FROM PLOT TO REGION: ASSESSING THE ROLE OF LAND USE IN TROPICAL

MONTANE FOREST STRUCTURE AND DYNAMICS

by

ADRIANA USCANGA CASTILLO

A DISSERTATION

Presented to the Department of Geography
and the Division of Graduate Studies of the University of Oregon
in partial fulfillment of the requirements
for the degree of
Doctor of Philosophy

September 2022

DISSERTATION APPROVAL PAGE

Student: Adriana Uscanga Castillo

Title: From Plot to Region: Assessing the Role of Land Use in Tropical Montane Forest Structure and Dynamics

This dissertation has been accepted and approved in partial fulfillment of the requirements for the Doctor of Philosophy degree in the Department of Geography by:

Lucas de Carvalho Ramos Silva   Chairperson
Patrick Bartlein   Core Member
Leigh Johnson   Core Member
Richard York   Institutional Representative

and

Krista Chronister   Vice Provost for Graduate Studies

Original approval signatures are on file with the University of Oregon Division of Graduate Studies.

Degree awarded September 2022

DISSERTATION ABSTRACT

Adriana Uscanga Castillo

Doctor of Philosophy

Department of Geography

September 2022

Title: From Plot to Region: Assessing the role of land use in tropical montane forests structure
       and dynamics

Forest disturbance and land use are strong drivers of forest structure, composition, and dynamics and yet, their role in shaping tropical montane landscapes is poorly understood. The overarching goal of my dissertation is to broaden our understanding on the role of land use in shaping forest structure and forest dynamics in tropical montane landscapes, with a particular focus on aboveground biomass (AGB). Using the Northern Mountains of Oaxaca (NMO), Mexico, as a study system, I investigate changes in vegetation across space and time, particularly in an ecosystem known as tropical montane cloud forest (TMCF).

The NMO has experience forest disturbance by land use for centuries. Deeply influenced by regional and global socioeconomic forces, land use has changed over time, modifying montane landscapes accordingly. Tropical mountains are currently experiencing large rates of forest loss related to the expansion of agricultural commodity production. Land-use and land-cover change, transformations of land tenure regimes, landscape management strategies, the development of policies related to agricultural production and forest protection, and the environmental conditions that define vegetation growth, are all factors that intertwine to define current and future forest dynamics. Thus, in this project I analyze various aspects of land use in shaping forest structure and dynamics, including the local and regional effects of land-use intensity on tropical montane forests, ways to include these effects at regional scales through forest structure models, and current land use dynamics taking place in the NMO.

In the first chapter I explain the global relevance of tropical mountains and I introduce the foundational concepts of my dissertation, including forest structure and succession, a brief overview of land use in the study region, and the significance of my research. In the second chapter I analyze the relative roles of land use and environmental factors on AGB spatial

patterns, as well as the relationship between forest structure and tree diversity. I conclude that land use has a larger role in shaping AGB spatial patterns, and that the relationship between tree diversity and AGB is positive but weak. In chapter three I use remote sensing data to study recent small-scale disturbance related to land use in TMCF. Seeking for novel methods to incorporate land use effects on forest structure in AGB estimates, I found several remote sensing variables that have the potential to be used as input variables in AGB predictive models. These variables are derived from Landsat time series that track vegetation cover change over time. I conclude with providing some recommendations on the use of these variables. In chapter four I assess trends of forest loss and forest conservation in the NMO over the last two decades. Here, I provide a map of the spatial distribution of forest loss and the ecosystems that have been affected the most. I show that forest loss in the NMO has increased in the last six years. I discuss possible driving causes of forest loss, including its relation to the establishment of cattle ranches and agricultural production, and assess the effects of the forest conservation projects taking place in the region. Finally, in the last chapter I summarize the main results of my dissertation.

CURRICULUM VITAE

NAME OF AUTHOR: Adriana Uscanga Castillo

GRADUATE AND UNDERGRADUATE SCHOOLS ATTENDED:

    University of Oregon, Eugene
    Universidad Nacional Autónoma de México, Mexico City

DEGREES AWARDED:

    Doctor of Philosophy, Geography, 2022, University of Oregon
    Master of Science, Biology, 2016, Universidad Nacional Autónoma de México
    Bachelor of Science, Biology, 2013, Universidad Nacional Autónoma de México

AREAS OF SPECIAL INTEREST:

    Landscape Ecology; Geospatial Science; Ecology of Tropical Forests; Agroecology and
    Food Systems; Social-Ecological Systems; Cartography and Data Visualization

PROFESSIONAL EXPERIENCE:

    Graduate Employee, Cartography and Data Visualization, University of Oregon, 2021-
       2022

    Graduate Employee, Instructor and Teaching Assistant, University of Oregon, 2021-2022

    Research Assistant, Institute of Ecology, Universidad Nacional Autónoma de México,
       2016-2017

    Research Assistant, INIFAP, México, 2012-2013

GRANTS, AWARDS, AND HONORS:

    Rippey Dissertation Writing Grant, From Plot to Region: Assessing the role of land use
       in tropical montane forests structure and dynamics, Department of Geography,
       University of Oregon, 2022

    NACIS Student Map Competition, 19 Years of Forest Loss in the Northern Mountains of
       Oaxaca, Mexico, North American Cartographic Information Society (NACIS), 2021

    Bill Loy Award for Excellence in Cartography, 19 Years of Forest Loss in the Northern
       Mountains of Oaxaca, Mexico, Department of Geography, University of Oregon, 2021

Sandra F. Pritchard Mather Graduate Fellowship, Department of Geography, University of Oregon, 2020

Doug Foster Community-Building Award, Department of Geography, University of Oregon, 2020

Tinker Field Research Grant, Center for Latino/a and Latin American Studies, University of Oregon, 2019

Best Student Poster AAG Rural Geography Specialty Group, Examining causes and consequences of regime shifts in human-environment systems of the Mexican Cloud Forest, American Association of Geographers (AAG), 2018

Honorable Mention for outstanding undergraduate thesis, Morphological foliar variation in wild and domesticated cotton in Mexico (in Spanish), XIX Mexican Conference on Botany, Sociedad Botánica de México, 2013

PUBLICATIONS (selected):

Uscanga, A., López, H., Piñero, D., Emerson, B.C., Mastretta-Yanes, A. (2021). Evaluating species origins within tropical sky-islands arthropod communities. *Journal of Biogeography*, 00:1-12. doi: 10.1111/jbi.14144

Arroyo-Laember, D., Uscanga, A., Piña Tejeda V.M., Vázquez Barrios, V., Reverchon, F., Rosell, J.A., Escalante, A.E., Peña-Ramírez, V.M., Benítez, M., Wegier, A. (2020). Cognitive maps across multiple social sectors: shared and unique perceptions on the quality of agricultural soils in Mexico. Frontiers in Sustainable Food Systems, 4:522661. https://doi.org/10.3389/fsufs.2020.522661

Sosa-Aranda, I., Ek del-Val, Hernández-Martínez, G., Arroyo-Laember, D., Uscanga, A., Boege, K. (2018). Response of lepidopteran herbivore communities to crop management in coffee plantations. Agriculture, Ecosystems and Environment, 265(1): 37-44. https://doi.org/10.1016/j.agee.2018.05.018

ACKNOWLEDGMENTS

Finally, I would like to especially thank my lovely sisters and my parents. Your teachings, unyielding support, continuous encouragement, and love kept me going in tough times and you were always in my mind in the happy moments. Thank you for loving me and taking care of me always. I would not be in this place without you.

To my family.

TABLE OF CONTENTS

LIST OF FIGURES

LIST OF TABLES

Table   Page

CHAPTER 1
INTRODUCTION

Tropical Mountains

Mountains are probably one of the most popular geological landforms among humans. Considered as places of contrasts, mountains have inspired poets and artists, aroused the curiosity of explorers and researchers, provided the setting for the domestication and diversification of several crops, constituted sacred spaces, and hosted armed conflicts over contested territories. In the social imaginary, mountains are mighty, dangerous, untamed places, and at the same time they are regarded as fragile, vulnerable, and endangered by global environmental change.

Mountains are rich places both environmentally and culturally. Home to at least one tenth of the global population, mountains exhibit the highest levels of biodiversity on Earth (Rahbek et al. 2019; FAO 2002). Hence, they are considered biodiversity hotspots (Hoorn, Perrigo, and Antonelli 2018; Spehn, Rudmann-Maurer, and Körner 2011). They also capture vast amounts of freshwater that benefit local inhabitants and people living downstream, a feature that made them earn the title of "world's water towers" (Immerzeel et al. 2020). Additionally, they have recently been acknowledged for their potential to stock large amounts of carbon (Spracklen and Righelato 2014). Many of these features are enhanced in mountains located in the tropics. Tropical mountains harbor some of the most biodiverse and carbon-rich ecosystems, and are more humanly populated than mountains in temperate regions (Körner et al. 2017).

Tropical mountains have bewildered researchers for more than two centuries. Alexander Von Humboldt's description of Mount Chimborazo in Ecuador, published in 1807, revolutionized our thinking of the distribution of ecosystems and their relationship to climate and topography (Moret et al. 2019). Not only do elevation gradients in tropical mountains mirror the climatic conditions of a latitudinal gradient from the equator to the poles, but they also exhibit a wide array of unique climates −in close proximity to one another− resulting from the combination of elevation, aspect, relief, distance to the ocean, and changes in air pressure and oxygen availability (Trew and Maclean 2021; Graham and Fine 2008). Thus, tropical mountains capture a larger portion of the temperature-precipitation climate space in shorter distances than lowlands, resulting in a great vegetation turnover displayed as layers of ecozones, with their

16

respective intrinsic variation, laid one after the other along an elevation gradient (Rahbek et al. 2019).

Plant communities and the life they support change along elevation gradients up tropical mountains (Hoorn, Perrigo, and Antonelli 2018). At lower elevations, warm temperatures give place to tropical evergreen or deciduous forests, depending on the precipitation regime. If mountains are exposed to ocean winds, air moving up the elevation gradient expands and cools, reaching a water condensation point that results in the formation of clouds at ground level (fog). The frequent presence of fog determines another ecozone where cloud forests are found. These unique ecosystems are the main focus of the present dissertation. The next ecozone is usually drier and colder, and mainly comprises coniferous forests. Finally, if the mountain is tall enough, the upper layers exhibit alpine vegetation–short shrubs and grasses– followed by snow caps (Rahbek et al. 2019). Because all these ecosystems are found at relatively short distances (in contrast to the latitudinal gradient), and in a predictable sequence, and because there are several mountain ranges in the tropics, tropical mountains are considered natural laboratories (Cavelier 1996; Tito, Vasconcelos, and Feeley 2020). That is, tropical mountains are conceived as sites where hypotheses regarding the relationship between plant communities and their environment can be tested. As of late, this has been particularly important in the face of the rising threat of climate change.

Forest Structure and Trajectories of Change

Some years after elevation gradients began to be described, the attention of researchers was drawn to the changes that vegetation experiences over time. Since the early 20th century, the sequence of plant communities assembled after a disturbance represented the chief focus of botanists like Henry Cowles and Frederic Clements (Egerton 2015). The description of plant community assemblages over time relies on the concept of succession. Succession refers to the sequential change over time of community composition and structure following disturbance (C. C. Chang and Turner 2019). Composition is defined as the types of vegetation and species that comprise a community, and structure refers to the horizontal and vertical arrangement of plants in space. Thus, common variables to describe forest structure include tree canopy height, tree density (the number of trees per area), and stand basal area.

For Clements, the final stage of succession represented a climax state, a permanent community–with a specific composition and structure–that defines an ecosystem (Clements 1936). Much research has been developed ever since, and yet, the idea of a stable state is still central to theoretical and applied ecological research. Although the predictability of forest succession has been contested (e.g., Norden et al. 2015), there are general trends that are expected to take place during this process. For example, in tropical forests, it is expected that the stand basal area and the number of large trees will increase over time, as well as the vertical layers of vegetation and the presence of lianas and epiphytes (Guariguata and Ostertag 2001). There is large variation in successional trajectories, however, and the increasing recognition of the dynamism of landscapes has fostered meaningful research on forest ecosystem change over time, especially in the light of current forest disturbance related to land-use -and climate change.

Disturbance is a central element of forest succession, not only because it marks its beginning, but also because it defines the spatial and temporal patterns of the process (Prach and Walker 2019). The intensity, frequency, and extent of a disturbance influence successional trajectories, since they modify the local environment. The availability of nutrients in the soil, the source of seeds for establishment, and the time available for recovery are all factors defining succession. For instance, thinning, wildfires, and recurrent landslides will have different effects on forest structure and composition (Pulsford, Lindenmayer, and Driscoll 2016). Moreover, disturbance has long-term effects, and plant communities are usually shaped by legacies of past disturbance (R. Chazdon 2003).

In tropical forests, the most common disturbance is related to land use (Yadvinder Malhi et al. 2014). The effect of agriculture in shaping forest structure and composition and driving deforestation has been at the center of several studies and academic debates. Currently, the main driver of tropical forest clearing is the production of agricultural commodities, such as palm oil, soy, and pasture for cattle (Curtis et al. 2018). The second driver is shifting cultivation, an agricultural technique practiced by small-scale farmers whereby land is cleared for cultivation, often through slashing vegetation and burning the site (slash and burn), followed by fallowing after a few agricultural cycles (Curtis et al. 2018; Pérez-García and del Castillo 2016). In turn, fallow lands begin a process of secondary succession in which vegetation regenerates (Velasco-Murguía et al. 2021). These patches of vegetation are known as secondary forests.

Permanent and shifting agriculture have different effects on forest landscapes, as do high-input (industrialized) and low-input agriculture. Notably, while in shifting cultivation vegetation is allowed to regrow, the establishment of cash crop plantations implies the permanent loss of forest (Bongers et al. 2015). Thus, different agricultural practices result in distinct successional trajectories of forest, and create different landscape dynamics (Tscharntke et al. 2005). The coexistence of small-scale agriculture, shifting cultivation, cash crop production, large plantations, and cattle ranches, along with several strategies of forest management in tropical regions, have encouraged researchers to think of tropical forests as dynamic communities embedded in complex landscapes, instead of as permanent, albeit fragile, communities in a climax state (I Perfecto, Vandermeer, and Wright 2009; Gardner et al. 2009; Yadvinder Malhi et al. 2014).

Land Use in the Highlands of Mesoamerica

This dissertation focuses on an intricate montane landscape located in southern Mexico where forests and agriculture have coexisted for centuries. As one of the cradles of agriculture, Mesoamerica has a long history of land use (Piperno 2011). Little is known about the effects of land use on vegetation before the Spanish conquest, even concerning regions or civilizations that have been more widely studied such as central Mexico or the Mayan culture (Urquijo Torres 2012). Highlands have been more widely associated with hunting and gathering than with the establishment of agriculture, especially because most of the large pre-Columbian settlements known to date are located in valleys (González-Abraham et al. 2015). This has led ecologists to think that montane forests were not commonly converted to agricultural lands before the colonial period, and that it was only in the colonial period, when indigenous populations were displaced to higher lands, that forest conversion expanded (Sánchez-Ramos and Dirzo 2014). However, this view is at odds with anthropological, archeological, and historical studies showing that important civilizations also thrived in the mountains, and not only at lowlands (Delgado 1966). Pottery, tombs, and small settlements found in montane lands show that these forested landscapes have been inhabited and used for more than five centuries, including for agricultural purposes (Chagoya Morgan 1986).

Better records on land use exist for the colonial and subsequent periods. From this moment on, the effects of land use on montane forests broadly mirror those provoked by the

incursion and development of capitalist agriculture in Latin America (I Perfecto, Vandermeer, and Wright 2009). Without intending to oversimplify the historical development of capitalist agriculture and the consequences it has brought to rural Latin America, this process can be summarized into five key historical moments of agrarian change: (1) the establishment of export-oriented cash crop plantations and large estates that produced crops for domestic markets during the colonial period (~1500-1830s); (2) the development of capitalist cash crop plantations from those formerly based on slave labor and the wider integration of estates' agricultural production into the world market, as landlords and the nascent merchant class gained political control and economic power in the newly independent nations (~1830s-1920s); (3) a transition from export to import of agricultural products, geared towards national industrialization that resulted in the abandonment of small-scale agriculture and the modernization of large-scale farms, causing rural economic stagnation (~1900s-1950s); (4) land reforms and the promotion of external inputs, mechanization, monocultures, and hybrid seeds through the Green Revolution, accelerating agricultural commercialization, and the end of the landed oligarchy (~1920s-1980s); and (5) further privatization of lands and a return to export-oriented agricultural production fueled by neoliberal globalization (~1980s-present) (Baer 1972; Bryceson 2000; Clapp 2012; Goodman and Watts 1997; Kay 2000; McMichael 2013).

In highland Mesoamerica, coffee became the leading crop amid the development of capitalist agriculture, and represented the main source of income, first for the landed oligarchy, and later for smallholders that in time began to grow and sell coffee in their own lands (E. F. Fischer and Victor 2014). With the establishment of coffee plantations in the 19th century, large areas of forest were cleared (Ivette Perfecto, Jiménez-Soto, and Vandermeer 2019). Coffee remains an important export product in the region, and is currently produced for a variety of markets, ranging from dominant international corporations to alternative supply chains such as Fair Trade, organic, and specialty markets (Clapp 2012; Topik, Talbot, and Samper 2010). By the mid-1970s, other export crops like vegetables and fruits were incorporated into the region's agricultural production (Imbach et al. 2017). These nontraditional crops are usually grown in smallholders' lands and commercialized through contract farming by cooperatives and exporters (Hamilton and Fischer 2005). Maize and beans are widely grown in the region, usually in the form of *milpas*, a traditional agricultural system wherein several crops–including maize, beans, and squash–are grown together in a way that maximizes nutrient and water use (Pérez-García

and del Castillo 2017). *Milpas* play a fundamental role in the peasant economy, though they are intended mainly for self-consumption, research has shown that maize production by small-scale farmers can also contribute to the local supply (Bellon et al. 2021; Arnés Prieto 2015; Isakson 2009). Currently, the most common land uses in tropical montane landscapes are small-scale farming of annual crops mainly in the shape of *milpas*—that can be found along the whole elevation transect; pasturelands and sugar cane production on the lower parts of the mountains; coffee production in medium-to-high elevation slopes; and logging at higher elevations where coniferous and oak forests are distributed (Martínez et al. 2009; Velasco Murguía et al. 2014; Cayuela, Benayas, and Echeverría 2006).

Forests in tropical mountains in general, and in the highlands of Mesoamerica in particular, are deeply influenced by the different uses that are given to land and how those uses change over time. Factors that define land-use and land-cover change include the price fluctuations of crops in the global market, changes in land tenure regimes, agricultural insurance programs, available technologies and infrastructure, forest conservation plans, and the development of policies related to both agriculture and forest protection. In particular, in the highlands of Mesoamerica there has been a transition from shifting agriculture to permanent agriculture and the establishment of cattle ranches, together with a decrease in coffee production, that have been shaping forest dynamics in the region in the last decades (Pérez-García and del Castillo 2017; SIAP 2020). Notably, most forests in southern Mexico are in either communal or *ejido* land—two forms of common property created after the Mexican Revolution as part of a land reform that granted land to small-scale farmers and territorial rights to indigenous communities. In the beginning of the 1990s, new legislation aimed at promoting land privatization allowed individuals to sell parcels of ejido land, thus opening the possibility of converting such lands into private property (Navarrete Romero 2015). Together, changes in land tenure regimes, and the intensification of agriculture and expansion of grazing lands for cattle, have deeply shaped tropical forested landscapes in the last decades.

This overview of land use in the highlands of Mesoamerica serves to contextualize the processes of land-use and land-cover change that are currently taking place in the Northern Mountains of Oaxaca, the mountain range at the center of this work. It is important to underscore that although my project comprises only the effects of recent disturbance on forest structure, land use and land cover change have been present in the area for a long time. Driven by local,

21

regional, and global forces, the specific form of current land uses may change, but the central role of land use in shaping these montane landscapes remains. Moreover, different land uses and management strategies influence landscape dynamics in distinct ways. Hence, it is fundamental to assess the role of land use and trajectories of landscape change in these mountains to understand the current state of forests and their potential future trends.

Overview of the Dissertation

The overarching goal of my dissertation is to broaden our understanding of the role of land use in shaping forest structure–including the amount of carbon forests can store– and forest dynamics in montane landscapes located in the Northern Mountains of Oaxaca (NMO), Mexico. Thus, I investigate changes in vegetation across space and time, particularly in an ecosystem known as tropical montane cloud forest (TMCF), and its surrounding ecosystems.

TMCF are defined as ecosystems that are frequently enveloped in clouds or mist (Fahey, Sherman, and Tanner 2016). Their distribution is determined by the upper and lower limits of ground-level clouds, and depends on the factors influencing cloud formation −such as temperature and humidity− which are in turn influenced by elevation and proximity to the ocean (Scatena et al. 2011). These forests tend to be close to the ocean and on topographically exposed landscapes, and they also exhibit great variation in elevation, soil type, and species composition (Fahey, Sherman, and Tanner 2016). TMCFs comprise only 1.4% of all tropical forests worldwide, but these ecosystems have been drawing more attention lately given their large role in water regulation and provision, the great amount of biodiversity they harbor, their recently acknowledged high capacity to store carbon, and their large rates of deforestation (M Mulligan et al. 2011). TMCF are also extremely beautiful and considered among the most threatened ecosystems under the current state of land-use and land-cover change and climate change (Bruijnzeel et al. 2011).

In Mexico, TMCF cover nearly 1% of the national territory and are distributed along tropical mountain ranges, usually between 1,500 and 2,500 m asl (although they can be found at lower and higher elevations depending on the exact elevation at which clouds are formed) (Toledo-Aceves et al. 2011). Despite their restricted distribution, they are an essential part of Mexican tropical montane forests given their exceptionally high number of endemic species (making them the ecosystem with the highest biodiversity per area in that country), and their role

in capturing water and regulating its flow downstream (González-Espinosa et al. 2012). The state of knowledge of carbon dynamics in TMCF remains scarce, which is one of the reasons I devoted two of my chapters to studying forest structure and aboveground biomass (where most of the carbon in tropical forests can be found).

Throughout the three following chapters, I answer questions related to forest structure and forest dynamics at local and regional scales. In chapter two, I draw data from the Mexican National Forest Inventory (FI) to estimate the magnitude and distribution of aboveground biomass (AGB) in TMCF located in the NMO. In doing so, I investigate the relative roles of environmental factors and land use in shaping AGB patterns across scales, as well as its relationship to tree diversity. Moreover, I analyze whether AGB is more strongly related to either the height of forest canopy, the basal area of a forest stand, or the density of trees, since these are forest structure variables that are used to estimate and map AGB at landscape, regional, and global scales. I found that AGB exhibits a wide variation in the region (8-400 Mg ha^{-1}) which stems from the diversity in landscape composition driven by the coexistence of fallows, young, and mature forests that result from land use spatial patterns. My results show that AGB spatial patterns can be best predicted by the interactive effects of land use and environmental factors, with land use having a larger role within the region, even overshadowing the effect of the climate.

In chapter three, I further explore the role of land use in shaping forest structure. I focus on potential methods that can be applied to incorporate the effects of land use on forest structure in AGB modeling and mapping. In this chapter I ask: (1) How can the recent disturbance history of a forest, assessed through remote sensing techniques, be used to estimate the effect of land use on forest structure? In turn, (2) how can these effects be incorporated into AGB models? Remote sensing provides a wide array of data that enables the analysis of vegetation change across large spatial areas almost in real time. To answer these questions, I used data from the Landsat program, a series of satellites that have acquired images of the Earth's surface since the 1970s. Landsat images have a spatial resolution of 30 meters and a temporal coverage of two weeks, which means that it is possible to build time series of several images per year with enough resolution to detect small-scale disturbance in tropical montane forests. Using Landsat time series, I tracked changes in vegetation cover of the FI plots located in the TMCF of the NMO (also analyzed in the previous chapter). With this method, I confirmed that montane landscapes

in NMO are very dynamic, with, for instance, 27% of the plots analyzed showing abrupt changes in vegetation (or forest clearings). I also found that the variation of vegetation indices (equations of light wavelengths that indicate vegetation greenness) over time can be used as a proxy for land use, which, if successfully incorporated into predictive models, could decrease the uncertainty associated with forest disturbance in AGB estimates.

In chapter four, I go beyond processes taking place in TMCF and assess trends of forest loss and forest conservation in the entire region over the last two decades. The main result of this chapter is a map with which I show the spatial distribution of forest loss, the ecosystems that have been most affected, and some of the lands spared to forest conservation. I found that forest loss in the NMO remained almost constant for many years but increased in the last six years, especially in the subregion known as Sierra Mixe. The most affected ecosystems are tropical evergreen forests and TMCF. The reasons behind the sudden increase in forest loss in 2015 are unclear, but agricultural surveys show a significant expansion of pasturelands in the last decade, suggesting that forest or shaded coffee farms conversion to cattle ranches may be driving forest loss in the region. In addition, land-use change due to illicit activities may also be playing an important role. On the other hand, community-based conservation projects are having a positive impact locally, especially in the subregion Ixtlán. Despite these very important efforts, forest loss surpasses forest gain in the region.

This dissertation constitutes my first attempt to link two foci of study that have commonly been analyzed in parallel, seldom showing explicit connections in the scientific literature: forest ecosystem dynamics and agrarian change. With its long-lasting focus on human-environment interactions, I believe Geography has much to offer in this regard. While most of the Earth's land is currently or has historically been used and modified by humans, assessing the role of land use in shaping forest landscapes is fundamental not only to enhance our current knowledge on forest ecosystem dynamics, but also to better suggest, support, and accompany processes of much needed forest regeneration and conservation. After all, as Hecht and Cockburn (1989) state in *The fate of the forest*, "if a region is denied its true history how can its future be honestly discussed?"

CHAPTER 2

LOCAL AND REGIONAL EFFECTS OF LAND USE ON SPECIES DIVERSITY AND ABOVEGROUND BIOMASS IN TROPICAL MONTANE CLOUD FORESTS

INTRODUCTION

Tropical forests play a fundamental role in the carbon cycle because they contain ~25% of the carbon in the terrestrial biosphere (Bonan, 2008). This carbon is stored in the living biomass of trees and other understory vegetation mainly allocated above the soil in stems, branches, and leaves, in what is known as aboveground biomass (AGB) (Holly K. Gibbs et al. 2007). Because AGB represents the main carbon pool in tropical forests, it also determines the amount of carbon loss to the atmosphere when these forests are disturbed (Houghton, Hall, and Goetz 2009; Pan et al. 2007). Moreover, AGB is expected to be related to forests structure and composition, and research has found it has a positive relationship with tree diversity suggesting an interesting synergy between carbon storage and biodiversity, two of the ecosystem features most threatened by current global environmental change (Sheil et al. 2016; L. Poorter et al. 2015). Thus, AGB is considered an essential variable in ecosystem science and an important input to Earth system models (Bojinski et al. 2014; Santoro et al. 2021).

The precise quantification of AGB in tropical forests remains a challenge, particularly in tropical montane forests (located above 1,000 m asl) where carbon has been historically understudied and underestimated (Spracklen and Righelato 2014; Cuni-Sanchez et al. 2021). Estimating AGB in tropical mountains is difficult because field data is sparse and remote sensing approaches are challenged by rugged terrain and frequent cloud cover (G. P. Asner et al. 2014; Ticehurst, Held, and Phinn 2004). Additionally, estimates have large uncertainties due to the significant spatial variation of AGB arising from two sources: (1) environmental factors, some of them linked to the elevation gradient imposed by mountain relief, and (2) forest disturbance patterns (Houghton, Hall, and Goetz 2009; D. B. Clark, Hurtado, and Saatchi 2015).

Ecosystems in tropical mountains are influenced by the environmental gradient imposed by elevation. As elevation increases, temperature decreases and vegetation is exposed to frequent cloud cover and fog (Gotsch, Asbjornsen, and Goldsmith 2020). This elevation gradient shapes forest structure and composition and gives rise to a distinctive ecosystem known as tropical montane cloud forest (TMCF), whose main environmental feature is its persistent immersion in

ground-level clouds. Fog, low temperatures, waterlogged soils, and nutrient limitation are all features found in TMCF that generally limit primary productivity (Fahey, Sherman, and Tanner 2016; Mark Mulligan and Burke 2005). Thus, research has found that AGB in TMCF is usually lower than in their lowland-forest counterparts and, more generally, that AGB in tropical mountains declines with elevation (Spracklen and Righelato 2014; G. P. Asner et al. 2014; C. A. J. Girardin et al. 2010). However, AGB patterns along elevation transects can be complex depending on how environmental factors other than temperature change with elevation (e.g., see climate-induced reversal of tree growth and water use in south- *vs* north-facing landscapes (Quadri, Silva, and Zavaleta 2021)), as well as their relative roles in shaping forest structural attributes (D. B. Clark, Hurtado, and Saatchi 2015). In fact, examples of TMCF that exhibit surprisingly high AGB, as well as patterns that do not conform to the general trend of AGB decreasing with elevation have been described (e.g., Cuni-Sanchez et al., 2017; de la Cruz-Amo et al., 2020), which suggests that more research is needed to understand how AGB changes along different environmental gradients.

The other large source of variation in AGB patterns in tropical mountains is forest disturbance. AGB decreases with forest disturbance, but increases shortly after a disturbance event following secondary succession, if the conditions allow new vegetation to establish, and surviving trees to keep growing (L Poorter et al. 2016). In TMCF, conversion to croplands and grazing lands for cattle represent the main source of disturbance (Bruijnzeel, Kappelle, Mulligan, & Scatena, 2011; Calderon-Aguilera et al., 2012). When croplands and cattle ranches are permanently established, AGB is also permanently removed, causing large carbon losses to the atmosphere (Mendoza-Ponce et al. 2018). However, in places where shifting agriculture is practiced and cash crops are grown in agroforestry systems, as in the case of many tropical mountains, vegetation is allowed to regrow after disturbance, resulting in AGB increases and, consequently, carbon gains (R. L. Chazdon et al. 2016; Velasco-Murguía et al. 2021). The coexistence of different agricultural systems and landholding sizes in tropical mountains (from small-scale farming to big cash crop plantations) results in patchy landscapes with forest at different successional stages surrounded by agricultural and grazing lands (del Castillo 2013; Ivette Perfecto and Vandermeer 2008; Gardner et al. 2009). These heterogeneous landscapes have been described as forest-agriculture mosaics and exhibit substantial AGB variation across space (Adhikari et al. 2017).

Despite the fundamental role that land use plays in shaping carbon distribution in tropical mountains, land use effect on AGB patterns remains poorly understood (K. H. Erb et al. 2018). Considering more than 60% of forested ecosystems around the globe currently experience some sort of land use (Grantham et al. 2020), this represents a fundamental knowledge gap. Furthermore, this lack of understanding is probably a large source of uncertainty in AGB estimates because AGB is usually measured at local scales in forests considered to be undisturbed and these measurements are then extrapolated to regional scales without explicitly accounting for the effect of land use variations across scales (De Jong 2013).

With the aim of contributing to a better understanding of the relative roles of environmental factors and land use on shaping AGB patterns across scales, here, we focus on a TMCF region located in southern Mexico that is subjected to both an environmental gradient and a land-use intensity gradient. Three research questions guide our study: (1) How much AGB do TMCFs hold and how is it spatially distributed at the local, landscape, and regional scales? (2) How is AGB related to tree diversity in the study region? and (3) How does land-use intensity shape AGB patterns along an elevation gradient? We hypothesize first, that AGB in this TMCF will be larger than reported in regional and global estimates as has been the case for other cloud forests studied recently (e.g., Cuni-Sanchez et al., 2021), and further, that its spatial distribution will be driven by forest structural attributes, particularly by tree height, as in other TMCF described in the Neotropics (G. P. Asner et al. 2014; C. Girardin et al. 2014). Secondly, we expect to find a positive correlation between tree diversity and AGB as has been found in lowland tropical forests (Arasa-Gisbert et al. 2018; L. Poorter et al. 2015) and in Mexican TMCF along land-use intensity gradients (Vizcaíno-Bravo, Williams-Linera, and Asbjornsen 2020). Finally, we predict that environmental factors and land use will have a compounding effect on AGB along the elevation gradient where lower land-use intensity and cooler temperatures will decrease AGB with increasing elevation.

METHODS

Study Area

We delimited a study area following a tropical montane cloud forest (TMCF) regionalization conducted by Toledo-Aceves *et al.* in 2011 based on geomorphology, forest cover, watershed margins, rivers, and cultural differences (such as presence of indigenous groups). We focused on

the Northern Mountains of Oaxaca (NMO), a region that harbors some of the most biodiverse forests in Mexico and includes the largest and most continuous TMCF, and where forest conservation is considered a critical priority (Toledo-Aceves et al. 2011). In the NMO, TMCF are found on hillslopes and humid ravines with frequent fog and drizzle. Soils in these forests usually develop from the weathering of metamorphic rocks and volcanic outcrops, they tend to be deep, and rich in clay and organic matter (Torres Colín 2004). This region has a long history of land use with shifting agriculture, some permanent agricultural and grazing lands, and several types of coffee farms (including sun and shaded coffee) interspersed with forests, creating a forest-agriculture mosaic. To define the distribution of TMCF within NMO we used the official map of vegetation and land-use series V published by the National Institute of Statistic and Geography (INEGI) in 2013 (INEGI 2013) (Figure 2.1).
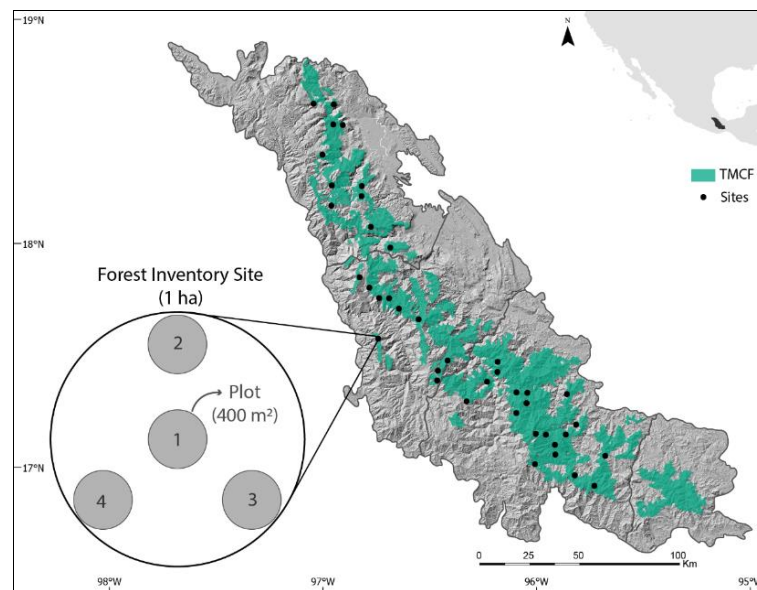
Figure 2.1. Forest Inventory sites (n= 40, black points) within Tropical Montane Cloud Forest (TMCF) distribution (in green) in the Northern Mountains of Oaxaca (NMO), located in the south of Mexico. A zoomed-in site shows the hierarchical nested sampling design carried out by the Forest Inventory (FI) where four plots of 400 m^2 were established in one-hectare sites.

Data Collection and Processing

We gathered and integrated information on forest structure and composition, climate, topography, and land use, from different sources into a single dataset. The main data source for

28

this work is the publicly available Mexican National Forest Inventory (FI) database, which contains information on forest structure and composition, as well as forest disturbance. From this database we estimated forest structural attributes, AGB, and land-use variables. To complement these data, we obtained information on mean annual temperature and precipitation from WorldClim (Fick and Hijmans 2017). Lastly, we retrieved topographical information from NASA's Shuttle Radar Topography Mission digital elevation data (SRTM, (Farr et al. 2007)). A detailed description of the foregoing variables can be found below (see also Table S2.1 for a summary of the variables used in this study).

Forest inventory sites. We assessed forest structure and composition using FI database. FI data collection was carried out between 2009 and 2014 following a systematic hierarchical nested sampling design with 1-ha circular sites as the main sampling unit. All sites were established 25 km apart from each other in a grid-like fashion (CONAFOR 2015). Within each site, four circular plots of 400 m^2 were established. One in the center of the site, and the other three in a north, southeast, and southwest direction, respectively, at 45.14 m from the central plot (Figure 2.1). All trees, lianas, shrubs, palm trees and ferns within the plots with a diameter at breast height (DBH) larger than 7.5 cm were taxonomically identified and sampled for height, DBH, and basal area (BA). Information about the geographic location, vegetation type, and land ownership of each site was also documented. Additionally, signs of forest disturbance were assessed in each site and recorded (CONAFOR 2015). For selecting FI sites relevant to our study, we performed a spatial intersection in QGIS 3.16 between FI sites and a NMO shapefile, the latter acquired from the National Commission of Biodiversity (CONABIO) GeoPortal (CONABIO 2012). This selection was further refined to obtain FI sites located exclusively in TMCF (see *Data Selection and Quality Control* section below).

It is important to note that FI sampling was not directed only towards undisturbed or 'old-growth' forests. On the contrary, this systematic sampling enabled the collection of data on a diversity of landscapes, many of them mosaics of different land cover classes including agricultural and grazing lands, coffee farms, and forests at different successional stages. Therefore, the Mexican FI provides a unique opportunity to test the effect of landscape composition and land use on forest structure and composition. This sampling design also made possible an analysis across spatial scales. Here, we processed data at two sampling levels. On the one hand, we used the 400 m^2 plots as our smallest sampling unit to describe forest structural

attributes and tree diversity (hereafter, plot level data). With this information we assigned to each plot to an approximate successional stage and estimated AGB. On the other hand, we used 1-ha sites to understand AGB spatial variation in relation to environmental factors and land-use intensity at the landscape and regional scales (hereafter, site level data).

Forest structural attributes and aboveground biomass estimation. Based on FI raw data, we derived three structural attributes at plot level that were then averaged by site: (1) stem density, i.e., the number of trees per hectare; (2) basal area, defined as the sum of the cross-sectional surface area of trees per hectare; and (3) Lorey's height, which is a measure of forest stand height weighted by its basal area.

We used allometric equations to calculate the AGB of every alive tree measured in 160 plots in 40 FI sites within our study region (Figure 2.1). A total of 4,106 trees belonging to 148 species were recorded. To correct for possible typos and identify synonyms in taxonomic names we collated our list of species with the Taxonomic Name Resolution Service using the correctTaxo function in R package BIOMASS (Réjou-Méchain et al. 2017). Then, we searched for all possible allometric equations published in the scientific literature that would match our species list. We found 47 allometric equations described at species or genus levels (Table S2.2 and references therein) with which we estimated the AGB of 2,700 trees. For estimating AGB of the remaining trees whose allometric equation has not been described, we used a generic allometric equation developed by (Jérôme Chave et al., 2015) for tropical trees based on tree wood density (ρ), height (H) and DBH (D):

$$\text{AGBest} = 0.0673(\rho D^2 H)^{0.976}. \qquad\qquad (1)$$

All allometric equations we used estimate AGB using a combination of trees' DBH and height, except for Chave et al.'s generic equation (eq.1) that also requires a wood density value. DBH and height were measured in the field and are available in the FI database. We searched for the wood density value of each species or its closest relative in global wood density databases using the function BIOMASS::getWoodDensity, which provides a wood-density value per tree and its associated standard deviation (calculated with repeated measurements of wood density at species, genus or family levels).

We calculated AGB as the sum of the biomass of each individual tree at plot level, and AGB per site as the average of the plot AGB values at each site. There is always some uncertainty inherent to upscaling biomass estimates from trees to forest stands that arises from the propagation of errors in field data collection, allometric equations, wood density estimates, and forest variation. To account for this uncertainty, we estimated the AGB standard deviation at plot level following error propagation through a Monte Carlo statistical simulation informed by field data using the BIOMASS::AGBmonteCarlo function. To do so, we used wood-density standard deviations, and assumed 95% of field data samples have a low DBH error and the remaining 5% a high DBH error (close to 5 cm), and that all field data samples have a height error of 10%, as suggested in (Jerome Chave et al. 2004). To estimate AGB error at the site level, we assumed standard-error independence between plots and used the following equation (eq. 2):

$$\varepsilon_{site} = (\varepsilon_{plot1}^2 + \varepsilon_{plot2}^2 + \varepsilon_{plot3}^2 + \varepsilon_{plot4}^2)^{1/2} \,. \tag{2}$$

Tree diversity. We used field measurements of species richness (S), i.e., the total number of species, and species abundance to calculate Shannon diversity index (H) in each plot using the R package *vegan* (Magurran 2013; Oksanen et al. 2020). To obtain total S per site, we calculated the total number of unique species sampled in the four plots within a site, and calculated H again using this combined species total. In this way, we obtained S and H at plot level, as well as total H and total S at site level.

Environmental variables. We focus on climate, topography, and their interactions as key environmental variables moderating the effect of land-use intensity on species diversity and ecosystem AGB. We extracted annual precipitation and mean annual temperature values at site level from WorldClim (bio12 and bio1, respectively) at ~1-km spatial resolution, using the R package *raster* (Hijmans 2021). We extracted slope (in degrees) and aspect values for each plot from NASA's STRM (~30-m resolution), using Google Earth Engine (Farr et al. 2007). We averaged plot values to obtain slope, and aspect at site level.

Land use variables. To quantify the effect of land use on AGB and tree diversity we defined three variables: (1) forest disturbance related to agricultural activities, assessed at the time of field data collection and available in the FI database; (2) forest disturbance related to cattle grazing activities, also provided by the FI; and (3) a land-use intensity gradient we built assessing the landscape composition of each site (i.e., the proportion of different types of land cover within a site) after a forest succession categorization at plot level. We obtained the first

two land-use variables from the FI disturbance database, which contains information about the cause and severity of vegetation disturbance at site level (CONAFOR 2009). The causes of disturbance are classified in 11 classes: fires, hurricanes, floods, roads, logging, land-use change, grazing, pests and diseases, power lines, mining, and urbanization. The severity of disturbance is classified in a four-category nominal scale: very low, low, medium, and high severity. Both the cause and severity of disturbance where qualitatively assessed during field data collection (CONAFOR 2009). Agriculture and grazing activities are reported within the categories of land-use change, grazing, logging, and fires with labels such as 'clearing for growing coffee', 'shifting agriculture', or 'conversion from forest to cattle ranch'. We reviewed all recorded disturbance causes in the database, identified, and extracted data related to agricultural and cattle grazing activities. Then, we assigned each site a disturbance severity value from 0, when no disturbance was reported, to 4, indicating high severity disturbance. Whenever a site presented more than one reported disturbance related to agriculture or grazing, we averaged the disturbance severity value.

To define the land-use intensity gradient we, first, identified the approximate forest successional stage of each plot to, then, calculate the proportion of forests at different successional stages present at each site. In general, shortly after croplands are abandoned or left fallow, TMCFs naturally regenerate showing an increase in tree density, height, and basal area. Over time, during secondary succession, tree height and basal area continue to increase but stem density decreases, representing a transition from young to mature forest (del Castillo, 2015). Other studies conducted in forest-agriculture mosaics in Mexican TMCF have shown that tree height, DBH, and tree density change through time after disturbance, which is useful for estimating an approximate stage of forest succession (Velasco-Murguía et al., 2021). To assign a successional stage to each plot, we classified all FI plots with a k-means cluster analysis using their structural attributes, including tree height, DBH, and stem density. K-means cluster analysis is a non-hierarchical procedure in which the user must define the initial number of centers. We ran the analysis with two, three, four and five initial centers and 25 randomly sampled sets each using the R package *stats* (Figure S2.1) (R Core Team 2021). Then, using the R package *NbClust*, we selected the best number of clusters by comparing 30 indices commonly used to obtain the optimal classification resulting from a cluster analysis (Charrad, Ghazzali, Boiteau, & Niknafs, 2014). A classification in three clusters was supported by most indices. Thus, we

assigned each plot to one of three groups: cluster one was defined as young fallows because it groups together plots with very low tree density, low basal area, and low tree height; the second groups together forest plots with high tree density, and medium basal area and tree height, thus, we defined it as young forest; we defined cluster three as mature forest because it groups together plots with very high basal area and tree height, but medium tree density (Figure 2a). We would like to acknowledge that forest succession is a continuum and a complex process (Chazdon, 2003; Norden et al., 2015). Here, however, we classified forest succession in discrete categories as a methodological approach conducted for the sake of the analysis. This approach has proven to be useful for understanding biomass accumulation over time after forest disturbance (Chazdon et al., 2016; Poorter et al., 2016).

Once plots were classified into three successional stages, we assessed the composition of young fallows, young and mature forests in each site. Interestingly, most of the sites have plots that fall across different successional stages, showing the patchiness in these forest-agriculture mosaic landscapes. To describe this patchiness, we assigned a value from 1 to 3 to each successional stage where young fallows = 1, young forest = 2, and mature forest = 3. Then, we defined a site forest proportion value (eq. 3) adding up the values of all successional stages within a site and normalizing the value to get a number from 0 to 1.

$$Forest\ proportion = \frac{SS - minSS}{maxSS - minSS}, \tag{3}$$

SS is the sum of the successional stage categories of the plots in a site, minSS is the minimum possible SS value present in a site and maxSS is the maximum possible SS value present in a site. Considering there are four plots in each site, minSS is always 4 (when all plots within a site are young fallows), and maxSS is always 12 (when all plots within a site are mature forests). This way, a forest proportion value from 0 to 1 is assigned to all sites, where 0 represents sites dominated by young fallows, 1 represents sites dominated by mature forests, and everything in between are sites with a combination of forests at different successional stages. Assuming sites dominated by young fallows experience greater intensity of land use and sites where most plots are classified as mature forest have experienced less land use, we estimated a land-use intensity gradient using the inverse of our forest proportion variable (eq.4). Similar approaches have been used to describe land-use intensity in tropical landscapes (Ivette Perfecto, Jiménez-Soto, and Vandermeer 2019; Tscharntke et al. 2005), where forest cover is inversely related to agricultural

intensification and, consequently, can be used as a proxy for quantifying land use at landscape scales.

$$Land\text{-}use\ intensity\ =1-forest\ proportion, \tag{4}$$

It is important to note that other causes of forest disturbance unrelated to direct land-use can result in land-use intensity gradient values closer to 1, such as pest outbreaks. However, agriculture and cattle ranching expansion have been identified as main causes of forest disturbance in TMCF (Calderon-Aguilera et al. 2012; Toledo-Aceves et al. 2011), and there is a positive correlation between our land-use intensity variable and the presence of forest disturbance related to agricultural and grazing activities reported in the FI disturbance database (Figure S2.2). Therefore, we are confident that forest proportion in this case is related to land use, and other sources of disturbance were excluded from the analysis.

Data Selection and Quality Control

To make sure that all FI sites selected correspond to our study system, we filtered FI sites further using the following key features of TMCF stated in the scientific literature as criteria: (1) sites should be within an elevation range of 1,000 and 2,800 m asl; (2) sites should receive at least 1,000 mm of annual precipitation; (3) sites should be described as cloud forest in the vegetation type column of the FI database; and (4) all sites must have epiphytes (Fahey, Sherman, and Tanner 2016; Jardel Peláez et al. 2014; Scatena et al. 2011; Torres Colín 2004).

We also performed some data quality control, homogenizing missing data values, correcting places names and removing diacritics, and filtering out rows with missing information. Additionally, we removed plots with many unidentified species or where most trees were dead. Because some plots are in places impossible to collect field data (such as very steep ravines), not all sites have four sampled plots. To avoid a biased sampling design, we selected only sites where four plots were sampled. After applying these filters, we ended up with a dataset of 160 plots within 40 sites located between 16.89 and 18.61 degrees N and -95.66 and -97.02 degrees W, within the distribution of TMCF (Figure 2.1).

Statistical Analyses

We deployed well-established statistical methods to answer each of our three main questions using two main sampling levels: plot level (n= 160), representing fairly homogeneous forest stands in an area of 400 m2; and site level (n = 40), conformed by 4 plots, representing the

heterogeneous nature of these landscapes in an area of 1 ha. All statistical analyses were performed in R version 4.1.1 (2021) and are described in the following sections that address the research questions (Q1-Q3) raised in the introduction.

Q1. How much AGB do TMCFs hold and how is it spatially distributed? To gain a general sense of the amount of AGB in TMCF and its variation, we calculated basic summary statistics of all variables at site level and estimated the correlation between variables. Because the plots within FI sites are at different successional stages, we were able to assess how AGB and forest-structural attributes change over secondary succession. To test whether stem density, tree height, basal area, wood density and AGB are significantly different in forests at different successional stages, we carried out five one-way analyses of variance (ANOVA).

We analyzed which structural attribute better explained AGB distribution in these forests as well as AGB distribution across trees of different size. Research shows that in some TMCF tree height is more strongly related to AGB than other structural attributes (e.g., (G. P. Asner et al. 2014)), in others, basal area and the density of very large trees play a larger role in explaining AGB distribution (Cuni-Sanchez et al. 2017). We analyzed the relationship between AGB and stem density, tree height, basal area, and wood density at plot level (n= 160) using linear regressions.

To explore the contribution of tree size to AGB and stem density we employed a similar approach as Cuni-Sanchez et al. (2021) and classified trees into six size classes based on their DBH: <10 cm, 10-20 cm, 20-30 cm, 30-40 cm, 40-50 cm, and >50 cm. Then, we calculated the proportion of stem density and AGB represented by each tree size class in every forest plot. We used one-way ANOVAs to assess whether tree size classes contribute to stem density and AGB in different proportions. To test if the contribution of tree size classes to stem density and AGB varies between forests at different successional stages we conducted two two-way ANOVAs using size class, forest successional stage, and the interaction between size class and successional stage as explanatory variables. Additionally, we conducted one-way ANOVAs to test whether the contribution of each tree size class to stem density and AGB is statistically different between forest plots at different successional stages, as well as to test whether the contribution to stem density and AGB varies between each tree size class within young fallows, young and mature forests. All statistically significant ANOVAs were followed by post-hoc Tukey tests, to determine the statistically significant different groups.

Q2. How is AGB related to tree diversity in the study region? To understand the relationship between AGB and tree diversity and richness in TMCF, we performed a series of linear regression analyses. We log-transformed AGB, given it has a long-tailed distribution in our dataset, in our dataset and assessed its relationship with species richness (S) and diversity using the Shannon diversity index (H) in TMCF plots (n= 160) and sites (n = 40) fitting linear regressions. Analyzing these relationships at both sampling units offered the possibility to test, first, whether the relationship between AGB and diversity is scale-dependent (as some studies have shown e.g., (L. Poorter et al. 2015)), and whether this relationship changes in forest stands at different successional stages. Thus, we visualized the results at plot level (smaller scale), considering the successional stage of each plot, and site level (larger scale).

Q3. How does land-use intensity shapes AGB patterns along an elevation gradient? We explored the relationships among tree biomass, diversity, environmental variables, and land use in TMCF sites using multiple linear regression models. First, to reduce the number of environmental variables, we computed a principal component analysis (PCA) of elevation, precipitation, temperature, and slope. Aspect is not a continuous variable and lacks variation in our dataset because most sites face either south or west, so aspect was excluded from the analysis. The first principal component (PC1) explained 68% of the variation and is correlated with temperature, precipitation, and elevation. Thus, PC1 represents an environmental gradient from warmer-and-moister sites at lower elevations to cooler-and-drier sites at higher elevations (Figure S2.3). Slope represents the second component, therefore, is unrelated to PC1. Thus, we selected PC1 and slope as our environmental predictors. We fitted a model with log-transformed AGB as the response variable and tree diversity, environmental gradient, slope, and the three land-use variables as predictors. Then, following a model-selection approach similar to (Tredennick et al. 2021), we performed variable selection by comparing the full model against a series of reduced models in which each predictor is dropped in a stepwise fashion (Lumley 2020). We selected the best model comparing their adjusted R^2, Mallows' Cp (CP), and Bayesian Information Criterion (BIC). To test for spatial autocorrelation, we calculated the Moran's I statistic for the residuals of the final model using a neighborhood distance of 10, 25, and 50 km, and visualized the spatial distribution of residuals with a map.

RESULTS

AGB in TMCF within the NMO is large and driven by basal area and the density of big trees

Forest structure and AGB show wide variation at both plot and site levels. In fact, some of the plots are completely devoid of trees (and AGB), while others surpass 500 Mg ha^{-1}. At site level, average AGB is 137.49 ± 121.29 Mg ha^{-1}, and it ranges from as low as 8.26 to as high as 414.52 Mg ha^{-1} (Table 2.1). Variation in structural attributes within and among sites is also large. For instance, average stem density in all 40 sites is 641.56 ha^{-1} but some sites have as few as 81.25 trees ha^{-1} while others almost reach 2,000 trees ha^{-1}. Similarly, the variation in tree height is large, going from about 5 to 25 m (Table 2.1).

Table 2.1. Summary statistics of structural attributes, aboveground biomass (AGB), tree diversity and richness, environmental and land-use variables in Tropical Montane Cloud Forest sites (n= 40).

Variable	Min (± S.E.)	Max (± S.E.)	Mean (± S.D.)
Forest structural attributes and AGB			
Stem density (tree ha^{-1})	81.25 (±15.72)	1806.25 (±444.10)	641.56 (±355.23)
Basal area (m ha^{-1})	2.26 (±0.64)	51.08 (±6.57)	20.42 (±13.48)
Lorey's height (m)	5.92 (±0.68)	24.91 (±1.00)	12.46 (± 4.63)
Average wood density (g cm^{-3})	0.32 (±0.02)	0.76 (±0.01)	0.56 (± 0.14)
Aboveground biomass (Mg ha^{-1})	8.26 (±1.02)	414.52 (± 19.29)	137.49 (± 121.29)
Tree diversity and richness			
Species richness	18	4	8
Shannon	0.51	2.41	1.49
Environmental variables			
Mean annual temperature (°C)	10.58	22.35	16.98
Annual precipitation (mm)	1026	3204	1883
Slope (degrees)	13.19	47.57	25.55
Elevation (m asl)	1042	2790	1863
Land-use variables			
Disturbance by agriculture	0	4	0.52
Disturbance by cattle grazing	0	4	0.25
Land-use intensity	0	1	0.68

The large variation in AGB and structural attributes found in TMCF sites stems from the diversity in landscape composition found in these forest-agriculture mosaics and it is driven by

the successional stage of each plot. In young fallows, tree density is low, and trees are short and thin (Table 2.2 and Figure 2.2). As forest succession develops, all these structural attributes increase in magnitude. Thus, young forests show larger trees and higher stem density than young fallows (Table 2.2 and Figure 2.2). In mature forests, the density of trees decreases as trees become even taller and bigger (Table 2.2 and Figure 2.2). As a result, AGB in forests at different successional stages is significantly different (ANOVA, $p< 0.001$, Figure 2.2f Table S2.3). In young fallows, AGB averages only 33.38 Mg ha^{-1}, in young forests this value notably increases to 151.69 Mg ha^{-1}, while in mature forests it reaches 354.86 Mg ha^{-1} (Table 2.2). On average, mature forests contain more than twice the biomass found in young forests, and about ten times more than young fallows. However, both young and mature forests contain similar proportions of the total measured AGB, due to the differences in the number of plots classified in each successional stage, accounting for about 47 and 43% of the total number of plots, respectively. In contrast, young fallows account for the remaining 10% of the total AGB measured in these 160 plots. The ANOVAs we performed to analyze structural differences among forests at different successional stages show that all attributes are statistically different in all three categories (young fallows, young forest, and mature forest) (Table S2.3). Wood density is the only structural attribute that is not statistically different between young and mature forests, although it is significantly lower in young fallows (Figure 2.2 and Table S2.3).

Table 2.2. Structural attributes and tree aboveground biomass (AGB) in forest plots (n= 160) at three different successional stages: young fallows (F), young forest (Y), and mature forest (M). Differences in structural attributes and AGB between different successional stages are statistically significant (ANOVA, $p < 0.05$, Table S2.3, Figure 2).

	F (n= 69)		Y (n= 62)		M (n= 29)	
	Mean	**S.D.**	**Mean**	**S.D.**	**Mean**	**S.D.**
Stem density (tree ha^{-1})	275.00	166.55	986.69	444.38	775.86	313.14
Basal area (m ha^{-1})	6.87	4.43	24.75	9.33	43.42	13.28
Lorey's height (m)	9.37	3.55	11.76	2.36	21.31	3.12
Average wood density (g cm^{-3})	0.49	0.13	0.57	0.08	0.57	0.08
AGB (Mg ha^{-1})	33.38	32.63	151.69	92.04	354.86	151.60
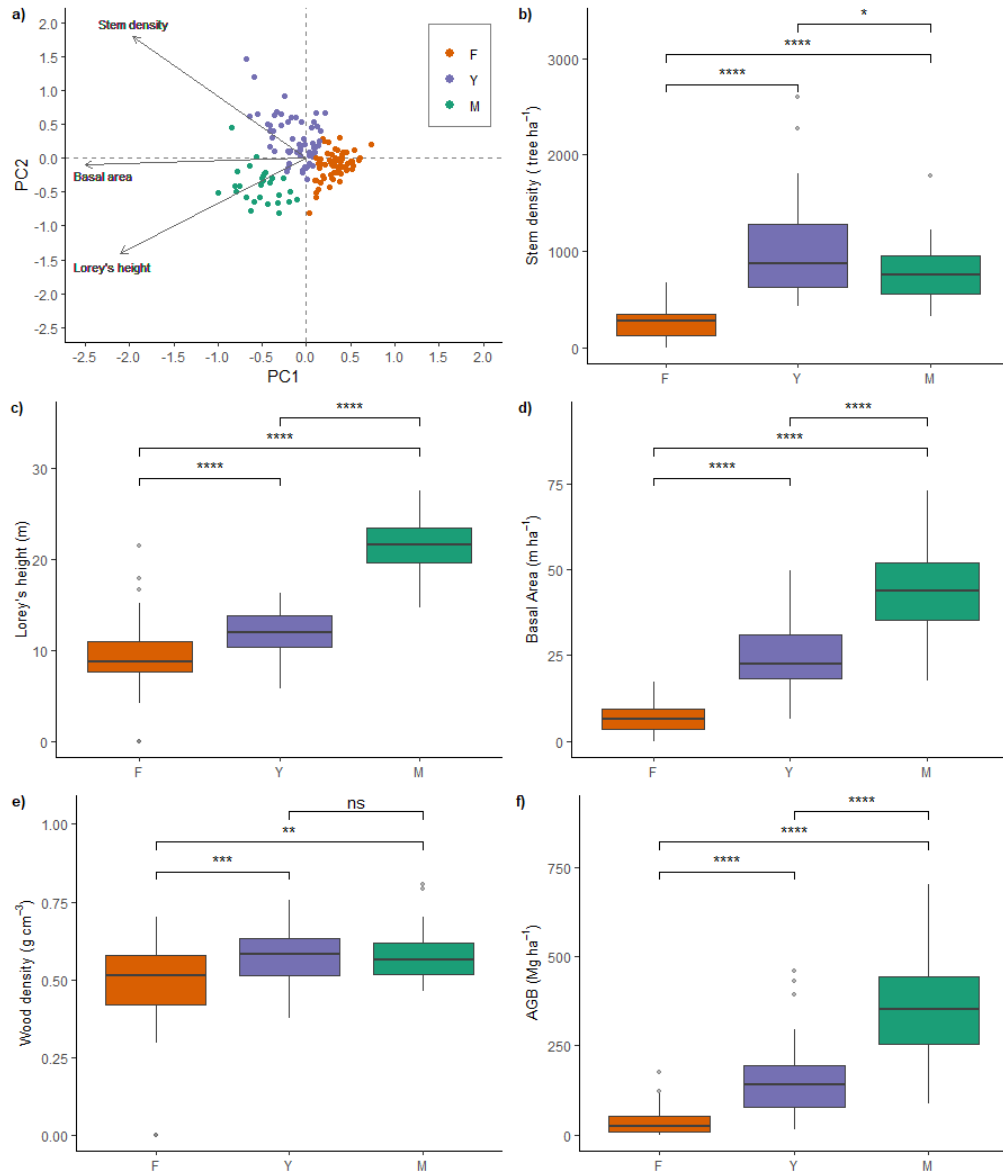
Figure 2.2. a) Results of k-means analysis based on forest structural attributes measured in the field and visualized with a PCA showing three clusters representing young fallows (F, in orange), young forest (Y, in purple), and mature forest (M, in green) in TMCF plots (n= 160). Comparison of b) stem density, c) Lorey's height, d) basal area, e) wood density, and f) aboveground biomass (AGB) between young fallows (F), young forest (Y), and mature forest (M). Boxes cover the interquartile range (IQR), the horizontal line within boxes shows the median, and values 1.5 times larger or smaller than the IQR are shown in dark gray points. Asterisks indicate statistically significant differences resulted from Tukey HSD tests as follows: ****$p < 0.0001$, ***$p < 0.001$, **$p < 0.01$, *$p<0.05$, and ns represents a non-significant difference. Results of ANOVAs and Tukey HSD tests can be found in Table S2.3.

The structural attribute that best explains AGB distribution is basal area (linear regression, $p < 0.001$, adjusted $R^2 = 0.86$, Figure S2.4b). Despite tree height and stem density have a positive relationship with AGB (linear regressions, $p < 0.001$, adjusted $R^2 = 0.47$, and $p < 0.001$, adjusted $R^2 = 0.18$, respectively), larger values show ample variation and data spreads out at the higher end of the curves, resulting in poor linear fits (Figure S2.4). Log-transforming AGB improves data visualization in these cases, highlighting that the relationships of stem density and tree height with AGB in TMCF is not linear (Figure 2.3). In fact, plots with the highest stem densities are not the ones showing greater AGB. On the contrary, AGB is greater in plots with stem densities closer to 1,000 trees ha^{-1} (Figure 2.3a). In contrast, the highest trees are found in plots with the greatest AGB, but variation in these plots is large and some show high AGB magnitudes (greater than 400 Mg ha^{-1}) with trees shorter than 20 m (Figure 2.3c). Wood density does not show a clear relationship with AGB, suggesting there are trees with high and low density across all plots (Figure 2.3d). There are not plots with high AGB whose trees show only low wood density, but this trend is probably controlled, at least partially, by the number of trees in each plot.
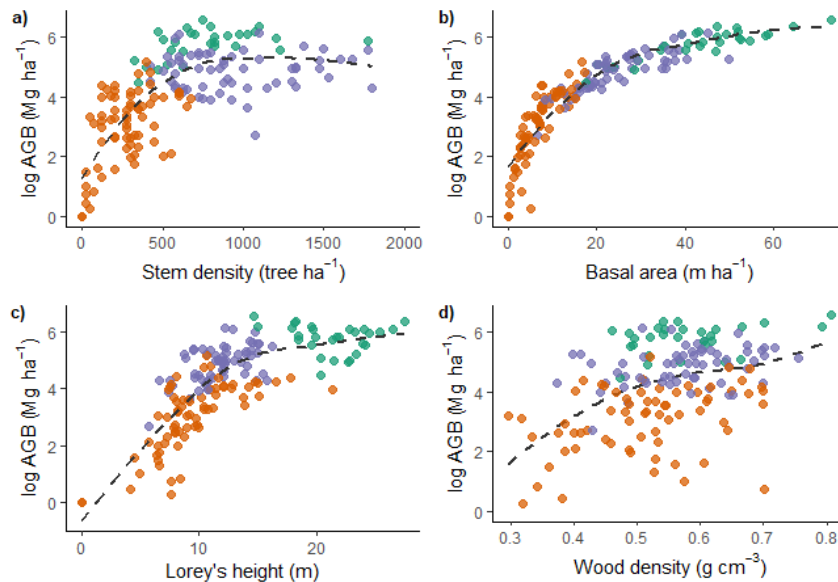
Figure 2.3. Relationship between log-transformed aboveground biomass (log AGB) and (a) stem density, (b) basal area, (c) Lorey's height, and (d) wood density in TMCF plots (n = 160) overlaid by their local regression curves (black dashed lines). Forest successional stage in plots is displayed in colors as follows: young fallows (F) in orange, young (Y) in purple, and mature (M) forests in green.

In these landscapes there is a large proportion of small trees (DBH < 20 cm), and trees with a DBH greater than 30 cm are uncommon (Figure S2.5a and Table S2.4). In most plots, trees between 10 and 20 cm of DBH represent almost 50% of the total number of trees. In contrast, trees with a DBH larger than 50 cm were found only in 51 out of 160 plots. When present, these large trees rarely account for more than 10% of the total number of trees. Despite their lower abundance, large trees contribute the most to total AGB, particularly the largest ones (DBH > 50 cm, Figure S2.5b and Table S2.4). Interestingly, this pattern changes in forest plots at different successional stages. The two-way ANOVAs on tree size contribution to stem density and AGB show that both size class and successional stage are statistically significant, as well as the interaction between them (Table S2.5 and Figure S2.6). Although the proportion of stems across tree size classes remains somewhat constant between young fallows, young forests, and mature forests (Figure 2.4a), their contribution to AGB is variable (Figure 2.4b, Table S2.6 and Table S2.7). In mature forests, larger trees (DBH > 50 cm) stand out as the main contributors to total AGB despite their low abundance. However, in young and very young forests the contribution to total AGB is very similar across all size classes. In all cases, small trees (DBH < 10 cm) contribute significantly less to total AGB despite representing a considerable proportion of stem density in all three successional stages, especially in mature forests, where the proportion of AGB represented by the smallest trees barely reaches 1% (Figure 2.4b).

The patterns of tree-size contribution to the total number of stems and AGB in forests at different successional stages can be explained by the progression of structural attributes over time (Figure 2.2). Young fallows have small AGB and small numbers of trees. Thus, the few but large trees that do exist in these plots represent a large proportion of the total amount of AGB (although this is not statistically different from the contribution to AGB by other size classes). In young forests the number of large trees is also small, but stem density in general is higher than in young fallows. Because there are many small-to-medium trees in young forests, they represent the greatest portion of AGB, and very large trees do not stand out as significant contributors to total AGB. In contrast, in mature forests the number of trees is lower but larger trees are more common, and thus larger trees stand out as the main contributors to AGB there (Figure 2.4).
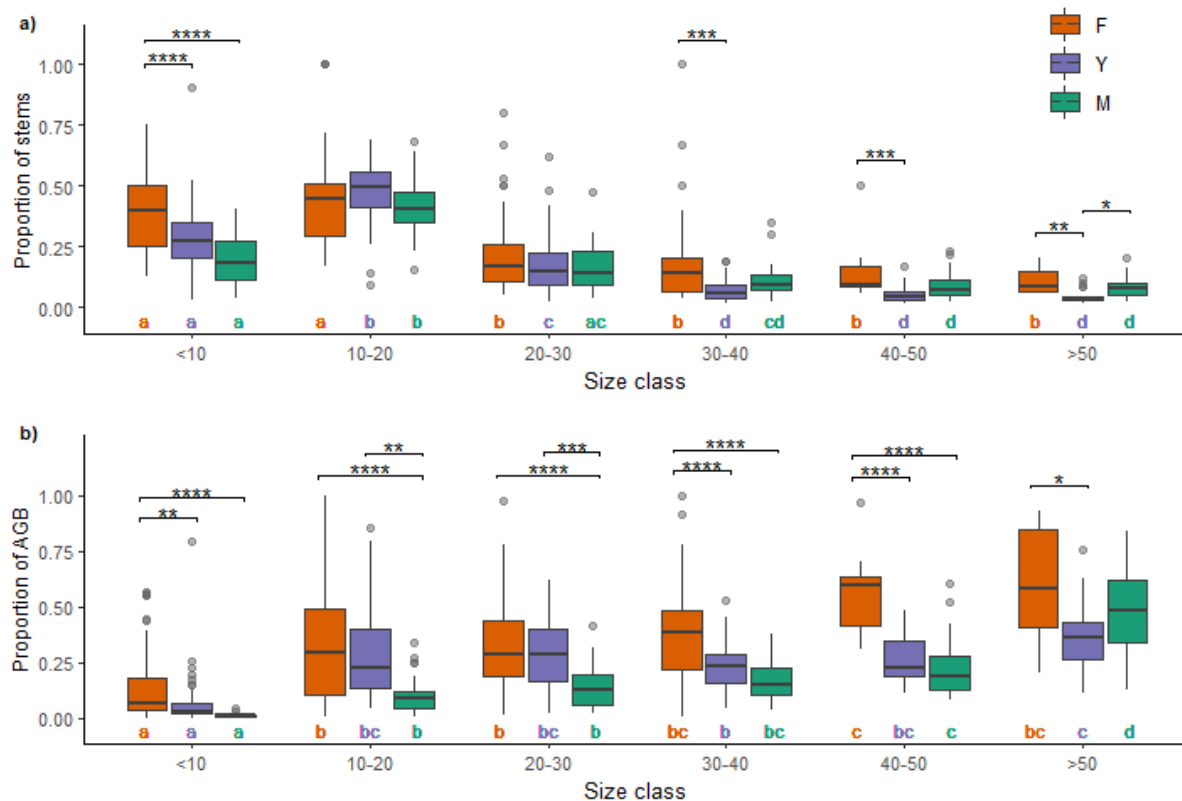
Figure 2.4. Contribution of tree size categories to a) stem density and b) aboveground biomass (AGB) in young fallows (F, shown in orange), young forest (Y, shown in purple), and mature forest (M, shown in green) plots in TMCF (n= 160). Trees were categorized in six size classes based on their DBH. Boxes cover the interquartile range (IQR), the horizontal line within boxes shows the median, and values 1.5 times larger or smaller than the IQR are shown in dark gray points. Asterisks indicate statistically significant differences between forests at different successional stages within each tree size class tested with one-way ANOVAs and Tukey tests (results shown in Table S2.6). Statistical significance: ****$p < 0.0001$, ***$p < 0.001$, **$p < 0.01$, *$p<0.05$. Non-significant differences are not shown. Letters indicate statistically significant differences between tree size classes within young fallows (F, shown in orange), young forest (Y, shown in purple), and mature forest (M, shown in green) resulted from one-way ANOVAs and Tukey tests (results shown in Table S2.7). Boxes sharing a letter are not statistically different.

The relationship between AGB and tree diversity is weak and scale-dependent

We found a total of 148 tree species in the region, with *Quercus*, *Saurauia*, and *Pinus* the most abundant genera. We analyzed the relationship between AGB and tree diversity and richness at site and plot levels. Although we were expecting a linear positive relationship between these variables, they show a positive but weak correlation with correlation coefficients near 0.2 and near 0.3 when AGB is log-transformed (Figure S2.2). We tested how AGB changes in relation to tree diversity and richness using Shannon diversity index (H) and species richness (S). Our

42

results show that at site level neither H nor S have a clear relationship with AGB (linear regressions, p= 0.96, R^2= -0.02, and p= 0.24, R^2= 0.01, respectively), even when log-transforming AGB (Figure 2.5a and 2.5b), and none of the linear regressions are statistically significant. When we analyzed the relationship between AGB and tree diversity at plot level, we found a weak but significant positive relationship, especially when using S (Figure 2.5c and 2.5d). In both cases, AGB slightly increases with tree diversity showing statistically significant linear regressions when AGB is log-transformed, although the R^2 in both cases is low (R^2= 0.08 for H and R^2= 0.11 for S). Despite we were expecting a clearer trend between AGB and tree diversity over different successional stages, all three successional stages show wide variation in H and S. Thus, sites with a larger composition of mature forests show greater AGB but not necessarily greater tree diversity, suggesting these two variables follow slightly different trends in forest-agriculture mosaics.
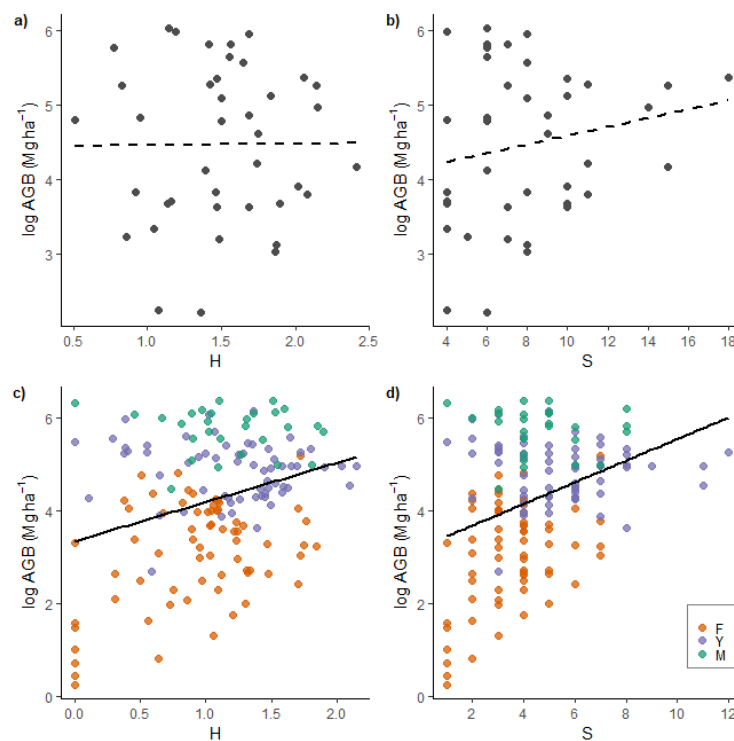
Figure 2.5. Relationship between log-transformed aboveground biomass (log AGB) and Shannon diversity index in TMCF (a) sites (n= 40) and (c) plots (n= 160); and between log AGB and species richness (S) in TMCF (b) sites (n=40) and (d) plots (n= 160), overlaid by their linear regression curves (significant regression: solid line, non-significant regression: dashed line). Forest successional stage in plots is displayed in colors as follows: young fallows (F) in orange, young (Y) in purple, and mature (M) forests in green.

Environmental and land-use gradients: AGB increases with elevation and decreases with land-use intensity

Tree AGB in TMCF sites is controlled mainly by land use, and secondly by environmental factors. Here, we assessed both land use and environmental factors with multiple linear regression models. Through a stepwise model selection process, we found the best model as the one having the lowest BIC, large explanatory power (high R^2), and where all predictors are statistically significant (Table 2.3). The best model includes three variables: land-use intensity gradient, forest disturbance related to agriculture, and slope ($p < 0.05$, adjusted $R^2 = 0.811$, Table 2.4, Figure S2.7). From the three variables, land-use intensity controls AGB the most, showing a strong relationship with AGB (linear regression, $p < 0.001$, adjusted $R^2 = 0.72$, Figure 2.6a). Adding forest disturbance driven by agriculture to the model improves its explanatory power and it seems to be the second most relevant predictor of AGB (Table 2.3). Similarly, adding slope improves the linear regression model and it is the third most relevant variable in all models. However, from the three predictors included in the first model, slope is the least influential in determining AGB patterns in TMCF (Table 2.4). The residuals of this model do not show spatial autocorrelation (Figure S2.7d). We computed Moran's I statistic for neighborhoods of 10, 25, and 50 km of distance and all of them resulted non-significant ($p = 0.517$, $p = 0.604$, $p = 0.187$, respectively, Table S2.8).

The second-best model includes six predictors (Table 2.3). It adds environmental gradient, disturbance by grazing, and Shannon diversity index (H) to the three most relevant predictors included in the first model (i.e., land-use intensity, disturbance by agriculture, and slope). Although this model shows high R^2 and the lowest CP, one of the predictors, H, is only marginally significant and it has a higher BIC value than the best model. Despite adding H to the model improves its explanatory power, both H and S are the least relevant predictors of AGB. This resonates with the weak relationship found between tree diversity and AGB explained in the previous section, and it is supported by the dissimilar behavior shown by land-use intensity in relation to AGB and H (Figure 2.6), where land-use intensity and AGB are strongly correlated ($p < 0.001$, adjusted $R^2 = 0.72$) but land-use intensity and H are not ($p = 0.70$, adjusted $R^2 = -0.02$).

44

Table 2.3. Results of stepwise model selection process comparing seven multiple linear regression models of aboveground biomass as a function of land-use, environmental, and species diversity and richness variables. Shown are the number of predictors considered in each model ordered from most to least relevant (top to bottom), as well as their statistical significance (***p < 0.001, **p < 0.01, *p<0.05, ∘p<0.10), adjusted R^2, Mallows' C_p (CP), and *Bayesian Information Criterion* (BIC). Shown in bold are the highest adjusted R^2, and lowest CP and BIC.

Predictors	Number of predictors considered in the model						
	1	2	3	4	5	6	7
Land-use intensity	***	***	***	***	***	***	***
Disturbance by agriculture		**	**	***	***	***	***
Slope			**	*	**	**	**
Environmental gradient				0.16	0.13	*	0.10
Disturbance by grazing					0.16	*	*
Shannon diversity index						∘	∘
Species richness							0.30
Adjusted R^2	0.729	0.769	0.811	0.816	0.821	0.833	**0.834**
CP	26.089	17.600	8.928	8.746	8.606	**7.089**	8.000
BIC	-45.958	-49.672	**-55.251**	-53.753	-52.336	-52.689	-50.339

Table 2.4. Results of the multiple linear regression selected as the best model to explain aboveground biomass patterns in TMCF. This model includes three predictors: slope, land-use intensity gradient, and disturbance by agricultural activities.

Variable	Coefficient	S.E.	t	p
Slope	0.027	0.009	3.064	0.004 **
Land-use intensity	-2.425	0.266	-9.088	< 0.001 ***
Disturbance by agriculture	-0.279	0.080	-3.478	0.001 **
b= 5.406; F= 57.07; df (3, 36); p < 0.001; adjusted R^2= 0.811				
***p < 0.001, **p < 0.01, *p<0.05, ∘p<0.10				
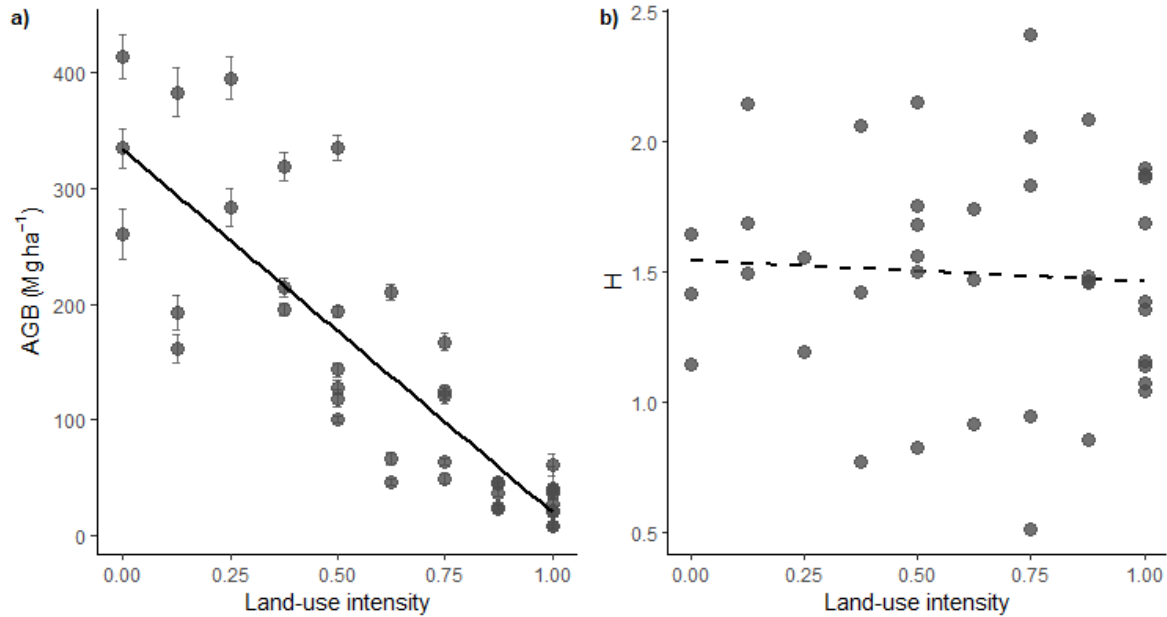
Figure 2.6. Relationship of land-use intensity with a) aboveground biomass (mean ± SE) and b) tree diversity estimated with Shannon diversity index (H) in TMCF sites (n= 40) overlaid by their linear regression curves (significant regression: solid line, non-significant regression: dashed line). Landscapes dominated by mature forests are at the lower end of the land-use intensity gradient and those dominated by fallows and young forests have high land-use intensity values. See text for details on how the land-use intensity gradient was calculated.

Interestingly, environmental gradient (which comprises temperature, precipitation, and elevation) is not included as a relevant predictor in the best model. Although the second-best model does include environmental gradient, this variable does not seem to fundamentally control AGB in TMCF landscapes within the region and it is significant only when disturbance by grazing and tree diversity are also included (Table 2.3). The environmental gradient variable has a statistically significant relationship with AGB ($p < 0.05$, adjusted $R^2 = 0.185$, Figure 2.7a) where warmer and more humid sites at lower elevations (closer to 1,000 m asl) exhibit smaller AGB than sites at higher elevations that have a relatively cooler and drier climate. Additionally, this environmental gradient is related to the land-use intensity gradient. Sites at lower elevations show larger land use and forest disturbance than sites at higher elevations ($p < 0.05$, adjusted $R^2 = 0.372$, Figure 2.7b). The fact that land use exerts a strong effect on AGB, in addition to be related to the environmental gradient, results in the latter being only marginally relevant when both predictors are considered.
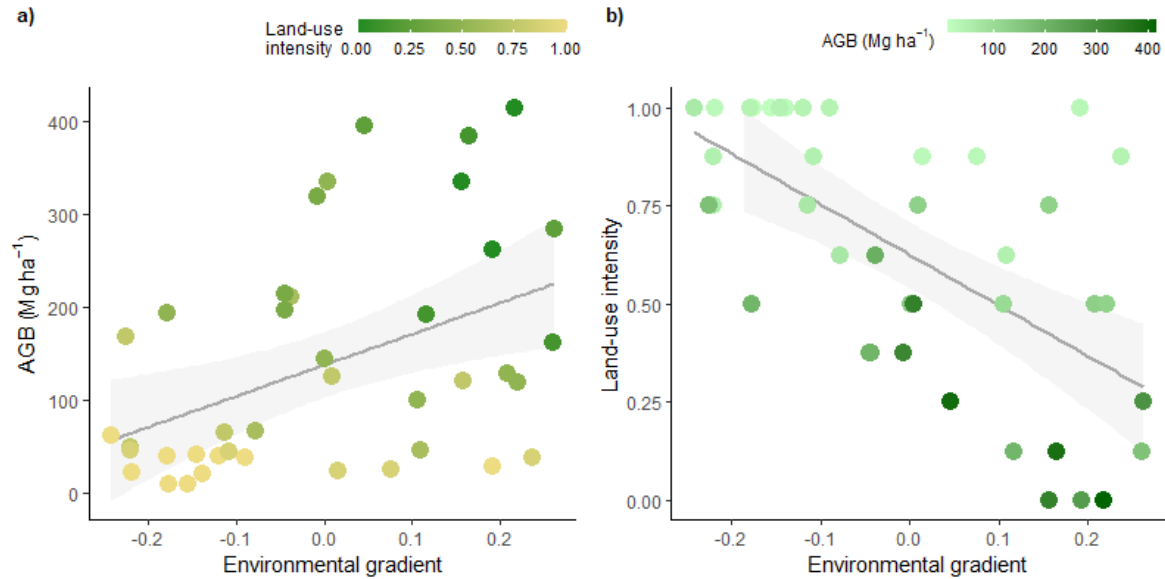
Figure 2.7. Linear regression curves between a) aboveground biomass (AGB) ($p < 0.05$, adjusted $R^2 = 0.185$), and b) land-use intensity ($p < 0.05$, adjusted $R^2 = 0.372$) as a factor of environmental gradient in TMCF sites (n= 40) overlaid by their linear regression with 0.95 confidence interval (gray line). Negative values in the environmental gradient show warmer and more humid sites at lower elevations and positive values represent cooler and drier sites at higher elevations. See text for details on how the environmental gradient variable was calculated.

DISCUSSION

Tropical forests represent 64% of the total AGB stored in forests around the globe (Santoro et al. 2021). Although most of it is in lowland tropical forests, large amounts of AGB have also been estimated in tropical mountains (Spracklen and Righelato 2014). In Mexico, TMCF covers 1.8 million hectares, representing 1.8% of the total forest area in the country (CONAFOR 2018). Although studying AGB is undoubtedly relevant, it has not been thoroughly examined in this ecosystem. Using the Mexican FI data collected from 2009 to 2014, we estimated AGB in a TMCF region in southern Mexico to understand the magnitude and distribution of AGB in these forests, as well as its relationship to tree diversity, environmental factors, and land use. We focused on the NMO, which harbor the largest and most continuous area of TMCF in the country, and where forest conservation is considered a critical priority (Toledo-Aceves et al. 2011).

The magnitude of AGB across TMCF around the globe ranges from 77 to 785 Mg ha^{-1} (Spracklen and Righelato 2014). This wide range stems mainly from the natural variation found in this ecosystem, but part of it can also be attributed to methodological approaches for

estimating AGB. Natural variation in AGB is given by forest composition and environmental variables such as elevation, precipitation, and soil nutrients, the age of forest stands as well as the effect of forest management and the amount of forest disturbance present in each site (C. A. J. Girardin et al. 2010; Marshall et al. 2012; D. B. Clark, Hurtado, and Saatchi 2015; Xia et al. 2019; Ali et al. 2019; Y Malhi, Baldocchi, and Jarvis 1999). Additionally, methodological decisions can also increase the variation found in AGB estimates. For instance, different fieldwork sampling designs, including the size and location of plots, and allometric equations selected to estimate AGB may yield slightly different results (D. B. Clark, Hurtado, and Saatchi 2015; Jerome Chave et al. 2004; van Breugel et al. 2011; Burt et al. 2020; Feldpausch et al. 2012). Here, we approached these challenges by (1) analyzing AGB patterns across environmental gradients, (2) calculating the successional stage of all plots analyzed, (3) using a structured nested sampling design to avoid biases during the establishment of plots, cover a wide spectrum of locations, and diminish scale-dependent errors, and (4) using allometric equations explicitly designed for the trees and ecosystem under study and, when specific equations were unavailable, complementing with a well-tested generic equation as well as considering error propagation in our final estimates.

AGB magnitude and distribution in TMCF of the NMO

The sites we studied consist of heterogeneous landscapes where forest patches are interspersed with agricultural and grazing lands, as commonly found in tropical forests (Yadvinder Malhi et al. 2014; Gardner et al. 2009; I Perfecto, Vandermeer, and Wright 2009). Thus, sites show a variety of landscape compositions from those dominated by mature forest to those mostly covered by young fallows, shifting agriculture, coffee farms, and grazing lands. Consequently, AGB values in the 40 sites studied are highly variable. Average AGB is 137.49 ± 121.29 Mg ha^{-1} falling within the range found by Spracklen and Righelato (2014) for TMCF around the globe, although slightly lower than the average value they report for this ecosystem in the neotropics (247 Mg ha^{-1}). In comparison to AGB estimates reported in pan-tropical maps, our results are in line with Santoro et al's (2021) and Avitabile et al's (2012) values for the region, but lower than those in Saatchi et al's (2011). When compared to AGB estimates in TMCF in Mexico, our results agree with those found by Álvarez-Arteaga et al. (2013) and Vizcaíno-Bravo et al. (2020). However, our AGB estimate is higher than the average value reported in the FI results for TMCF at the national level, where TMCF averages 75.41 Mg ha^{-1} (CONAFOR 2018). This discrepancy

can be surprising at first because our estimates were calculated from a subset of the FI data set. However, it is probable that TMCF in the NMO contains larger amounts of AGB than other TMCF in the country. For instance, the difference between AGB measured in TMCF within the NMO by Álvarez-Arteaga et al. (2013) (an average of about 278 Mg ha^{-1}) and that obtained by (Leija-Loredo et al. 2018) in Hidalgo, Mexico, (29 Mg ha^{-1} on average) is significant. It is important to note that forests at different successional stages are not distinguished in the FI national averages reported by vegetation type, nor are land use intensity or other types of disturbance considered. Thus, the inclusion of disturbed forest sites could lower FI's national AGB average for TMCF, placing it at the lower end of the pantropical range.

Here, we found that average AGB changes in forest plots at different successional stages. In mature forest (n= 29), AGB averages 354.86 Mg ha^{-1} which is closer to Saatchi et al's (2011) estimate for the region and higher than AGB estimates found by Spracklen and Righelato (2014) in neotropical montane forests. In contrast, young forests (n= 62) show an average AGB of 151.69 Mg ha^{-1}. Other studies that have analyzed the difference in AGB between mature forests and forest in secondary succession usually find greater AGB in the former (Aragón et al. 2021), although this difference is not always statistically significant (e.g., Vizcaíno-Bravo et al. (2020)) and depends heavily on forest stand age (Requena Suarez et al. 2019). These results show that forests in secondary succession can sequester carbon in large quantities, highlighting their ecological significance (L Poorter et al. 2016). On the one hand, AGB in secondary forests, if allowed, will only increase until these forests grow to maturity or are disturbed again (R. Chazdon 2003; Cook-Patton et al. 2020; Silver, Ostertag, and Lugo 2000). On the other hand, forests in secondary succession are more common and widespread than mature forests and thus they represent a large part of the total biomass (Yadvinder Malhi et al. 2014). For instance, we found that both mature and young forests represent similar amounts of the total AGB measured in these sites because 82% of plots are in secondary succession. This probably holds true for other TMCF in the country given 54% of this ecosystem is classified as secondary forest (CONAFOR 2018). Thus, our results underscore the potential of secondary forests to store carbon in the future and their current relevance as a main component of total biomass.

The magnitude of AGB and its variation is defined mostly by forest structural attributes. The structural attributes studied here, including basal area, stem density, and tree height, are within the range found in other Mexican TMCF structure analyses (e.g. (Mejía, Meave, and Ruiz

2004; Meave et al. 1992; Arellanes Cancino 2000; Ruiz-Jiménez, Meave, and Contreras-Jiménez 1999; Williams-Linera 1991). The forest structural attribute that better explains AGB patterns in the study region is basal area. Although both tree height and stem density increase with higher AGB, they show high variability in sites with higher AGB values. In contrast, basal area has a tight relationship with AGB. This is at odds with the findings of studies conducted in other neotropical montane forests, where tree height has shown a closer relationship to AGB to the one found here (G. P. Asner et al. 2014; C. A. J. Girardin et al. 2010), but coincides with studies in Kenyan TMCF and Borneo's and northern South America's tropical forests where basal area and the density of largest trees seem to control AGB patterns (Cuni-Sanchez et al. 2017; Slik et al. 2010; Álvarez-Dávila et al. 2017). Tree density has a strong relation to AGB in montane tropical forests in eastern Democratic Republic of Congo (Imani et al. 2017), but this is not the case for TMCF in the studied area where sites with the highest density of trees are not the ones showing higher AGB. As in African tropical montane forests and Brazilian subtropical forests, the density of largest trees in our study region is a main contributor to total AGB (Cuni-Sanchez et al. 2021; Bordin et al. 2021). Despite large trees are uncommon and represent a small proportion of all trees present in a site, they account for most of the AGB measured. This is particularly important in mature forests, although young forests and young fallows show a similar pattern. Nevertheless, in forests in secondary succession trees of different size are equally relevant for accounting to the total biomass of a site.

Relationship between AGB and tree diversity

Although a positive relationship between AGB and tree diversity has been found in tropical forests (Arasa-Gisbert et al. 2018; L. Poorter et al. 2015; Vizcaíno-Bravo, Williams-Linera, and Asbjornsen 2020; Kothandaraman et al. 2020; Cavanaugh et al. 2014), we did not find it in our data. The relationship between AGB and tree diversity has been explored in tropical forests, partly because biodiversity and carbon storage are two fundamental ecosystem features that are under significant pressure due to current global environmental change (Rockström et al. 2009; Dinerstein et al. 2020). Here, statistically significant relationships between tree diversity and AGB were found only after log-transforming AGB and at plot level, suggesting that this relationship may be scale-dependent, weakening at larger spatial scales as other studies have pointed out (L. Poorter et al. 2015; Sullivan et al. 2017). Moreover, our results show a clearer relationship between AGB and tree diversity when species richness is used instead of Shannon

diversity index. Lack of a meaningful relationship between tree diversity and biomass has been found in other studies (Bordin et al. 2021; Cuni-Sanchez et al. 2017; Sullivan et al. 2017), where tree diversity does not increase in plots with higher AGB. It is probable that a synergistic relationship between carbon storage and biodiversity could be better explored with other indices such as rarefied species or focusing on functional instead of taxonomic diversity (Lourens Poorter et al. 2017; Shen et al. 2016). No doubt forest structure, composition, and function are interrelated, but more research is needed to understand how these relationships operate in TMCF as well as how they are influenced by environmental factors and land use.

Patterns of AGB along land-use and environmental gradients

From all factors analyzed in this study, land use and forest disturbance represented the most influential ones on AGB patterns across the region, even overshadowing the effect of climate and topography. This does not mean climate and topography have no effect on AGB as ample evidence suggest they do (Marshall et al. 2012; Spracklen and Righelato 2014; Cleveland et al. 2011; Hofhansl et al. 2015; Lewis et al. 2013; Taylor et al. 2017; Moser et al. 2008), rather, our results show that AGB patterns are driven by the compounding effect of environmental and land use factors where the relative role of land use is larger than that of the environment.

In our study area, both precipitation and temperature decrease with elevation creating an environmental gradient that has a significant relationship with AGB. AGB increases with elevation, contradicting the general expectation of AGB declining with elevation driven by cooler temperatures (Gregory P. Asner et al. 2009; Raich et al. 2006). Our findings are in line with other studies showing more complex AGB patterns along elevation transects, for instance, where AGB exhibits a unimodal distribution along elevation (i.e., higher AGB at mid-elevation), a bimodal distribution (i.e., higher AGB at the lowest and highest elevations with a dip in between), or no relation at all (de la Cruz-Amo et al. 2020; Imani et al. 2017; Álvarez-Arteaga et al. 2013; Marshall et al. 2012). Furthermore, our results agree with Alvarez-Arteaga et al.'s (2013) study where the highest AGB in TMCF within the NMO was found at 2,500 m asl. It is possible that the relationship between AGB and elevation changes according to the length of the elevation transect. For instance, here, we are only covering forests located between 1,000-2,800 m asl, and although this is a long transect, we cannot rule out the possibility that the relationship between AGB and elevation could change if we expand the altitudinal range to include sites in neighboring ecosystems at lower and higher elevations. If anything, these changes would only

underscore the complex relationship between forest structure, AGB, and elevation gradients (D. B. Clark, Hurtado, and Saatchi 2015).

Our results support the claim that upper montane sites can hold large amounts of AGB in spite of experiencing lower temperatures than their lowland counterparts (Cuni-Sanchez et al. 2021; Spracklen and Righelato 2014) while also suggesting that environmental factors other than temperature may be controlling AGB patterns in the study area (Clark et al., 2015). In fact, precipitation seems to be exerting a larger effect on AGB than temperature and could explain the lower values of AGB in lower and wetter sites. In contrast to temperature, that usually relates linearly to productivity, rainfall shows a humped relationship with productivity probably due to soil saturation limiting plant growth in places with very high precipitation (Taylor et al. 2017; Álvarez-Dávila et al. 2017). Indeed, soils in TMCF, including those studied in the NMO, are relatively acidic, waterlogged, and anaerobic (Roman, Scatena, and Bruijnzeel 2011; Álvarez Arteaga et al. 2008), all features that can lead to nutrient limitation and, consequently, to low aboveground primary productivity (Benner, Vitousek, and Ostertag 2011; Fahey, Sherman, and Tanner 2016).

In agreement with other studies assessing the role of topography on AGB patterns, here, we found that slope is a relevant factor in shaping biomass spatial distribution in TMCF (Arasa-Gisbert et al., 2018; Marshall et al., 2012). Slope steepness influences soil properties in several ways. Steep slopes exhibit soil erosion, influencing nutrients distribution and leaching, and negatively affecting tree growth and biomass accumulation (Marshall et al. 2012; Tsui, Chen, and Hsieh 2004). However, shallow slopes can result in poorly drained terrain causing nutrient limitations, especially in places with very high precipitation as noted above (Gregory P. Asner et al. 2009). Although our results support the latter process is occurring in our study region given the small but significant positive relationship between slope and AGB in combination with the very high precipitation levels in lower elevation sites, more research is needed to fully understand how precipitation and topography interact in these montane forests. These results suggest that factors such as soil nutrients, seasonality, microclimate, and topography may be more influential in controlling AGB patterns in the region than mean annual temperature and deserve more attention (Cuni-Sanchez et al. 2021; Marshall et al. 2012; Álvarez-Arteaga et al. 2013; Fisher et al. 2013; Álvarez-Dávila et al. 2017).

Besides the influence that the environment exerts on AGB patterns, forest disturbance and land use also change along elevation gradients and can reinforce, mask, or shift the effect of environmental factors (Marshall et al. 2012; de la Cruz-Amo et al. 2020). In our study, land use seems to reinforce the effect of the environmental gradient because sites experiencing stronger land-use intensity are located at lower elevations. Additionally, slope steepness plays a role in land use patterns as the probability of forest conversion to agricultural and grazing lands is lower in very steep slopes (Mendoza-Ponce et al. 2018), which could further reinforce the small but positive effect slope has on AGB in the region, showing yet another interaction between land use and environmental factors. Remarkably, regardless of the interactions that could exist between land use and environmental variables, land use by itself exerts the largest influence on AGB spatial distribution at both local and regional scales. At the plot level, forest stands are differentiated by the successional stage in which they are found, showing significant differences in their structural attributes and AGB content; at the site level, AGB is determined by the composition of the landscape where AGB values from as low as 36 to as high as 485 Mg ha^{-1} can be found within a single one-ha landscape due to the coexistence of young fallows, young and mature forests; at the regional level, the amount of land use across the landscape gives place to a pattern characterized by sites at lower elevations exhibiting lower AGB because land use is more widespread, and higher elevation sites with a tendency to present a larger composition of mature and secondary forests exhibiting greater AGB.

The effect of forest disturbance and land use on carbon stocks in general, and AGB in particular, has been acknowledged and studied for a long time at local (e.g., Aragón et al., 2021; Vizcaíno-Bravo et al., 2020), regional (e.g., Cuni-Sanchez et al., 2021; Marshall et al., 2012), and global scales (e.g., K. H. Erb et al., 2018). In all cases, research has found that land use reduces AGB because it implies the removal of forests for the establishment of other land covers with a smaller capacity to accumulate biomass, such as grasses and crops. Here, we took a landscape approach based on forest properties to assess land use and assumed that a larger composition of young fallows and young forests in the landscape is directly linked to higher land-use intensity (Tscharntke et al. 2005). Certainly, we found a linear decline of AGB along our land-use intensity gradient. Nevertheless, it is important to note that there are several approaches to study the effects of land use on ecosystem structure and function, and other features of land use not explored here, such as land-use history, inputs used, and landscape

configuration, can greatly influence AGB distribution across space in nonlinear and unexpected ways (K.-H. Erb et al. 2013; del Castillo 2015; R. Chazdon 2003; Kauffman, Hughes, and Heider 2009; Melito, Metzger, and de Oliveira 2018). For instance, in TMCF in Peru, biomass recovery rates are slower than expected after agroforestry lands are abandoned, suggesting a negative legacy effect on secondary succession (Aragón et al. 2021). In TMCF in the NMO, in contrast, small-scale disturbance caused by shifting agriculture reduces soil acidity and promotes the establishment of pioneer and generalist species, increasing biodiversity and facilitating a fastest recovery across the landscape, suggesting this type of land use plays a relevant role in this ecosystem dynamics (Velasco-Murguía et al. 2021). Understanding how different types of land use influence forest structure and composition across scales is paramount for improving AGB estimates.

The relationship between AGB and land use that we present here establishes a baseline for AGB estimates in the region that provides a general idea of the amount of biomass that these landscapes currently and can potentially accumulate. A thorough understanding of the effect of land use on AGB could, on the one hand, reduce the uncertainty found in the quantification of carbon stocks and emissions associated to land use and land cover change in the tropics. On the other, this knowledge could broaden the understanding of these landscapes potential to store carbon, which is fundamental for suggesting landscape management strategies aimed at sequestering carbon. Finally, studies like this one can help shed light on the problem of conserving ecosystem services while producing food in carbon and biodiversity rich places where agriculture represents a fundamental cultural heritage and the main source of income for their inhabitants, as in the case of tropical mountains.

CONCLUSIONS AND BRIDGE

TMCF in the NMO hold large amounts of AGB, mainly in mature forests but also in forests in secondary succession. AGB magnitude in mature forests is larger than expected but it fits within the reported values for this ecosystem if forests at different successional stages (including young fallows) are considered. AGB is determined by forest structural attributes, particularly by total basal area and the presence of large trees (DBH > 50cm). The relationship between AGB and tree diversity was week, unclear, and scale-dependent. More research is needed to explore whether a stronger relationship between these two ecosystem features can be found using other

diversity indices or functional instead of taxonomic diversity, as well as how this relationship changes across spatial scales.

AGB in TMCF within NMO increases with elevation. Although we were expecting to find shorter trees, lower stem density, and lower AGB as elevation increased as has been described in tropical montane forests in South America, we found the opposite trend. Furthermore, our results show that AGB patterns are influenced by the compounding effects of land use and environmental factors, where land use has a larger role. Although environmental factors such as temperature, precipitation, and slope seem to influence forest biomass in the region, their effect is weak. Analyzing other environmental factors (e.g., soil nutrients and seasonality) and studying a larger elevation gradient that includes other types of ecosystems could shed more light on the role of the environment in shaping AGB patterns in the region. The influence of land use on AGB is significant, larger than expected, and is not constrained to local scales. On the contrary, land use shapes AGB patterns at landscape and regional scales. Our results highlight the fundamental need of studying the effect of land use across scales to better understand patterns of AGB in the tropics and suggest landscape management strategies that attain the dual goal of producing food in a sustainable way while sequestering carbon and protecting biodiversity.

In the next chapter I further explore the effects of land use on forest structure as well as novel methods to incorporate such effects in AGB models. To do so, I use remote sensing imagery to analyze recent small-scale forest disturbance in vegetation cover change and variability.

CHAPTER 3

INCORPORATING RECENT LAND USE IN REGIONAL MODELS OF
ABOVEGROUND BIOMASS OF TROPICAL MONTANE FORESTS

INTRODUCTION

Despite the large amount of evidence showing that land in most tropical forests is or has been used by humans, little attention has been given to the role that land use plays in shaping the spatial distribution of aboveground biomass (AGB), defined as the dry mass of living trees above the ground (K. H. Erb et al. 2018; Grantham et al. 2020). This shortcoming has permeated the very important efforts of mapping AGB at regional and global scales (e.g., (Saatchi et al. 2011; Avitabile et al. 2016; Cartus et al. 2014; Santoro et al. 2021)). AGB maps rely on remote sensing (RS) data to develop predictive models that are both fed by and validated with field observations (Laura Duncanson et al. 2021). In this process, a combination of passive and active RS is used to classify vegetation types and capture information on forest structure (Avitabile et al. 2016). Although undoubtedly powerful and useful, these approaches fail to explicitly consider land use in the modeling process. Ironically, one of the main applications of AGB maps is to measure future carbon flux to the atmosphere from land-use and land-cover change (LULCC) (e.g., (Baccini et al. 2017).

Common inputs to AGB models include: Light Detection and Ranging (Lidar) measurements (usually translated into canopy forest height models), normalized difference vegetation index (NDVI), annual averages derived from optical RS satellites (such as MODIS and Landsat), and topography products like the Shuttle Radar Topography Mission (SRTM) digital elevation data, among others (Laura Duncanson et al. 2021; Goetz et al. 2009). It could be argued that several of the RS products used as inputs implicitly consider land use. For instance, a forest canopy height model derived from Lidar is influenced by land use because forest structure (including tree height) is regulated by the progressive stages of secondary succession after disturbance (Guariguata and Ostertag 2001). Likewise, a vegetation classification derived from Landsat will include a cropland (or similar) class that can be excluded from the analysis (e.g., (Cartus et al. 2014). However, these approaches are problematic because different land uses can have similar RS signals and thus discarding certain land-cover classes results in a truncated analysis of the distribution of AGB, especially in areas where the limits between cropland and

56

forest are diffuse, as in agroforestry systems and forest-agriculture mosaics (Mercier et al. 2019; Mateo-Vega, Arroyo-Mora, and Potvin 2019). For example, a shaded coffee farm in a tropical mountain will have a very similar canopy height than its surrounding forest, but different AGB (Ensslin et al. 2015). If, however, it is categorized as cropland and excluded from the analysis, the role of trees and shrubs kept in agricultural lands, which could store a vast amount of carbon, ends up being underestimated (Zomer et al. 2016). Given the large role that land use plays in shaping carbon storage and distribution, we contend that it should be explicitly included in AGB models as an input variable, and not only as an *a posteriori* effect.

The neglect of the role of land use in shaping the distribution of AGB stems, in part, from methodological constraints. Assessing land use at a regional level with RS is challenging and requires other sources of information that are not always readily available, or are difficult to collect at large spatial extents (e.g. surveys or records on land management) (Bürgi, Östlund, and Mladenoff 2017). Additionally, LULCC is a complex process exhibiting dynamics occurring at a pace and spatial scale that static land-cover classes do not fully encompass (Kuemmerle et al. 2013; C. F. Brown et al. 2022). This problem is further enhanced by the common (and often inevitable) mismatch between dates of acquisition and processing of the input data (for instance, using field and RS data acquired in different years) (L. Duncanson et al. 2019). Moreover, the relative relevance of the factors influencing AGB distribution changes across scales. For instance, at the global scale, climate is the main control for plant productivity, but at a landscape scale, disturbance history can be a driver as strong as any other environmental factor in shaping AGB spatial patterns (Dahlin, Asner, and Field 2012). Thus, if AGB spatial distribution is mapped with a low-to-medium spatial resolution instrument (e.g., MODIS), the exclusive inclusion of environmental factors in the model could suffice. However, as AGB maps increasingly use medium-to-high spatial resolution data (e.g., Landsat), land use becomes more relevant and cannot be ignored.

Beyond the methodological challenges, disregarding the role of land use also stems from an epistemological issue. Analyses of forest structure, composition, and dynamics are, in many cases, still approached from a 'stability/fragility' paradigm where tropical forests are regarded as pristine and untouched, instead of as dynamic landscapes in constant flux (R. Chazdon 2003; Blanco et al. 2021). Hence, most of the field observations used to scale up AGB estimates come from field plots established in undisturbed forests, likely biasing the process of modeling and

validation across the roughly 53% of forests worldwide that are not considered primary (Gregory P. Asner et al. 2010; R. L. Chazdon et al. 2016; Rozendaal et al. 2022) Studying forests from this 'stability/fragility' framework increases the uncertainty associated to AGB estimates while feeding the idea that only "untouched" forests can store substantial amounts of carbon (Bongers et al. 2015). Therefore, this approach can have important consequences for the development and implementation of policies and landscape management decisions.

Fortunately, both methodological and epistemological limitations can be overcome. In fact, significant progress has been made in RS to improve the quantification of AGB, either through implementing new technologies, such as NASA's Global Ecosystem Dynamics Investigation (GEDI) (Laura Duncanson et al. 2022), better monitoring LULCC (C. F. Brown et al. 2022), or by simply making data more readily available to researchers and the general public (Gorelick et al. 2017). Likewise, important theoretical developments have been made regarding the understanding of forests as dynamic landscapes produced by disturbance, recovery, and resilience, which has been accompanied by a better understanding of the current and historical role of humans in these processes (L Poorter et al. 2016; Kennedy et al. 2014; Bürgi, Östlund, and Mladenoff 2017; Ellis and Ramankutty 2008). The present project is an addition to those efforts. With a focus on tropical mountains, this study explores novel ways to include land use in the analysis and quantification of AGB and its distribution.

Tropical mountains are home to 500 million people, who have used, modified, and in many cases protected montane forest for hundreds to thousands of years (Jackson and Scherr 1995). The main drivers of AGB in tropical mountains are not well understood yet. Studies on forest structure along elevation gradients have arrived at different conclusions about the relative roles climatic, topographic, and historical variables play in shaping the distribution of AGB (D. B. Clark, Hurtado, and Saatchi 2015). The fact that the uncertainty of AGB spatial models increases over steep terrain limits our understanding of biomass accumulation on tropical mountains even further (cf. Saatchi et al. 2011). Monitoring forests and quantifying AGB in montane landscapes is challenging since they are often overcast, which limits the availability of cloud-free imagery (Zhu et al. 2021), and active RS data loses accuracy over rugged terrain (Kutchartt, Pedron, and Pirotti 2022; Pang et al. 2022; Wu et al. 2021). However, tropical montane forests have received more attention recently, partly as a response to an increasing acknowledgement of their carbon sequestration potential, in combination with an increased rate

of forest loss mainly related to upslope expansion and agricultural intensification (Feng et al. 2021; Spracklen and Righelato 2014; Salinas et al. 2021). Spurred by the large amount of high-resolution data that have become available, meaningful developments have been done in the study of tropical montane forests, including improved estimates of AGB and better forest monitoring methods (Spracklen and Righelato 2014; DeVries, Verbesselt, et al. 2015). These studies show that RS analyses of tropical montane forests are feasible despite frequent clouds and rough terrain.

This study seeks to enhance our understanding of the role of small-scale disturbance, driven by land use, in shaping the magnitude and distribution of AGB in tropical mountains. To do so, we focus on the Northern Mountains of Oaxaca (NMO) in Mexico. We use Landsat imagery to extract time series of pixels that overlap with the Mexican National Forest Inventory (FI) plots established and surveyed between 2009 and 2014. We then address the following questions: (1) How can the recent disturbance history of a forest, assessed through Landsat time series, be used to estimate the effect of land use on forest structure? And, in turn, (2) how can these effects be incorporated into AGB models? We focus on Landsat for several reasons. First, Landsat has enough temporal and spatial resolution to detect vegetation cover change and trends linked to the small-scale disturbance caused by land use, even in mountainous regions with frequent cloud cover (DeVries, Verbesselt, et al. 2015). Second, being the program of satellites with the longest record of Earth's surface, Landsat provides the widest temporal window available to infer the effect of land use with RS data (Wulder et al. 2019). Third, clear relationships between optical RS observations and forest structural variables are difficult to establish. Yet, time series have seldom been used for this purpose, an application that has potential and it is worth exploring (Kennedy et al. 2014; Huang et al. 2010). Finally, active RS data over our study region and during the period in which the field data collection was carried out is not as widely available as is passive RS.

In the following sections we describe the two approaches we took for analyzing vegetation cover change through time as proxies of land use: the first one is based on detecting abrupt changes within time series, and the second one is based on the variation of vegetation indices over time. We conclude by providing some recommendations regarding the incorporation of land use in the study of forest structure with RS.

METHODS

Study area and data collection

This study was carried out in the Tropical Montane Cloud Forest (TMCF) located in the NMO (Figure 2.1). Highly dependent on the presence of clouds, this ecosystem is characterized by having a scattered distribution along the mountain range, which has been further exacerbated by a long history of land use. These montane landscapes exhibit patches of forest at different successional stages, shifting agriculture, some permanent agricultural and grazing lands, several types of coffee farms (including sun and shaded coffee), and other types of cash crops, all interspersed, creating a dynamic and complex forest-agriculture mosaic.

To delimit our study area, we used the official map of vegetation and land-use series V published by the National Institute of Statistic and Geography (INEGI) in 2013 (INEGI 2013) as well as the map of cloud forest regions created by Toledo-Aceves et al. (2011) available from the Mexican National Commission of Biodiversity (CONABIO) GeoPortal (CONABIO 2012) (Figure 2.1). Within this area, we selected 284 plots where forest structure was measured by the Mexican National Forest Inventory (FI) during a fieldwork campaign conducted from 2009 to 2014. Along with information on forest structure, we extracted the geographic location and elevation of each plot from the FI database, and we retrieved their slope (in degrees) from NASA's SRTM digital elevation data via Google Earth Engine (GEE) (Farr et al. 2007). In addition, we tracked forest cover trends and change over time for the 284 FI plots by using Landsat time series, where each plot (area= 400 m^2) is contained and represented by a single pixel (area= 900 m^2). To select the 284 pixels corresponding to each FI plot, we used the exact location of FI plots available in the FI database and selected the pixel that would overlap with the plot centroid. This way, we ensured most of the FI plot area is contained within, and represented by, a single Landsat pixel, even though their area, shape, and outline do not match exactly.

Forest structure and aboveground biomass estimation

FI data collection was carried out following a systematic hierarchical nested sampling design with four circular plots of 400 m^2, established in 1 ha circular sites: one in the center of the site, and the other three in a north, southeast, and southwest direction, respectively, at 45.14 m from the central plot (Figure 2.1). All sites were established 25 km apart from each other in a grid-like fashion (CONAFOR 2015). Within each plot, the height, basal area, and diameter at breast height (DBH) of every plant with DBH > 7.5 cm was measured and taxonomically identified.

We derived three structural variables from this information: (1) tree density, i.e., the number of trees per hectare; (2) basal area, defined as the sum of the cross-sectional surface area of trees per hectare; and (3) Lorey's height, which is a measure of forest stand height weighted by its basal area. Then, we estimated the AGB of 7,196 trees measured in the 284 FI plots using 47 allometric equations described at the species or genus levels. For species whose allometric equation has not been described, we used a generic allometric equation developed by Chave et al. (2015) for tropical trees (Table S2.2 and references therein). Following the methodology for estimating AGB carried out in chapter 2, we calculated AGB ± S.D. per plot by adding up the biomass of each individual tree and propagating errors through a Monte Carlo statistical simulation informed by field data and implemented in the R package BIOMASS (Réjou-Méchain et al. 2017). Because tree density, tree height (Lorey's height), basal area, and AGB have a heavily skewed distribution, the former three variables were sqrt-transformed and AGB was log-transformed for all statistical analyses (Figure S3.1).

Landsat time series extraction and cleaning

Using GEE, we extracted 284 Landsat time series, corresponding to 284 FI plots, from atmospherically corrected surface reflectance images acquired by Landsat-5 TM and Landsat-7 ETM+ sensors from 1993 to 2020 (Gorelick et al. 2017; Masek et al. 2006). Although Landsat imagery collection dates back to the 1970s, data of our study region before 1993 is very sparse and impossible to use in time series analyses (Solórzano, Gallardo-Cruz, and Peralta-Carreta 2020; Wulder et al. 2019). Removing clouds and foggy pixels from the time series was particularly important to avoid false forest disturbance detection (i.e., cloudy periods that can be mistakenly interpreted as forest disturbance in the time series). To detect and remove clouds from the time series, we first applied a cloud mask using the CFMask algorithm in GEE (Foga et al. 2017), through which we obtained 91% overall accuracy of ground and cloud pixels. Secondly, we calculated a cloud index (CI) using the blue, green, red, NIR and SWIR bands (Table 3.1) and searched for a threshold value that removed the cloudy pixels that were not eliminated by the cloud mask, while keeping as many ground pixels as possible (Zhai et al. 2018). We found an optimal CI value of 2.8, with which we reached an overall accuracy of 94.4% (Table S3.2). Overall accuracy, commission, and omission errors of cloudy *vs* ground pixels were conducted by selecting and classifying 500 random pixels. Although removing

cloudy pixels decreased the number of observations per time series from an average of 606 to 166, all years were well represented in every plot (Table 3.2).

Table 3.1. Remote sensing indices used in this study. B = blue band, G = green band, R = red band, NIR = near infrared band, SWIR = short-wave infrared band.

Index	Equation	Reference
Cloud Index (CI)	$(NIR+2*SWIR)/(B+G+R)^2$	Zhai et al. 2018
Normalized Difference Vegetation Index (NDVI)	$(NIR-R)/(NIR+R)$	Robinson et al. 2017
Enhanced Vegetation Index (EVI)	$2.5*(NIR-R)/(NIR+6*R-7.5*B+1)$	Jarchow et al. 2018
Normalized Difference Water Index (NDWI)	$(NIR-SWIR)/(NIR+SWIR)$	Gao 1996

To increase the comparability between remote sensing and FI data, we trimmed the end of time series to match the year of field data collection. Field data collection was carried out over a time span of 5 years; thus, some time series are shorter than others. For instance, forest plots where fieldwork data was collected in the year 2009 span a period of only 16 years, but those measured in 2014 cover a 21-year-period. In addition, the time series are irregular (i.e., the number of pixels varies over time and does not follow a regular pattern) and the number of observations varies within and across time series and years. Moreover, within individual time series, there are more observations during the dry season (October to April) and during the years where Landsat-5 TM and Landsat-7 ETM+ overlap (Table 3.2). The number of observations ranges from 58 to 330 across time series, and depends on the geographic location of the FI plot and the year of data collection (Table 3.3). Plots that fall in areas where two Landsat scenes overlap exhibit more observations, but those with more frequent cloud cover have less. In addition, Landsat-7 gaps due to the scan line corrector failure after 2003 increased the irregularity of time series. Despite these challenges, the minimum average number of observations per year over all the time series analyzed is 5.

Table 3.2. Number of observations, mean and S.D. of observations per year in total and in each season (dry or rainy) in 284 FI plots from 1993 to 2014 after cloud removal, and after being trimmed at the end for matching the date of field data collection. Each observation is equivalent to one Landsat pixel.

Year	Total		Dry season		Rainy season	
	No. obs.	Mean obs. ± S.D.	No. obs.	Mean obs. ± S.D.	No. obs.	Mean obs. ± S.D.
1993	3034	10.5±3.96	1765	6.13±2.46	1269	4.39±2.01
1994	3216	11.1±4.36	1804	6.26±2.29	1412	4.92±2.49
1995	2801	9.69±2.90	1507	5.29±1.80	1294	4.56±1.44
1996	2626	9.09±3.85	1637	5.66±2.55	989	3.60±1.73
1997	1972	6.82±3.36	1294	4.48±1.78	678	2.70±1.89
1998	3183	11.0±3.82	2109	7.30±2.19	1074	3.77±2.23
1999	3331	11.5±4.89	1889	6.54±2.55	1442	4.99±2.86
2000	4637	16.0±5.54	2681	9.28±2.48	1956	6.77±3.60
2001	3475	12.0±3.96	1914	6.62±2.67	1561	5.40±1.98
2002	1944	6.85±2.68	1096	3.86±1.04	848	3.27±1.88
2003	1725	6.07±2.06	1210	4.26±1.63	515	1.87±0.88
2004	1443	5.12±2.59	961	3.41±1.39	482	2.13±1.48
2005	1722	6.08±2.06	891	3.15±1.49	831	2.99±1.27
2006	1490	5.27±2.31	870	3.07±1.30	620	2.45±1.46
2007	2136	7.52±2.34	1550	5.48±1.77	581	2.31±1.12
2008	1825	6.36±2.20	1214	4.27±1.54	611	2.18±1.09
2009	2315	8.15±2.78	1322	4.65±1.99	993	3.53±1.30
2010	1891	8.01±2.25	1382	5.86±1.76	509	2.33±0.937
2011	1797	9.82±3.30	1433	7.83±2.58	364	2.12±0.942
2012	885	5.78±2.49	578	3.78±1.47	307	2.27±1.42
2013	452	6.19±2.28	240	3.29±1.64	212	3.03±1.39
2014	183	5.90±2.52	119	3.84±2.30	64	2.21±1.29

To study forest cover trends and change, we calculated three commonly used vegetation indices (VI): Normalized Difference Vegetation Index (NDVI), Enhanced Vegetation Index (EVI), and Normalized Difference Water Index (NDWI) (Table 3.1). These VI have been widely used, alone or in tandem, for analyzing forest cover trends and disturbance (e.g., (DeVries, Verbesselt, et al. 2015; DeVries, Decuyper, et al. 2015; Berveglieri et al. 2021; Wang, Lu, and Haithcoat 2007)). Both NDVI and EVI are sensitive to changes in vegetation greenness, while NDWI is sensitive to changes in liquid water content of tree canopies (Gao 1996).

Recent history of forest disturbance in FI plots

We approached the study of forest disturbance over time in two ways: first, we detected forest clearings using the algorithm Breaks For Additive Seasonal Trend (BFAST) implemented in the

R package BFAST (Verbesselt et al. 2010). Secondly, we calculated several variables associated with the variation of vegetation indices over time, such as mean, standard deviation, and coefficient of variation (Figure 3.2).

BFAST decomposes time series into trend, seasonal, and reminder components, and detects abrupt changes (breakpoints) in the time series trend by fitting the data iteratively to a piecewise linear model. This algorithm also characterizes the magnitude and direction of change, whereby larger breakpoints represent abrupt changes in the vegetation, such as forest clearings (Verbesselt et al., 2010). Here, we applied BFAST to NDVI time series to detect forest disturbance by means of an ordinary least squares-moving sums of residuals model (OLS-MOSUM), with a level of 0.05 and a dummy seasonal trend. To run BFAST, we used untrimmed time series, which included observations from the year 1993 to 2020. Although TMCF has seasonal variation, most of the cloudy pixels removed belonged to the rainy season and thus a seasonal pattern was not discernible in all years (Table 3.2).

Once BFAST was applied to every time series, we recorded the date and magnitude of each breakpoint. We validated breakpoints using Planet high resolution images available from 2016 to the present (Planet Team, 2017). In the 284 time series analyzed, only 13 breakpoints were detected from 2016 to 2021. To produce a larger list of breaks to test, we extracted another 100 NDVI time series, corresponding to 100 pixels (or training points) from a TMCF landscape adjacent to one of the FI plots (Figure S3.2). We then applied BFAST by following the foregoing process. For every breakpoint detected between 2016-2021 in both the training points and the FI plots, we visually examined if a forest clearing truly took place via Planet Explorer high resolution images (Planet Team, 2017). After testing 35 breakpoints, we found that forest clearings occurred when a breakpoint had a magnitude greater than |0.15|, where positive breakpoints were usually preceded by a slow decline of NDVI undetected by BFAST, followed by a fast NDVI increase (Table S3.3). To avoid overestimating forest clearings, we discarded breakpoints with a magnitude smaller than |0.15| and those detected after field data collection. The final breakpoint dataset comprised 189 breakpoints detected in 76 FI plots. Finally, we summarized this information by calculating the total number of breakpoints per plot and the time elapsed between FI data collection and the last breakpoint (hereafter 'time since last disturbance') (Figure 3.1).

Our second approach consisted in calculating NDVI, EVI, and NDWI mean, standard deviation (S.D.), coefficient of variation (C.V.), minimum (min) and maximum (max) values per year and over the entire time series, to grasp the general trend of each time series and its variation within and across years. To obtain measurements of the inter-annual variation of vegetation indices, we averaged annual S.D., C.V., min, and max values. We assumed that smaller values of mean annual S.D. and mean annual C.V. would correspond to more stable plots with less forest cover change, and that higher min and max values would correspond to larger forest cover maintained over time. Finally, we calculated the same metrics for the year of field data collection.

This way, we constructed a data set of variables derived from RS data (hereafter RS variables) comprising the total number of breakpoints, time since last disturbance, and several summary statistics of the time series, including mean annual S.D., mean annual C.V., mean annual min and max values of NDVI, EVI, and NDWI, as well as mean, S.D., C.V., min, and max values of these indices in the entire time series and in the year of field data collection (Figure 3.1). RS variables were calculated using pixel values from 1993 until the year of field data collection.

Figure 3.1 (next page). (A) Example of NDVI time series of a FI plot showing the variables used in this study, where the three vertical black dashed lines represent the breaks detected by BFAST, the solid gray line indicates the date of field data collection, the purple horizontal line represents time since last disturbance (TSLD), horizontal green dotted lines are NDVI mean value and its S.D. (shown also in panel B), and the big triangle represents the minimum NDVI value found in the time series. (B) NDVI time series period showing each year's minimum NDVI value in small triangles (abbreviated as NDVIa min in text), and annual NDVI mean value with its S.D. in gray horizontal lines and boxes (abbreviated in text as NDVIa mean, and NDVIa S.D., respectively). (C) NDVI time series period exemplifies the breakpoint validation process, where Landsat (orange diamonds) and PlanetScope (purple crosses) images were visually inspected to detect abrupt changes in vegetation cover. Satellite images indicate their acquisition date. (D) Landsat-7 true color images (first row), Landsat-7 NDVI images (second row), and PlanetScope images (third row) used to validate breakpoints detected by BFAST for the period shown in panel C. The squares and arrows point to the tracked pixel.

A

B

C

D
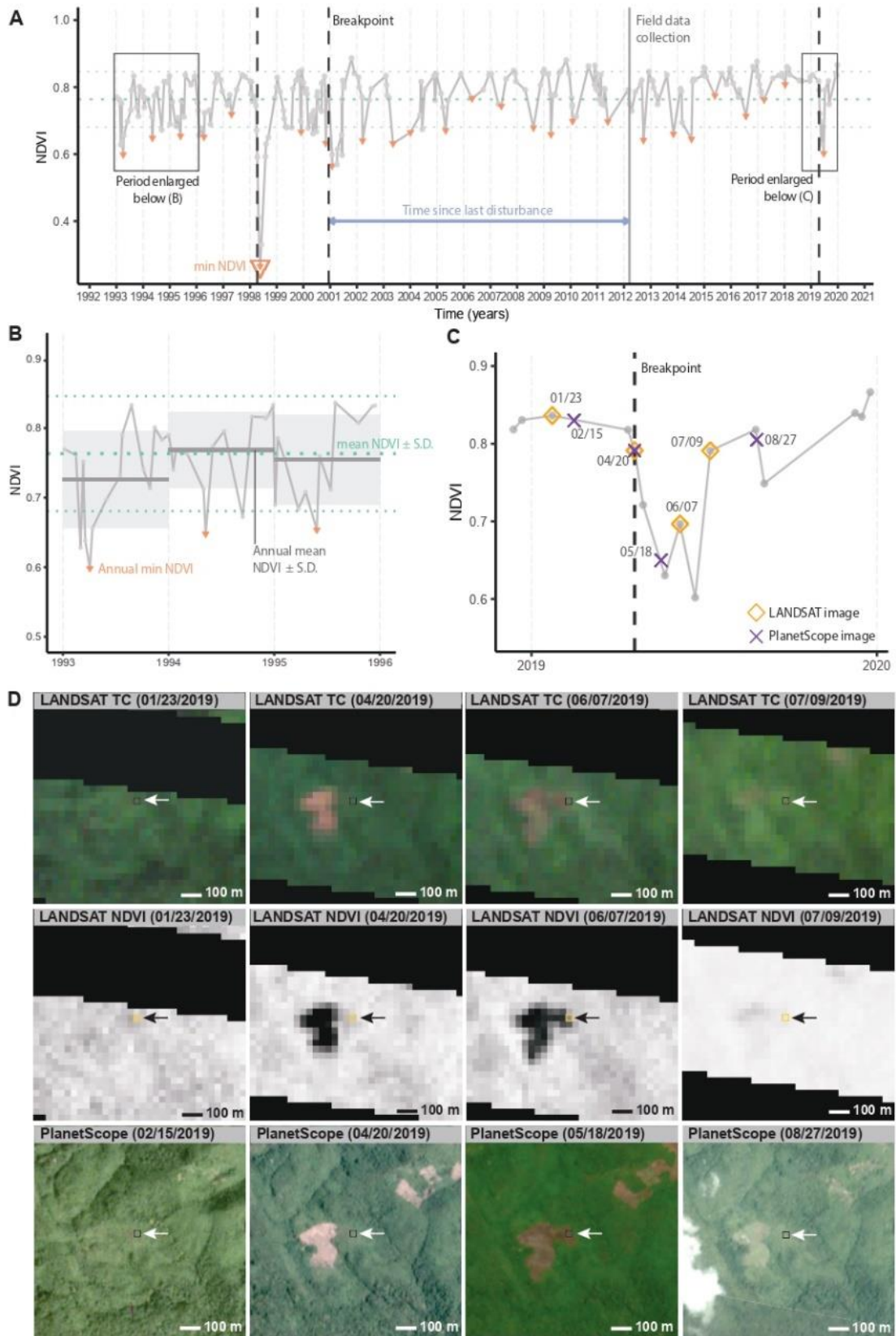
Selection of remote sensing variables

We calculated the correlation coefficient between forest structure variables (tree density and height, basal area, and AGB) and RS variables, and, following a common approach for model exploration, we removed all variables with $\rho < |0.3|$ (Tredennick et al. 2021). Our final RS dataset consisted of 10 variables, including total number of breaks, time since last disturbance (TSLD), average of the annual NDVI S.D. (NDVIa S.D.), NDVI S.D., NDVI minimum value found in the time series (NDVI min), NDVI coefficient of variation, NDWI S.D., NDWI minimum value found in the time series (NDWI min), the average of the minimum yearly values found in the NDWI time series (NDWIa min), and average of the annual NDWI S.D. (NDWIa S.D.) (Figure S3.2).

Statistical analyses

Statistical analyses were conducted at two levels: plots (n= 284) and sites (n= 39) (Figure 2.1). To explore the effect of forest disturbance measured through breakpoints (total number of breakpoints and TSLD) on forest structure, we used data at plot level. We classified plots in two groups according to the presence or absence of breakpoints, and assessed through t-tests whether plots that have had forest clearings in the recent past show differences in forest structure. Additionally, we further analyzed how forest structure variables change over time after the last disturbance, exclusively using the 76 FI plots with breakpoints. We tested the statistical significance of these changes with linear regressions.

To explore whether optical RS variables can improve the predictability of forest structure and AGB, we used multiple linear regression models. This analysis was conducted at site level to avoid spatial autocorrelation and overestimation of forest structure variables measured in small plots (Araza et al. 2022). Thus, we summarized information at site level averaging all variables of every plot within each site. We only used sites where information for all four plots was complete and available (n= 39). To avoid multicollinearity, we removed both RS variables with very high correlation coefficients between them ($\rho > |0.9|$) and which showed a very similar relationship with forest structure variables. We fitted four different models with forest structure and AGB as response variables; and elevation, slope, mean TSLD, most recent value of TSLD found in site, average number of breaks, NDVIa S.D., NDVI S.D., NDVI min, NDWIa min as predictors. Structure variables were transformed to comply with normality. Then, we performed variable selection by comparing a full model, which included all RS variables, against a series of

reduced models in which each predictor is dropped in a stepwise fashion (Lumley, 2020). We selected the best model comparing their adjusted R^2, Mallows' Cp (CP), and Bayesian Information Criterion (BIC). All statistical analyses were performed in R version 4.1.1 (2021).

RESULTS

Forest structure and aboveground biomass in tropical montane cloud forest

FI plots exhibit wide variation in tree density and height, basal area, and AGB (Table 3.3). AGB shows a value of 109.67 Mg ha^{-1}, on average, but some plots reach 700 Mg ha^{-1}, while others are completely devoid of trees, and thus, of living tree biomass. At site level, AGB ranges from 8 to 414 Mg ha^{-1}, showing an average of 120 Mg ha^{-1} (Table 3.4). Tree density in TMCF sites averages 660 ha^{-1} but can reach 1,806 trees ha^{-1}. While there are FI plots within sites with no trees, all 1-ha sites have a tree density of at least 80 trees ha^{-1}. Trees in TMCF are 12 m tall on average. However, Lorey's height max value is 25 m. Basal area ranges from values as low as 1.5 to those as high as 51 m ha^{-1} at site level. From previous studies, we know that forest structural variation in this ecosystem is related to land use, climate, and topography, with the former having the largest role (see chapter 2). Thus, for understanding the relationship between forest structure and disturbance, we used Landsat time series data to detect recent changes in forest cover.

We assessed the recent history of forest disturbance in FI plots using two approaches: (1) detecting forest clearings with BFAST using NDVI time series, and (2) assessing the annual and total variation of NDVI and NDWI values over time.

Landsat time series and selected remote sensing variables

Time series length varied from 16 to 21 years, depending on the year of field data collection. Although time series are irregular, on average, they are composed of 166 observations over time, and all of them have at least five observations per year and 58 observations in total (Table 3.3). We found a total of 189 forest clearings (breakpoints detected with BFAST) in 76 out of 284 plots (i.e., ~27% of all sampled plots). The total number of observations per plot and the effective detection of breakpoints show that the issue of cloud contamination in optical RS imagery can be successfully overcome using a cloud mask in combination with a cloud index.

Table 3.3. Summary statistics of forest structure variables, time series characteristics, and remote sensing variables in TMCF plots (n= 284), showing their minimum (min), mean, and maximum (max) values. Breakpoints represent forest clearings. Abbreviations are: AGB, aboveground biomass; No. obs., number of observations in time series; No. obs. per year, number of observations per year in time series; TSLD, time since last disturbance; NDVIa S.D., mean annual NDVI S.D.; NDVI min, NDVI minimum value found in the time series; NDWIa min, mean annual minimum NDWI. See figure 3.2 for further details on remote sensing variables calculation.

Variable	All plots (n= 284)			Plots with breakpoints (n= 76)			Plots with no breakpoints (n= 208)		
	Min	Mean (±S.D.)	Max	Min	Mean (±S.D.)	Max	Min	Mean (±S.D.)	Max
Tree density (tree ha^{-1})	0	592.95 (541.47)	2600	0	530 (205)	2175	0	616 (431)	2600
Lorey's height (m)	0	11.58 (5.05)	27.52	0	8.89 (3.66)	24.1	0	12.6 (5.15)	27.5
Basal area (m ha^{-1})	0	17.58 (15.07)	73.013	0	10.6 (10.4)	46.8	0	20.1 (15.7)	73.0
AGB (Mg ha^{-1})	0	109.67 (133.60)	758.79	0	50.7 (63.3)	259	0	131 (146)	759
No. obs.	58	166 (48.8)	330	109	195 (57.9)	330	80	158 (38.8)	274
No. obs. per year	5.12	8.41 (2.79)	16	1	10.2 (5.42)	32	1	8.13 (3.75)	32
No. of breakpoints	0	0.52 (1.31)	9	1	2.09 (1.89)	9	0	0	0
TSLD (years)	0	15.92 (5.27)	21	0	8.99 (5.61)	20	-	-	-
NDVIa S.D.	0.03	0.05 (0.01)	0.09	0.03	0.06 (0.01)	0.09	0.03	0.05 (0.01)	0.09
NDVI S.D.	0.04	0.06 (0.01)	0.12	0.05	0.08 (0.01)	0.12	0.04	0.06 (0.01)	0.10
NDVI min	0.24	0.51 (0.10)	0.65	0.24	0.39 (0.08)	0.60	0.30	0.55 (0.06)	0.65
NDWIa min	-0.07	0.21 (0.08)	0.38	-0.07	0.15 (0.09)	0.33	0.02	0.24 (0.06)	0.38

Table 3.4. Summary statistics of forest structure and remote sensing variables in TMCF sites (n = 39). Values are averages of those found in the four plots contained in each site. Abbreviations are: TSLD, time since last disturbance; NDVIa S.D., mean annual NDVI S.D.; NDVI min, NDVI minimum value found in the time series; NDWIa min, mean annual minimum NDWI.

Variable	Min	Mean (±S.D.)	Max
Tree density (tree ha^{-1})	81.25	659.94 (389.96)	1806.25
Lorey's height (m)	5.92	11.69 (4.36)	24.91
Basal area (m ha^{-1})	1.56	18.53 (12.77)	51.08
AGB (Mg ha^{-1})	8.26	120.58 (144.98)	414.52
No. of breakpoints	0	2.46 (4.96)	27
Most recent TSLD (years)	0	14.21 (6.66)	21
Mean TSLD (years)	3.75	15.93 (4.80)	21
NDVIa S.D.	0.03	0.05 (0.01)	0.08
NDVI S.D.	0.04	0.06 (0.01)	0.10
NDVI min	0.26	0.50 (0.10)	0.62
NDWIa min	-0.04	0.20 (0.08)	0.33

Breakpoints were validated using PlanetScope high-resolution images (daily coverage and pixel size of ~3 m) where we found a threshold magnitude value of |0.15|. This means that NDVI changes > |0.15| were recorded as abrupt changes in forest cover, and NDVI changes < |0.15| as natural variation. Once breakpoints were detected, we summarized information by plot. We calculated the total number of breakpoints in each time series, the average number of breakpoints over all plots sampled, and the time elapsed between the last breakpoint detected and the time of field data collection (TSLD). The average number of breakpoints is 0.5 because, despite none were detected in 208 plots, it was common to find more than one in several time series. In fact, the average number of breakpoints in the 76 plots where forest clearings were detected is 2 (Table 3.3). Besides number of breakpoints and TSLD, we calculated mean, min, max, S.D., and C.V. per year and throughout the entire time series of three VI: NDVI, EVI, and NDWI.

In itself, the variable selection process is an interesting result, as it gives insight on which variables are potentially more informative for understanding land use effects on forest structure. For selecting them, we calculated the correlation among all RS and forest structure variables and removed all RS variables that were poorly related to forest structure ($|\rho<0.3|$). In the variable selection process, we reduced the dataset from 44 RS variables to only 10 (see *Selection of remote sensing variables* section above). Interestingly, maximum and mean values of the three evaluated VI did not yield meaningful results. Rather, the variation of VI over time showed a

70

clearer relationship with forest structure. The selected variables represent the variation in NDVI and NDWI and their minimum values found over time. Although we initially calculated EVI as well, this index did not show a strong correlation with forest structure variables and was dropped in the variable selection process. Therefore, subsequent analyses were conducted only with NDVI and NDWI. The RS variables calculated only for the year of data collection (annual NDVI, EVI, and NDWI mean values and variation from 2009 to 2014) were also dropped due to their weak correlation with forest structure.

RS variables show high correlation between them (Figure S3.3). For instance, NDVImin, NDWImin and NDWIa min values are negatively correlated with the number of breakpoints detected in a time series, which means that the minimum values of NDVI and NDWI were found in time series with breakpoints. In addition, the S.D. of both NDVI and NDWI is negatively correlated with VI's minimum values, suggesting that time series that show lower VI values are also the ones showing more variation. NDVI and NDWI values range, respectively, from 0.24 to 0.98 and -0.32 to 0.72 over all time series, with mean values of 0.746 and 0.29.

The effect of recent land use on forest structure

To test the effect of forest disturbance on forest structure, first, we classified plots in two groups: those with breakpoints detected and those without, and compared their tree density, tree height, basal area, and AGB using t-tests (Figure 3.2). Forest structure variables were statistically different between the two groups ($p < 0.05$) (Figure 3.2 and Table S3.4). All plots with breakpoints show lower tree density, tree height, basal area, and AGB, than plots with no breakpoint. It is important to note that the group with no breakpoints shows more variation in forest structure, with some plots exhibiting low basal area, AGB, and tree height (Figure 3.2).
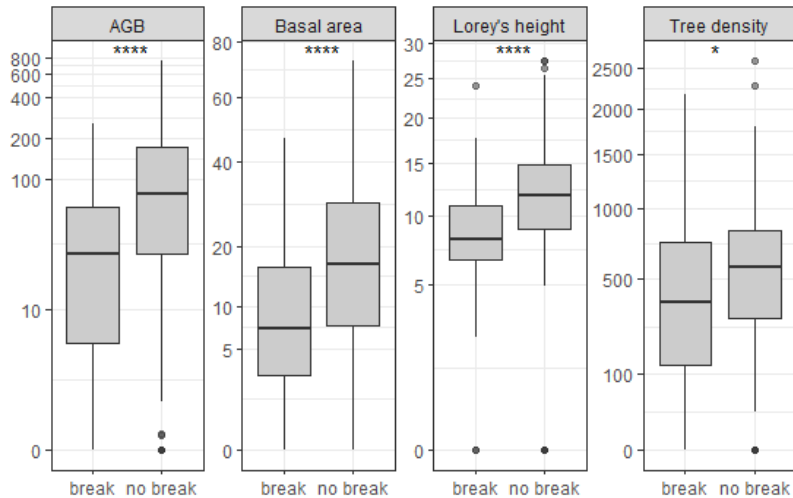
Figure 3.2. Comparison of forest structure variables between FI plots with breakpoints (break) and without breakpoints (no break) detected by BFAST, including (A) sqrt-transformed basal area (m ha^{-1}), (B) log-transformed aboveground biomass (log AGB, Mg ha^{-1}), (C) sqrt-transformed Lorey's height (m), and (D) sqrt-transformed tree density (tree ha^{-1}). Boxes cover the interquartile range (IQR), the horizontal line within boxes shows the median, and values 1.5 times larger or smaller than the IQR are shown in dark gray points. Asterisks indicate statistically significant differences between plots with and without breaks tested with t-tests ($p < 0.05$) (results shown in Table S3.4). Statistical significance: ****$p < 0.0001$, ***$p < 0.001$, **$p < 0.01$, *$p<0.05$, ns = non-significant.
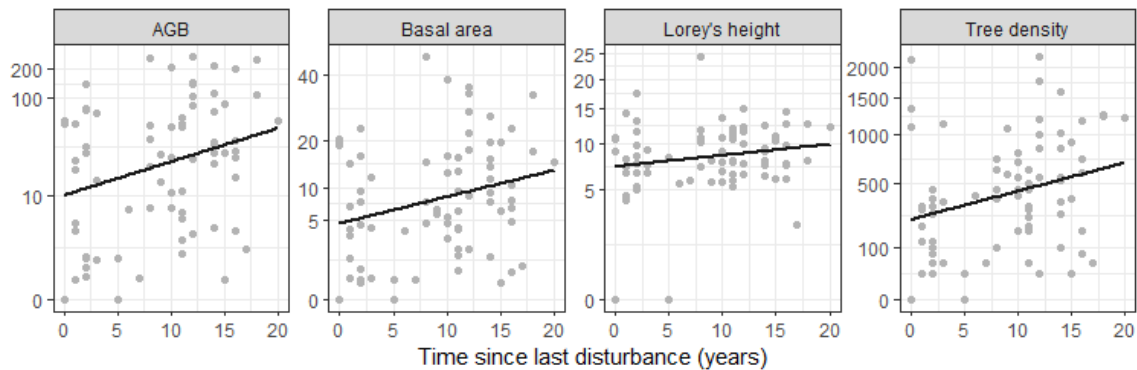
Figure 3.3. Forest structure variables over time after the last breakpoint detected by BFAST (time since last disturbance, TSLD) in FI plots with breakpoints shown in light gray points (n= 76). Black lines show linear regressions between TSLD and log-transformed AGB (p= 0.01, adjusted R^2= 0.06), sqrt-transformed basal area (p= 0.02, adjusted-R^2= 0.05), sqrt-transformed Lorey's height (p= 0.1, adjusted-R^2= 0.01), and sqrt-transformed tree density (p= 0.01, adjusted-R^2= 0.06). Forest structure variable units as in Figure 3.3.

72

We also assessed the effect of TSLD on forest structure. TSLD is capped at 21 years because our starting point is the year 1993 and the last year of field data collection is 2014. Because of this, we could not test forest structural change after disturbance on periods longer than 21 years. To avoid underestimating TSLD in time series with no breakpoints, we analyzed the relationship between forest structure and TSLD only in the 76 plots that have been disturbed in the last 16-21 years. Almost all structural variables increase with TSLD and show statistically significant linear regressions ($p < 0.05$), except for Lorey's height (Figure 3.3). However, they show large variation and their R^2 values are (Figure 3.3 and Table S3.5). For instance, the maximum value of AGB found in FI plots with breakpoints is 259 Mg ha^{-1}, which is higher than the AGB we would expect to find in a disturbed forest (Table 3.3). On the other hand, several plots with 15 or more years since the last disturbance show lower values of basal area (< 5 m ha^{-1}), AGB (<10 Mg ha^{-1}), tree height (<5 m) and tree density (< 500 ha^{-1}) than expected (Figure 3.4). These results are in line with the large variation of forest structure variables found in the no-breakpoints group (Figure 3.2).

To assess which RS variables are relevant for making predictive models of forest structure and AGB, we performed multiple linear regression models with data grouped at site level. Model predictors were elevation, slope, and the seven RS variables that remained after reducing our RS dataset (we removed RS variables that show very high correlation between them): mean and min TSLD, mean number of breaks per site, NDVIa S.D., NDVI S.D., NDVI min, and NDWIa min. For each response variable (AGB, basal area, Lorey's height, and tree density), a full model including all variables was computed and compared with models using subsets of variables (Lumley, 2020). We selected the best models as those presenting the lowest BIC and CP, and highest R^2 (Table S3.6). The best models always include elevation and at least one RS variable; most of them have two or three predictors (except for basal area that has five predictors), and all of them have an adjusted $R^2 > 0.3$ (Table 3.5).

The most relevant variables for predicting forest structure and AGB are elevation, slope, NDVI S.D., NDVIa S.D., and NDWIa min, where S.D. has always a negative relation with forest structure variables and NDWI annual minimum values a positive one (Figure 3.4). Importantly, the number of breaks in a site, and a site average TSLD, were removed from the models during the stepwise selection process and are not fundamental for predicting forest structural variables and AGB through linear regression models (Table S3.6). The forest structure variable that was

better predicted is basal area, with an adjusted R^2 of 0.57, followed by Lorey's height (Table 3.5). Although AGB shows a statistically significant relationship with the predictors, the R^2 of this model is 0.43 and it only includes one RS variable (NDVI S.D.).

Table 3.5. Multiple linear regression models of forest structure variables and aboveground biomass (AGB) as a function of elevation, slope, and remote sensing variables in TMCF sites (n= 39).

BASAL AREA (sqrt-transformed)				
b= -1.312; F= 11.32; df (5, 33); p < 0.001; adjusted R^2= 0.575				
Predictors	**Coefficient**	**S.E.**	***t***	***p***
Elevation	0.001	0.0003	4.930	<0.001
Slope	0.031	0.019	1.555	0.129
NDVI S.D.	-62.33	24.56	-2.537	0.016
NDVIa S.D.	64.97	36.09	1.800	0.081
NDWIa min	8.472	3.657	2.317	0.026
LOREY'S HEIGHT (sqrt-transformed)				
b= 4.095; F= 16.71; df (2,36); p < 0.001; adjusted R^2= 0.452				
Predictors	**Coefficient**	**S.E.**	***t***	***p***
Elevation	0.0004	0.0001	3.159	0.003
NDVI S.D.	-21.27	4.600	-4.624	<0.001
TREE DENSITY (sqrt-transformed)				
b= 3.85; F= 10.63; df (2,36); p < 0.001; adjusted R^2= 0.336				
Predictors	**Coefficient**	**S.E.**	***t***	***p***
Elevation	0.005	0.001	3.176	0.003
NDWIa min	47.049	12.19	3.859	<0.001
AGB (log-transformed)				
b= 4.51; F= 10.56; df (3,35); p < 0.001; adjusted R^2= 0.430				
Predictors	**Coefficient**	**S.E.**	***t***	***p***
Elevation	0.0008	0.0002	3.572	0.001
Slope	0.031	0.016	1.973	0.056
NDVI S.D.	-36.67	8.510	-4.309	<0.001
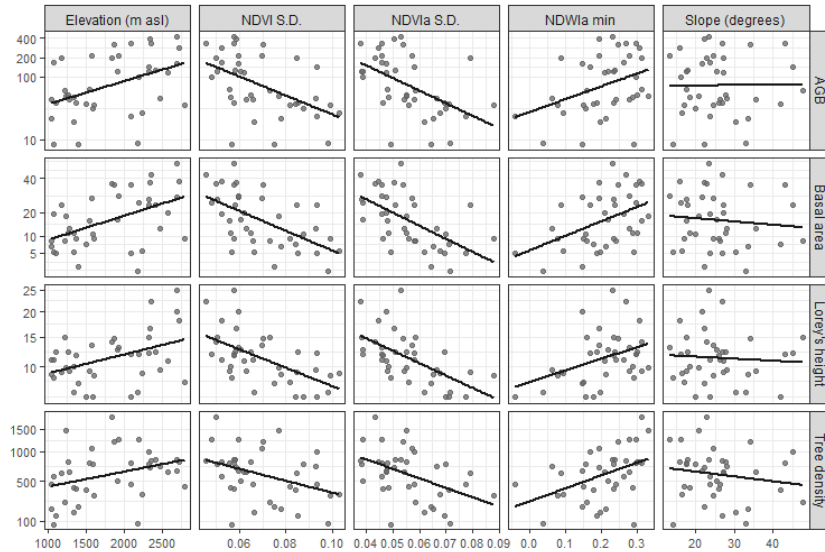
Figure 3.4. Relationship between forest structure variables and the five predictors included in the best multiple linear regression models (models shown in Table 3.5), including elevation (m asl), NDVI S.D. of time series, average of annual NDVI S.D. (NDVIa S.D.), average of annual NDWI minimum value (NDWIa min), and slope (degrees). Linear regressions are shown in black. Forest structure variable units as in Figure 3.3.

DISCUSSION

Aboveground biomass in cloud forests of the Northern Mountains of Oaxaca

Many studies have relied on forest inventory data to study forest structure and estimate AGB, since they provide ample spatial coverage with a systematic sampling design (Mohren et al. 2012). Here, we used FI data to assess basal area, tree density, Lorey's height, and AGB in TMCF located in the NMO. TMCF landscapes in the studied region show a great variation in forest cover and structure, from sites with only eight trees and AGB of 8 Mg ha^{-1}, to sites with thousands of trees and AGB of 414 Mg ha^{-1}. The average value of AGB found (120 Mg ha^{-1}) is in line with other estimates calculated in TMCF around the globe (77-785 Mh ha^{-1}) and in Mexico (75 Mg ha^{-1}) (Spracklen and Righelato 2014; CONAFOR 2018). Compared to the average AGB reported for Mexican TMCF, our estimate is higher, but compared to the values shown in pan-tropical maps for this region, the average AGB we found is lower (e.g. Saatchi et al. 2011). These discrepancies arise both from methodological approaches and the natural variation of biomass accumulation in tropical mountains.

Several factors determine the accumulation of AGB in a site, including environmental ones, such as climate, topography, and the availability of nutrients in the soil; as well as factors related to forest disturbance, such as the frequency, severity, and time of recovery after disturbance (D. B. Clark, Hurtado, and Saatchi 2015; K. H. Erb et al. 2018). In TMCF found in the NMO, disturbance by land use, elevation, and precipitation seem to have a large role in driving AGB magnitude and distribution (see chapter 2). Modeling all the factors driving AGB patterns is challenging. To estimate AGB at local scales, forest structure is surveyed, and the biomass of each tree is calculated using allometric equations (Rojas-García et al. 2015). At larger spatial extents, however, surveying forests directly in the field is unrealistic (Jérôme Chave et al. 2019). RS has been widely used to overcome this challenge (Laura Duncanson et al. 2021). However, RS-based maps of AGB have done a better work including environmental factors (climate, topography, soil) than those related to disturbance, despite forest monitoring during and after disturbance with RS is an important field of study in continuous development (DeVries, Decuyper, et al. 2015; White et al. 2017). Here we used RS imagery (Landsat and PlanetScope) to assess recent disturbance that took place before field data collection in the FI plots established in the TMCF of the NMO.

Estimating recent forest disturbance using Landsat time series

Although steep terrain does not represent a problem for optical RS, cloud contamination does. To counteract this problem, it is important to use imagery with high temporal coverage and filter out cloudy pixels. Landsat time series have been widely used to monitor forests even in tropical mountains with frequent cloud cover (DeVries, Verbesselt, et al. 2015). Landsat satellites have a returning cycle of two weeks, and they are out of phase by one week, resulting in an 8-day repeat coverage during periods where the two satellites are in orbit (for instance, from 2000-2012, when both Landsat 5 and Landsat 7 were active) (Wulder et al. 2019). Using Landsat imagery, we obtained time series with enough observations per year to assess vegetation change over time, even after removing cloudy pixels and during the years of biweekly (as opposed to weekly) repeat coverage (Table 3.2). The number of observations in the studied time series were determined by cloud frequency and the overlapping period of Landsat satellites and scenes. Cloudy pixels were more frequent during the rainy season and, thus, the time series are more populated from May to October; there are more observations between 2000-2012 than before

2000 and after 2012, and some plots fall within the overlapping space of two Landsat scenes, increasing their coverage over time.

Removing contaminated pixels was a fundamental step in this study. In addition to applying a cloud mask as most other studies do, we also calculated a cloud index (Table 3.1) and, following Zhai et al (2018), removed all pixels with a CI value lower than 2.8. This was particularly useful because, besides being frequently overcast, TMCF are regularly immerse in ground-level clouds (fog), particularly in the dry season (Gotsch, Asbjornsen, and Goldsmith 2020). Ground-level clouds can have a different spectral signature than clouds that form in the upper sky. Thus, foggy pixels were not always masked out by the CFMask. Using a cloud mask and a CI threshold value we reached a ground pixel accuracy of 94%. Making sure that time series observations were cloud-free was essential to avoid overestimating vegetation cover change due to commission errors (DeVries, Verbesselt, et al. 2015).

We assessed forest disturbance by detecting abrupt changes in FI plots vegetation cover and by estimating the variation of VI over time. It is important to note that disturbances unrelated to land use can also increase the variability in vegetation cover over time and trigger a change in forest cover. For instance, fires, pest outbreaks, and landslides can all be tracked from space using satellite imagery because they influence forest cover and, with it, the spectral reflectance of land's surface (Frolking et al. 2009). However, land use is the most common cause of forest loss in the NMO and thus, we did not distinguish different types of disturbance (Toledo-Aceves et al. 2011). Unfortunately, Landsat coverage over our study area before 1993 is scarce and impossible to use in time series analysis (Solórzano, Gallardo-Cruz, and Peralta-Carreta 2020). Thus, the length of time series ranged from 16-21 years depending on the time of field data collection (that took place from 2009 to 2014). Nevertheless, periods of 16-21 years are enough for gaining insight into the land use dynamics of the studied forests.

Abrupt forest cover changes were assessed with BFAST. Out of 284 plots, 76 were cleared at least once over the two decades before field data collection. Within 1-ha sites, the average number of breakpoints over time is 2.46, and 23 sites (out of 39) show no disturbance during the evaluated period. Several plots exhibit recurrent breakpoints (Table 3.3), suggesting that vegetation is repeatedly cleared. In fact, the average TSLD is 9, which means that disturbed plots are, on average, cleared every 9 years. Different types of land use create distinct disturbance regimes. For instance, shifting cultivation creates cycles of forest clearing and

77

regrowth (Frolking et al. 2009). Thus, forest plots that are part of a shifting cultivation cycle may exhibit several breakpoints in their time series, depending on the length of the fallow periods (Jiang, Li, and Feng 2022). However, other types of land use could also result in repetitive breakpoints depending on the management and the sequence of land-cover change. For example, this could occur in a cleared forest stand that is converted to an agroforestry system, whose management implies the periodic reduction of vegetation cover, or in a forest turned into a coffee farm and then into grazing land. These dynamics are not uncommon in tropical mountains, including the NMO (del Castillo 2013). Moreover, research has shown that disturbed forests (degraded or secondary) are more often cleared and converted to agricultural or grazing lands than old-growth forests (Reid et al. 2019; Ochoa-Gaona and Gonzôlez-Espinosa 2000; Heinrich et al. 2021). This explains why only one quarter of forest plots show breakpoints, but most of them show two or more clearings.

FI plots with breakpoints show lower basal area, tree height, tree density, and AGB than forests with no breakpoints (Figure 3.2). As expected, the difference in tree density between plots with and without breakpoints was not as large as that in the other forest structure variables, because forests in secondary succession have greater tree density than old-growth forests (Ruiz-Jiménez, Meave, and Contreras-Jiménez 1999; Meave et al. 1992). Interestingly, plots with breakpoints have an average AGB of 50.7 Mg ha^{-1} and most of them do not surpass 100 Mg ha^{-1}. This means that the presence of breakpoints can be used to flag forest pixels to avoid overestimating AGB. Notably, plots with no breakpoints show large forest structure variation. For instance, some undisturbed plots have an AGB < 10 Mg ha^{-1} while others attain values larger than 500 Mg ha^{-1}. This wide variation has three possible explanations: (1) breakpoints were underestimated in time series that correspond to FI plots with very low AGB; (2) forest plots with very low AGB were converted before 1993 and never recovered from the disturbance; and (3) forest degradation decreased AGB in certain FI plots, but this type of slow change is not detected as a breakpoint.

Underestimating breakpoints could occur if the NDVI magnitude threshold we selected is higher than needed so that forest clearings with an NDVI magnitude lower than |0.15| occurred. The selection of a magnitude threshold depends on the type of forest studied. For instance, DeVries et al. (2015) used a magnitude threshold of 0.06 for monitoring Afromontane forests of southern Ethiopia in a Biosphere Reserve where stable time series were expected. In contrast,

Gao et al. (2021) used a threshold of |0.2| in Mexican tropical dry and temperate forests, where it was expected that seasonal variation resulted in large NDVI change. In our case, the landscapes studied are heterogenous and encompass lands with different levels of vegetation cover (agroforestry systems, agricultural lands with scattered trees, secondary and old-growth forests) and thus, we were expecting large NDVI variation that, in case of change, would show an equally large magnitude. Therefore, we limited breakpoint detection to NDVI changes that occurred clearly as an event of complete vegetation cover loss, which we found at a magnitude of |0.15|. On the other hand, slow forest disturbance, such as forest degradation, can result in low values of AGB and will not trigger an abrupt change in NDVI (DeVries, Verbesselt, et al. 2015). Hence, forest disturbance could be underestimated if forest degradation is more common than forest conversion. Additionally, research showing high levels of deforestation in the 1980s and 90's suggests that LULCC in these landscapes was common before the beginning of the studied time series (Gómez-Mendoza et al. 2006). FI plots with low AGB but no breakpoints could have been disturbed before 1993 and maintained stable afterwards, showing a steady NDVI time series.

FI plots with breakpoints also show great variation in forest structure in relation to the TSLD (Figure 3.3). Although all forest structure variables increase over time, the relationship between TSLD and forest structure was not as clear as we were expecting. AGB was the variable showing a more significant change over time. However, there are several plots with breakpoints in the last five years showing similar AGB values than plots with more than 15 years since the last disturbance. This suggests that vegetation is not always allowed to regenerate after an abrupt change, and also that in some events of abrupt change large trees are left alive, maintaining some AGB even if the land is almost completely cleared. Indeed, research conducted in the NMO has shown that establishing permanent agricultural lands and cattle ranches has become more common in the last decades (Velázquez et al. 2003). Moreover, maintaining trees in agricultural and grazing lands is a common practice among small-scale farmers (Fuentealba and González-Esquivel 2016; Zomer et al. 2017). Together, the fact that 27% of plots show breakpoints over 16-21 years, that several FI plots were cleared repeatedly, the large variation in plots with no breakpoints, and the large variation of forest structure over time after a disturbance, show the dynamism of changes in land use and vegetation in the region.

Gradual change is not considered in an approach based on detecting breakpoints but could also be informative. To consider gradual change, we computed basic summary statistics of NDVI and NDWI time series. Interestingly, the variation in VI over the time series, assessed through their S.D. and their minimum values, was more informative for assessing forest structural change over time than average and maximum values. Average NDVI values are often employed in AGB models. However, they are mainly used for distinguishing vegetation cover and do not show strong relationships with forest structure variables (Saatchi et al. 2011). Here we found that historical trends of vegetation cover and its variation over time can be assessed with VI time series and that they are relevant for predicting forest structure.

The RS variables that show stronger relationships with forest structure are: NDVIa S.D., NDVI S.D., and NDWIa min. Notably, RS variables are corelated. As plots show more variability in their vegetation cover over time (i.e., disturbance), their S.D. increases making it more likely to find lower VI values (i.e., lower VI min). AGB, basal area, and tree height decrease with forest disturbance, which explains why VI minimum values and S.D. show a relationship with forest structure (Figure 3.4). From all RS variables analyzed, NDVI S.D. was the best predictor of forest structure and AGB, except for tree density. NDWI was more informative in predicting tree density than other VI. NDWI is related to the content of liquid water in the forest canopy (Maki, Ishiahra, and Tamura 2004). Thus, forests with lower tree density also show the lowest NDWI values. Tree density, however, is not the best predictor of AGB. Forests in secondary succession tend to have a higher number of trees −albeit smaller and thinner−than older forests (Guariguata and Ostertag 2001). Thus, old-growth forests hold greater amounts of biomass, especially in large trees, than forests in secondary succession. Because of this, basal area and tree height are better predictors of AGB in TMCF (Cuni-Sanchez et al. 2017). Tree height is usually assessed with active RS in AGB models. However, estimating basal area has proven to be more difficult (S. Brown, Narine, and Gilbert 2022). Surprisingly, we found that NDVI S.D., NDVIa S.D., and NDWIa min greatly improve the predictability of basal area. In fact, computing multiple linear regression models using RS variables, slope, and elevation as predictors, we found an adjusted-R^2 of 0.6 for basal area. These results hint to the wide array of possibilities that could be developed for implementing recent forest disturbance in AGB models.

Implementing land use in aboveground biomass models

Despite forest disturbance related to land use influences the magnitude and distribution of AGB in tropical forests, it is rarely included in regional AGB estimates (K. H. Erb et al. 2018). Our results suggest that the variation of VI and their minimum values over time can be greatly informative in predicting forest structure and AGB. Although more sophisticated models are usually applied for mapping AGB, here, using linear regression models, we explored the relationship between RS variables of forest disturbance and forest structure variables, including basal area, Lorey's height, tree density, and AGB, adding only two environmental variables as predictors (slope and elevation). With these simple models, we obtained statistically significant relationships between RS variables of recent disturbance and forest structure. Surprisingly, the number of breaks and TSLD were not relevant predictors, although they proved to be important variables for understanding the variation in AGB and forest structure resulting from the dynamic processes of forest cover change in the region.

Implementing land use in regional models of AGB has been challenging, in part, due to the lack of informative data. Using time series of VI is a common approach in forest monitoring that has not been applied for modeling the distribution of AGB. Given the large amount of RS data and the computer power now available, it is feasible to assess the recent disturbance history of pixels through summarizing VI time series information. Whether a forest pixel has been abruptly or gradually disturbed, the record persists in the satellite imagery archives. Harnessing this opportunity could increase our understanding of AGB spatial patterns while reducing the uncertainty in AGB maps. Variables such as number of breakpoints, NDVI S.D., and annual NDWI minimum values are not difficult to calculate and are good candidates to be tested as inputs.

Caveats and recommendations

Our approach to study recent forest disturbance in TMCF has some important limitations. First, our approach is time-constrained. Although we used the satellite imagery with the longest record of Earth's surface, Landsat provides data for the last ~50 years at best (and about 30 years for our study area) (Solórzano, Gallardo-Cruz, and Peralta-Carreta 2020; Wulder et al. 2019). However, forest disturbance has long-term effects that are not captured by RS imagery (Aragón et al. 2021; R. Chazdon 2003). Second, analyzing VI time series allows us to detect changes in vegetation cover that we linked to land use because it is the most common disturbance found in the NMO.

Yet, other types of disturbance taking place in the area (e.g., fires Cruz-López et al. 2019) have similar RS signals, although possible different effects on forest structure and recovery. A limitation of this approach is its incapability to identify different types of disturbance. Even if the detected disturbance is related to land use, with this approach is not possible to identify whether the change in vegetation is permanent or temporal, nor the exact type of LULCC that took place. Despite these limitations, summarizing VI time series information is a promising approach to include recent forest disturbance into AGB modeling. To do so it is important to: (1) remove all cloudy and foggy pixels from the time series to avoid commission errors when detecting vegetation disturbance; (2) use the longest record available to extract VI time series and trim them to the closest point to field data collection; (3) detect breakpoints and flag all pixels that have been disturbed in the recent past (even if those pixels display high NDVI values, it is almost certain that they cannot have more than 100 Mg ha^{-1}); (4) calculate basic summary statistics of NDVI and NDWI, particularly NDVI S.D. and NDWI minimum values, and used them as inputs in AGB models along with other sources of information. Combining these time series summary statistics with active RS variables could be especially useful, as the former have a stronger relationship with basal area and the latter with forest canopy height, complementing the information needed to estimate AGB. Finally, we recommend conducting time series analyses of land use related disturbance at a meaningful spatial scale. Imagery of medium-to-high spatial and temporal resolution would yield better results than coarse-grained data.

CONCLUSIONS AND BRIDGE

Forest disturbance and its effects represent a large component of uncertainty in AGB estimates. Here, with the aim of improving our understanding of land use influence on biomass accumulation, we analyzed the effect of recent small-scale disturbance on forest structure with optical RS satellite imagery and FI data in the TMCF of the NMO. Our objective was twofold. First, we wanted to estimate the effect of small-scale forest disturbance on TMCF structure using Landsat time series; and second, we explored possible ways in which these effects could be incorporated into AGB models. We found that Landsat time series have the potential to add power to AGB models and decrease uncertainty related to forest disturbance. In particular, we found that NDVI S.D. and NDWI minimum values of Landsat time series are related to forest structural variables, especially to basal area and tree density, which can potentially complement

active RS data that is better related to tree canopy height. We also showed that forest change detection with BFAST can be applied to flag pixels that have experienced recent disturbance, adding information that could be easily missed if only a snapshot of a VI is used. Finally, our results reveal the dynamism that the studied landscapes experience; a dynamism that, if successfully accounted for, can improve AGB models, especially at landscape and regional scales.

The following chapter uses another remote sensing approach to assess the trends of forest loss across the entire region. Given the relevance that land use has on forest dynamics and distribution (shown in this and the previous chapter), I analyze the relationship between forest loss trends and agricultural production in the NMO. In addition, I investigate the forest conservation efforts developed in the region and critically assess how forest conservation can be conducted in tropical montane landscapes.

CHAPTER 4

FOREST LOSS AND CONSERVATION IN THE NORTHERN MOUNTAINS OF OAXACA, MEXICO, IN THE LAST TWO DECADES

INTRODUCTION

Tropical forests are currently under great stress due to climate change and widespread deforestation (Morello et al. 2018; Yadvinder Malhi et al. 2014). A combination of land-use and land-cover change (LULCC), hurricanes, drought, and fires is diminishing the extent of tropical forest worldwide (França et al. 2020). Although several regulations to decrease the rate of deforestation in tropical countries are in place (Furumo and Lambin 2021), tropical forest loss still surpasses forest gain (FAO 2016; Hansen et al. 2013). According to Global Forest Watch (GFW), 11.1 million ha of tropical forest were lost in 2021 (Weisse and Goldman 2022), a higher figure than the seven million ha yr^{-1} reported by the Food and Agriculture Organization (FAO) for the first decade of the 21st century (FAO 2016). These trends indicate that tropical forest loss is still on the rise.

Forest loss in the tropics is mainly driven by the expansion of agriculture and the establishment of cattle ranches (H K Gibbs et al. 2010). Commodity-driven deforestation amounted for 27% of total forest loss between 2001 and 2015, whereby forests are cleared to establish grazing lands, soy, or palm oil plantations (Curtis et al. 2018). Shifting agriculture[1] is the second most common cause of forest loss in the tropics, representing 24% of forest cover change. In contrast to permanent agriculture and cattle ranches, in shifting agriculture land is left to fallow, allowing forest to regenerate (Velasco-Murguía et al. 2021). Thus, the difference between forest loss and deforestation is more difficult to establish with remote sensing in places with shifting agriculture than in those with forest conversion to permanent agriculture (Jiang, Li, and Feng 2022). Shifting cultivation alone rarely causes deforestation, unless it occurs along with other causes of forest loss such as wood extraction and expansion of infrastructure (Geist and Lambin 2001). Deforestation in places where shifting agriculture is the main proximate cause of forest loss is usually related to shorter fallow periods and other forms of agricultural

---

[1] An agricultural technique based on field rotation in which land is cleared for cultivation and, after a few agricultural cycles, left to regenerate. Many small-scale farmers practice shifting agriculture (also known as swidden agriculture) in tropical mountains.

intensification impacting forests at landscape scales (Tscharntke et al. 2005; Byerlee, Stevenson, and Villoria 2014; Phelps et al. 2013).

Tropical forest loss has drawn public attention, partly due to the fundamental role these forests play in global and regional climate stability, biodiversity, and the provision of ecosystem services (Bonan 2008; Gardner et al. 2009). This applies to mountain regions, where both forest loss and the evidence showing the large amount of carbon they can accumulate have increased (Spracklen and Righelato 2014; Feng et al. 2021). Although forest loss in tropical mountains is beginning to be of larger concern, global estimates of forest cover change (like those reported by GFW) do not distinguish lowlands from uplands. Tropical mountains are equally subjected to both LULCC and climate change. However, their effects and consequences on forest distribution and dynamics may be different from those in lower lands because of their biophysical properties (including relief, soil nutrients, and climate). Despite the important efforts made by the scientific community to study montane landscapes in tropical regions, processes of forest dynamics (including LULCC) and the effects of a changing climate in tropical mountains are not yet well understood.

Thus, with the aim of expanding the characterization of forest loss in tropical mountains, here I analyzed forest loss trends in the Northern Mountains of Oaxaca (NMO), Mexico. The NMO harbors some of the most biodiverse forests in that country, including the largest and most continuous tropical montane cloud forest (TMCF), as well as large extensions of coniferous forests and tropical evergreen forests (Toledo-Aceves et al. 2011). The NMO is also home to about half a million people, out of which roughly 47% are indigenous (mainly Zapotec, Mixe, and Chinantec), and many are involved in farming (CEIEG 2022a, 2022b). The NMO has also been the stage of several local, but globally renowned, forest conservation projects (D. B. Bray et al. 2003). In the second part of this chapter, I analyze forest conservation efforts, many of which have been led by these indigenous groups, in tropical forests and their possible use in montane landscapes.

METHODS

The NMO, located in southern Mexico, exhibits a wide diversity of ecosystems going from tropical evergreen or deciduous forest at lower elevations, passing through cloud and oak forest at mid elevations, and coniferous forest at higher elevations. Croplands and grasslands can be

found in large extensions at lower elevations closer to Miguel Alemán Dam, and in small patches throughout the mountain range (INEGI 2013). Four subregions have been identified in the NMO, based on geomorphology, forest cover, watershed margins, rivers, and the presence of indigenous groups: Huautla-Zongolica, Ixtlán, Sierra Mixe, and Guevea de Humboldt (Toledo-Aceves et al. 2011).

To study forest loss trends in the region, I used the Global Forest Change product (GFC) developed by Hansen *et al.* in 2013, and available in Google Earth Engine (GEE) (Gorelick et al. 2017). GFC contains global maps of tree cover change from 2000 to 2019, at a spatial resolution of 30 m. I extracted GFC layers of my study area from GEE and overlapped them on a land-cover map created by the Mexican National Institute of Statistic and Geography (INEGI) in 2013 (INEGI 2013). I delimited the NMO region using a TMCF regionalization map acquired from the National Commission of Biodiversity (CONABIO) GeoPortal (CONABIO 2012). Then, I calculated the area of forest loss in the region and each subregion every year from 2000 to 2019, as well as the total amount of forest loss per land-cover type, in ArcGIS Pro (ESRI Inc 2020). Later, to assess the role of conservation projects in the region, I added a layer of protected natural areas created by the National Commission on Protected Natural Areas (CONANP), available through CONABIO's GeoPortal (CONANP 2019). It is important to note that these areas have been voluntarily registered as protected lands by local communities.

Because most cases of forest loss in the tropics are related to agricultural expansion and intensification, I also extracted data from the Mexican Agricultural Information Service (SIAP) available online (SIAP 2020), and calculated the area devoted to agriculture and agricultural production (in tons) in the NMO from 2003-18.

Importantly, neither forest gain nor regrowth are considered in this analysis because even though shifting cultivation is commonly practiced by smallholders in the region, monitoring forest regrowth during fallow periods is more difficult than detecting forest cover loss and is not included in the GFC product. There is a layer in GFC that displays forest gain, but the area of forest gain in the region was negligible and thus, was excluded from the analysis.

RESULTS AND DISCUSSION

19 years of forest loss in the Northern Mountains of Oaxaca
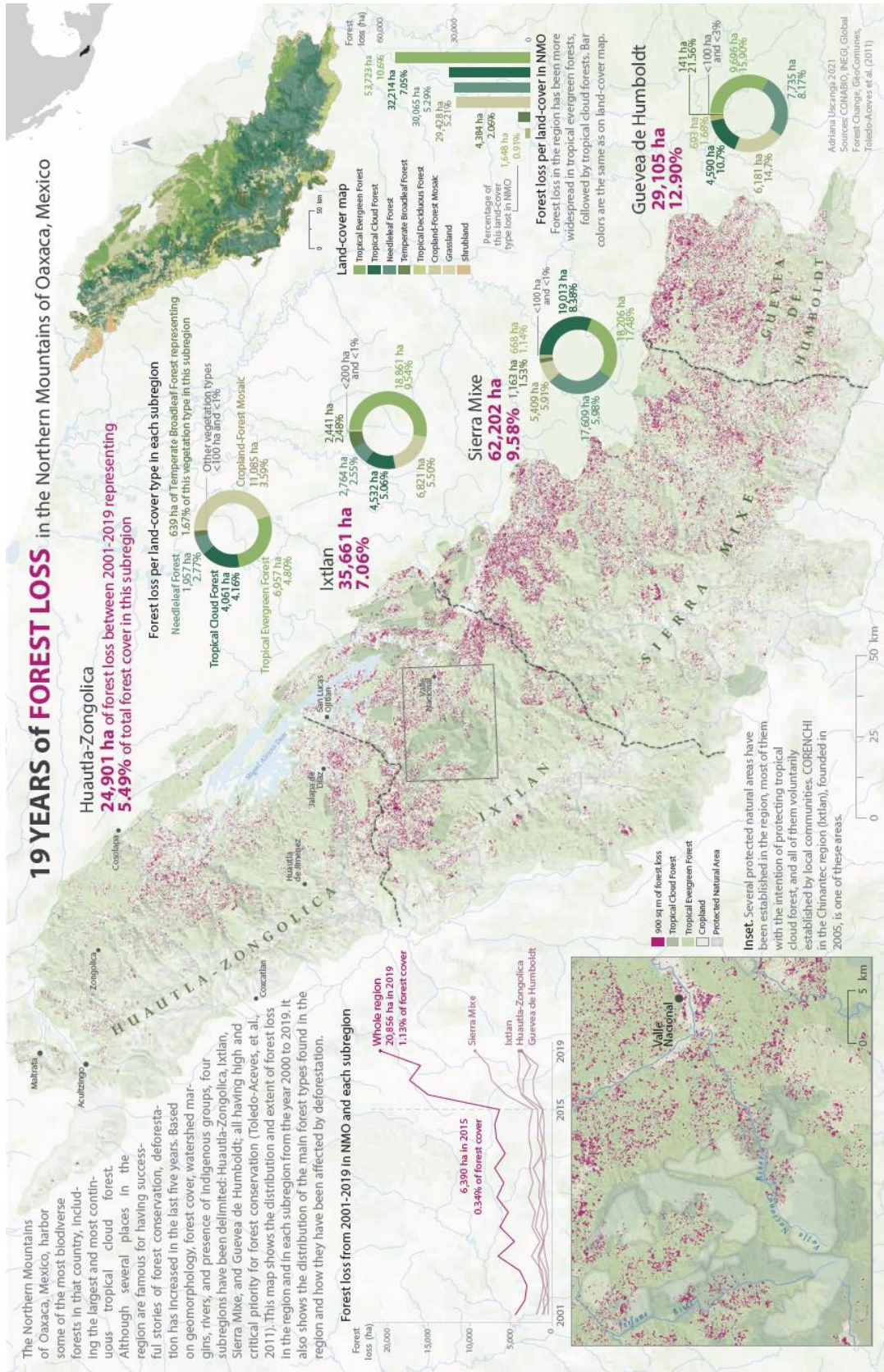
Figure 4.1. Map of the Northern Mountains of Oaxaca showing forest loss trends and vegetation type affected.

From 2000 to 2015, around 5,000-6,000 ha of tree cover were lost every year, representing between 0.2 to 0.3% of the total forest cover per year (Figure 4.1). From 2015 to 2016, however, tree cover loss tripled, and by 2019 it reached its highest point at 20,856 ha, representing 1.13% of the total forest cover in the region. This means that the rate of forest loss in this area averaged 5,513.69 ha per year between 2000 and 2015 and increased to 17,291.23 ha per year after 2015 (i.e., a 213.6% increase). In total, the NMO lost 151,869 ha of forest cover in 19 years. The area of lost forest is similar to that found in other tropical mountains. For example, mountains in Southeast Asia lost around 11% of tropical forest between 2001-2019 (Feng et al. 2021), while the NMO lost around 8%. These trends are lower than the deforestation rates found by Gómez-Mendoza et al. (2006) between 1980 and 2000 in NMO, suggesting that forest loss in the region decreased during the first fifteen years of the 21st century. A decline in the rate of deforestation in the region has been reported before in other studies for that same period (Navarro Cerrillo et al. 2018). Although forest cover increase has been described in the region at local scales (cf. Velasco Murguía et al. 2014) at the regional scale, forest gain is overshadowed by forest loss and not well represented in the GFC product.

By overlaying the tree cover loss layers from GFC on a land-cover map, I assessed which vegetation type has experienced more forest cover change in the last two decades (Figure 4.1). The ecosystem most affected was tropical evergreen forest, which lost 10.6% of its area (53,723 ha). The second most affected ecosystem was TMCF, losing 7% of its area (32,214 ha). This coincides with the LULCC trends found in the state of Oaxaca around 2003, when evergreen forests were most affected, followed by TMCF and coniferous forests (Velázquez et al. 2003). However, these results show lower percentages of forest loss in comparison to those reported for the region between 1980-2000, where evergreen forests lost 40% of their area and TMCF lost 11% (Gómez-Mendoza et al. 2006). Moreover, there was a 5.2% decrease in tree cover of cropland-forest mosaics. These results are in line with the land-use intensity patterns I found in chapter 2, where areas at lower elevations (where tropical evergreen forest is found) experience more land-use related disturbance.

The spatial patterns of forest loss in the studied region are heterogeneous. While all subregions exhibit a stable state between 2001-2014 followed by a sudden increase in tree cover loss, Sierra Mixe stands out as the subregion with the highest forest loss area, especially after 2015 (Figure 4.1). In this subregion, tree cover loss occurred mainly in TMCF, which lost 19,013

ha of forest between 2000 and 2019, representing around 30% of the total tree cover loss in Sierra Mixe in these two decades. Tree cover loss in Sierra Mixe amounted to 62,202 ha in total, almost twice as much as in any other subregion in the NMO, representing 40% of the total forest cover that was lost in the region. Proportionally, however, Guevea de Humboldt lost more trees over these two decades, representing almost 13% of its tree cover, most of it in the tropical evergreen forest.

The causes behind tree loss in the NMO are not well understood. According to Gómez-Mendoza et al. (2006) and Velázquez et al. (2003), forests are cleared in the region mainly to allow for the establishment of croplands and grazing lands for cattle. However, these analyses were conducted before the sudden increase in tree cover loss in 2015, and are focused on previous decades. Whether the rate of agricultural and grazing lands expansion tripled by 2016 or another source of forest loss arose is still unknown. According to Geist and Lambin (2001), a diffuse spatial pattern of forest loss, as the one taking place in the NMO, results from shifting agriculture activities. However, given vast amounts of land in NMO are owned by smallholders, a patchy, diffuse pattern would be expected even if the land-use change underlying forest loss is related to establishing cattle ranches or permanent agriculture.

Using data from SIAP, I calculated the area devoted to agriculture and agricultural production (in tons) in the NMO from 2003 to 2018. I found a total of 72 crops grown in the region, of which pasture, maize, coffee, sugar cane, and lime are the most common.

Agricultural land in the region has gradually increased in area from 315,904 ha in 2003 to 423,402 ha in 2018 (a 34% rise), showing the highest value of 445,935 ha in 2014 (Figure 4.2). Although both agricultural area and production have increased over time, especially after 2010, none of them show a sudden increase after 2016. Remarkably, out of the five most common crops, the only one that increased in area is pasture, which covered an area of 18,447 ha in 2003 and of 172,011 ha by 2018 (Figure 4.2). Sugar cane production remained relatively constant over time, while the area devoted to maize and coffee production decreased. Pastureland expansion occurred in two moments: first, during a sudden increase from 2003 to 2006 followed by a stable period, and through a second rapid augment in 2011 and 2012, followed by another stable period that lasted until 2018. This means that the region experienced a ten-fold increase in grasslands, suggesting that the expansion of grazing lands for cattle is indeed a very important land-cover change in the region, which has become even more conspicuous as of late (Gómez-Mendoza et

al. 2006). Interestingly, the second largest increase in pastureland roughly mirrors the decline in coffee production area, which could suggest the existence of a process of land cover change from coffee farms to cattle ranches. Not surprisingly, the decline in area for coffee production coincides with the beginning of the coffee rust outbreak−a fungal disease caused by *Hemileia vastatrix* that infects coffee plant leaves causing severe decreases in productivity (Valencia et al. 2018; Torres Castillo et al. 2020).
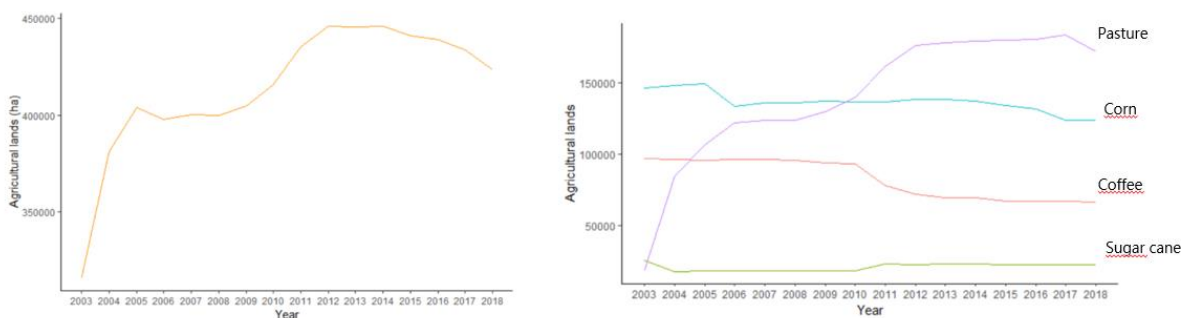
Figure 4.2. Total agricultural land (left), and agricultural land devoted to the four main crops, coffee (in red) sugar cane (in green), maize (in blue), and pastures (in purple) (right) through time (2003-2018) in the Northern Mountains of Oaxaca.

It is important to note that tree cover loss can occur in land-cover types other than forests. Here, following Hansen et al. (2013), I used a threshold of 50% of tree cover for defining a forest pixel. Given several crops are grown in combination with other trees in agroforestry systems, such as shaded coffee and cacao, it is completely plausible that these areas exhibit 50% of tree cover or more. Consequently, a land-cover change from shaded coffee to sun coffee or pasture could be classified as forest loss in GFC if tree cover (remotely sensed) declines significantly. Because coffee production is an important activity in the NMO, and coffee productivity has declined in the region (Figure 4.2), the possibility that the conversion of shaded coffee farms to sun coffee or other land uses has triggered tree cover loss in the region cannot be ruled out. Indeed, some local news outlets reported that farmers were opting for converting their coffee farms into grazing lands for cattle because coffee ceased to be profitable after the coffee rust hit the region (Vargas 2016).

Other causes of forest loss that cannot be discarded, but are difficult to study, are those related to unreported activities, such as deforestation for illicit crop production and illegal logging. Studies conducted in Central America have shown that narcotrafficking networks

engage in LULCC dynamics through seizing territorial control via land acquisitions, agro-industrial investments, and the development of transit infrastructure, thus becoming an important driver of forest loss (Tellman et al. 2020). Although a systematic analysis of unreported activities would be needed to assess whether the NMO is experiencing a similar situation, news reporting violence escalation and illicit poppy production in Sierra Mixe suggest that these activities may also have a role in the decrease of forest cover in the region (Cruz 2022; Manzo and Carrión 2022; Mundaca 2019). However, more research is needed to ascertain the underlying causes of forest loss increase in the last six years.

Processes of forest loss are usually complex, multifactorial, exhibit fundamental socioeconomic and political ties, and their causes (and often their consequences) extend beyond local scales (Geist and Lambin 2001; Lambin, Geist, and Lepers 2003; Seymour and Harris 2019). Tropical deforestation has been studied at global, regional, and local scales for several decades. Most studies conclude that agricultural expansion and forest clearing to produce commodities are the main proximate causes of forest loss (Curtis et al. 2018). For instance, Zeng, Gower, and Wood (2018) found that forest loss in the mountains of Thailand has been increasing due to the expansion of agricultural lands for growing maize, which, in turn, is related to the global market price of corn. In the Democratic Republic of Congo, in contrast, forest loss is related to mining activities and the expansion of what the authors call *the rural complex* into areas of primary forest (Potapov et al. 2012; Molinario, Hansen, and Potapov 2015). As previously mentioned, research conducted in Central America has found that narcotrafficking and other illicit activities are also relevant contributors to forest loss (Tellman et al. 2020).

Although population growth often appears as a main cause of forest loss in tropical deforestation studies, these claims are not always sustained by census data and often simplify the complex forces underlying deforestation (Lambin et al. 2001). Contrary to the prevailing narrative, Defries et al. (2010) found that urban population growth outside the forests (as opposed to rural population growth) and an increasing trend of agricultural production for export are the main drivers of forest loss in tropical regions. Furthermore, certain cultural activities actually increase tree cover, challenging the idea that local land use always degrades forests (Fairhead and Leach 2014). In some cases, population growth shows a positive relation with forest loss (e.g. Jha and Bawa 2006), but it is never the sole nor the underlying (ultimate) cause of forest cover change (Lambin et al. 2001). Generally, when population growth is directly

related to forest loss, there are underlying political or institutional mechanisms pushing people into forested and less populated areas. This has occurred, for instance, when governments seek control over contested territories and force people to relocate, or when people are displaced due to the establishment of forest management units (like national parks) or the criminalization of their traditional practices (Peluso and Vandergeest 2014). Population trends (both growth and decline) have different effects on forests, depending on the economic, social, political, and cultural characteristics locally shaping land use and management. In the NMO, for instance, forest loss has increased in the last decade, but population has remained constant and there are more people emigrating from the region than immigrating (CEIEG 2022a, 2022b), suggesting that socioeconomic and political drivers other than population growth are shaping forest cover change in the region.

Forest conservation in the Northern Mountains of Oaxaca

The understanding (or lack thereof) of forest dynamics and their socio-ecological causes and consequences can define what type of forest conservation projects are recommended, carried out, and supported. Despite the recent rise of forest loss in the NMO, this region has also been in the spotlight due to several successful stories of forest conservation, especially in the subregion Ixtlán, also known as *Sierra de Juárez* (e.g. D. Bray 2021). In the NMO, protected natural areas established and controlled by the government are nonexistent. Rather, local communities have developed different management strategies to protect their forest while producing timber and crops, or by carrying out ecotourism activities (Pazos-Almada and Bray 2018). Some communities have officially certified their territories as areas voluntarily designated for conservation (shown in Figure 4.1); others are enrolled in programs of payment for ecosystem services; and others have preferred to manage their territories without government interference (Pazos-Almada and Bray 2018; Velasco Murguía et al. 2014).

Interestingly, the subregion with more community-based conservation projects (Ixtlán) exhibits less forest loss than most areas in the NMO. Although forest loss in Ixtlán also increased in 2015, in the last two decades it lost 7% of its forest cover, most of it outside areas designated for conservation. In contrast, Sierra Mixe lost 9.6% and Guevea de Humboldt lost 12.9% during the same period. Moreover, some studies report forest gain in Ixtlán associated with the establishment of community-based conservation projects (Velasco Murguía et al. 2014). These

results suggest that forest conservation projects in Ixtlán have been successful in maintaining forests in designated areas for conservation.

The fact that forest loss has been uneven over the region, with Sierra Mixe experiencing three times the amount of forest loss than that experienced in other subregions, requires a deeper analysis. On one hand, it has been deemed difficult to establish and keep forest conservation projects in this subregion due to land tenure conflicts (Toledo-Aceves et al. 2011). The lack of established conservation strategies could be giving way to greater deforestation rates in the subregion in comparison to the others. This could also be true for the subregion Guevea de Humboldt, which also lacks structured conservation projects and lost a significant percentage of evergreen forest during the last decade. On the other hand, restraining productive activities in protected areas could result in the outsourcing of agricultural activities or wood extraction elsewhere, causing forest loss in other places, exemplifying what Clark and York have called "rifts and shifts" (B. Clark and York 2008; Meyfroidt et al. 2013). The displacement of land use across regions, and even across nations, has been described in cases showing forest recovery, where the local demand for food or wood is provided by imported goods, instead of being produced *in situ*, thus removing some pressure off local forests while transferring it to more distant ones (Pfaff and Walker 2010; Meyfroidt, Rudel, and Lambin 2010). Moreover, studies in other tropical montane regions have shown an increase in forest loss in lands surrounding protected areas following their establishment (Liu et al. 2022). Because most areas with forest conservation plans in the NMO have been developed by local communities that, besides sparing land for conservation, maintain productive lands with timber and self-subsistence agriculture, it is unlikely that they are shifting to an economy based on importing goods. Most likely, the community-based forest conservation conducted in Ixtlán provides a myriad of positive examples and ideas for other tropical montane regions (D. B. Bray 2020). Nevertheless, a thorough examination of the unintended consequences of forest recovery and conservation projects in the NMO has not been conducted. This is important not only to evaluate the benefits and consequences of the already established conservation plans, but also to assess whether similar forest conservation strategies could be successfully carried out in other tropical montane landscapes, including areas within the NMO.

The conversation around how to protect forests while producing food for the global demand has revolved around two opposite ideas: sparing land to protect forests while

intensifying agriculture in the remaining lands at one pole, or producing food with environmentally friendly agricultural practices while protecting forests in the same landscape at the opposite pole (Kremen 2015). Criticized by its simplistic approach, the land-sparing/land-sharing academic debate seems to be outdated (Bennett 2017; J. Fischer et al. 2014). In practice, however, limiting human activities in large portions of land in order to protect whatever *primary* forest is left is currently the most common conservation approach in tropical regions (Terraube and Fernández-Llamazares 2020; Seymour and Harris 2019). Meanwhile, an agricultural intensification model keeps dominating agricultural production and sprawling along with the expansion of agriculture itself (Zabel et al. 2019). It seems, then, that a land-sparing approach is the one ruling the conservation agenda globally. In this context, conservation projects like those taking place in Ixtlán provide practical and nuanced examples of the land-sparing *vs.* land-sharing scheme (J. Fischer et al. 2017). On one hand, the projects in Ixtlán are sparing land for protecting forests while producing agricultural or timber commodities, as well as self-subsistence agriculture. On the other hand, these projects retain some of the land-sharing principles, such as low-intensity agricultural practices and a community-based organization, where conservation plans are agreed on in assemblies, instead of being enforced and regulated by the government. Importantly, this marks a fundamental difference with fortress conservation (the extreme model of land-sparing), which prioritizes conservation at the expense of local livelihoods, displacing people from their homes and restricting their access to basic resources through law enforcement (West, Igoe, and Brockington 2006; Domínguez and Luoma 2020; Brockington and Igoe 2006).

Conservation agendas are moving beyond a strict land-sparing model as the human-rights and ethical problems brought by fortress conservation projects are highlighted, and the negative impact of certain modes of agriculture on tropical forests is demystified (Ravikumar et al. 2017; Domínguez and Luoma 2020). In this context, the role of agroecological systems as a possible solution to produce food while conserving forests is gaining attention (Perfecto and Vandermeer 2008; Perfecto and Vandermeer 2010). So is the fact that shifting cultivation does not always drive deforestation. For instance, FAO's *State of Forests* (2016) puts agroecology at the forefront of the conversation on forest conservation solutions. More broadly, the establishment of agroecological management at large scales has resulted in forest cover increase over the last decades in countries like Cuba, where agroecology is practiced at a national level (Betancourt 2020). Similarly, recent analyses on global forest loss trends like GFW explicitly nuance the role

94

of shifting agriculture as a proximate cause of deforestation (Curtis et al. 2018). This is essential, since accepting and understanding the current and historical role of agriculture in shaping forested landscapes is a first critical step in reframing the food-conservation challenge into a more inclusive conversation centered both in non-human and human wellbeing.

People living in the NMO have depended on forest resources and agricultural production for hundreds to thousands of years (de Teresa 2011). Despite the relationship that local communities have with their territories has been deeply shaken by colonization and the incorporation of agricultural production to capitalism, agriculture remains an important part of their livelihood (de Teresa 1999; Aquino Vásquez, Ramírez Juárez, and Clark Tapia 2021). In this way, peasant agriculture and indigenous traditions are entwined with migration (seasonal or permanent, national or international), off-farm work diversification, the incorporation of industrial agricultural techniques, and the integration of local products to the global market, shaping rural life in the mountains (S. Hecht 2010; Aquino Vásquez, Ramírez Juárez, and Clark Tapia 2021; Kay 2008). Regarding forest conservation, understanding this complex reality is fundamental for the future of tropical montane forests.

For several reasons, the NMO provides an excellent opportunity to carry out conservation plans where low-input, wildlife-friendly agriculture and sustainable forest management coexist. First, industrial agriculture is naturally limited in montane landscapes due to the steep terrain, hindering the use of machinery and the conversion of forest in very large extensions of land. Perhaps more importantly, the intensification of agriculture in tropical hillsides has multiple negative and undesirable effects on soils and water resources (Turkelboom, Poesen, and Trébuil 2008). Far from meaning that agriculture is completely unsuitable for tropical mountains, this means that non-industrial agriculture may represent a better strategy for the sustainable management of tropical montane landscapes. Second, rural life in the NMO is characterized by its deep roots in peasant agriculture[2], which can be a meaningful source of traditional knowledge on farming, as well as a fundamental element for food security in the region (Bocco 1991; Altieri, Anderson, and Merrick 1987; Rivero-Romero et al. 2016; Bellon et al. 2021). Third, in the state of Oaxaca, 82% of forests are owned by *ejidos* or communities−two forms of common

---

[2] In contrast to capitalist agriculture, peasant agriculture is based on subsistence production and simple commodity production, and it depends on family labor and access to land (Bryceson 2000; Akram-Lodhi and Kay 2010; De Janvry 1981). A peasant household constitutes simultaneously a unit of production, consumption and reproduction (De Janvry 1981).

property created after the Mexican Revolution as part of a land reform that granted land to small-scale farmers and territorial rights to indigenous communities (Madrid et al. 2009; Morett-Sánchez and Cosío-Ruiz 2017). Most forested land in the NMO is in communal land, where the collective decisions taken on the use of land have proven to be a successful path to sustainable forest management and regrowth (D. B. Bray 2020; Porter-Bolland et al. 2012).

CONCLUSIONS

In this chapter, I sought to describe the general trend of forest loss and conservation in the NMO and how they relate to land use. I found that forest loss in the NMO remained almost constant for many years but increased in the last six years, especially in the subregion Sierra Mixe. The most affected ecosystems were tropical evergreen forests and TMCF. The reasons behind the sudden increase of forest loss in 2015 are unclear, but agricultural surveys show a significant expansion of pasturelands in the last decade, suggesting that forest or shaded coffee farms conversion to cattle ranches may be driving forest loss in the region. In addition, land-use change due to illicit activities may also be playing an important role. These changes can have important implications for biodiversity and carbon dynamics, and must be monitored.

Although the area, rate, and time of change in the two data sets used here (SIAP and GFC) are not completely compatible, this comparison provides useful insights on the relationship between agricultural and forest cover change. The mismatch between both datasets is not surprising, since they are estimated in very different ways. SIAP depends on surveys at the municipality level and presents "broader-brush" information, while GFC is based on remote sensing data with a higher spatial resolution, but does not provide land-use information. To assess the fate of pixels experiencing forest loss with precision, it would be necessary to make land-cover maps that can be contrasted with SIAP, or other similar databases. The results shown here, then, are general trends that provide a starting point for future research.

Community-based conservation projects are having a positive impact locally, especially in the subregion Ixtlán, where most conservation projects are located, and which showed lower forest loss than other subregions. Other conservation lands exist in the region but are not included in the analysis due to lack of geographic data. These include forests managed sustainably by local communities and land under payment for ecosystems services. Despite local

communities are making very important efforts to protect forests, forest loss continues to increase, counteracting forest gain.

The effects of forest loss depend on the type of LULCC taking place. The spatial pattern of forest loss (small and scattered patches) points to a possible case of shifting agriculture, which could not necessarily lead to deforestation if vegetation is allowed to regrow. However, the substantial increase of pasturelands in the region suggest that forests are being converted to cattle ranches, indicating that at least a proportion of forest cover has been permanently lost. A deeper land system analysis with ground data is needed to assess if this is indeed the case, as well as the underlying cause driving the change.

Considering the current state of deforestation in the tropics and in the NMO, there is no doubt that conservation plans are urgently needed to protect tropical montane forests. It is fundamental, however, for these plans to understand the socioecological complexity of forest dynamics, avoid simplistic solutions based on mainstream and unquestioned narratives, and that local communities become the main actors of forest conservation. This is particularly important in regions like the NMO, where most forests are located in communal land and have a long indigenous history and tradition. The NMO thus provides, at the same time, an example of forest loss in tropical mountains, as well as the potential for holistic forest conservation that could arise from the complex rurality of the Global South.

CHAPTER 5
CONCLUSIONS

This dissertation sought to broaden our understanding of the role of land use in shaping forest structure and dynamics in tropical mountains. To do so, I used the Northern Mountains of Oaxaca as a study case, a mountain range located in southern Mexico. I investigated changes in vegetation across space and time within this region, with a particular focus on an ecosystem known as tropical montane cloud forest. Using a combination of remote sensing and field data, I answered questions related to the dynamics and structure of cloud forest at local and regional scales (hence the title "from plot to region"). While field data provided information at local levels, such as the number of tree species and their size, with remote sensing data I was able to work at broader temporal and spatial resolutions. The main results of this dissertation can be summarized in the following points:

(1) Tropical montane cloud forests are embedded in dynamic and heterogeneous landscapes that greatly influence their structure. Such dynamism is mainly driven by land use.

(2) Forest structure and aboveground biomass change along an elevation gradient. Forests at the lower end of the elevation gradient experience warmer and wetter conditions, as well as greater land-use intensity. As elevation increases, temperature, precipitation, and land-use intensity decrease. As a result, aboveground biomass increases with elevation, contrary to the expected trend. This spatial pattern can be best predicted by the interactive effects of land use and environmental factors, with land use having a larger role within the region.

(3) The relationship between species diversity and aboveground biomass is weak and scale-dependent.

(4) It is possible to incorporate the effect of land use on forest structure in models and maps of aboveground biomass using remote sensing data. Specifically, forest disturbance events and trends can be assessed using algorithms that detect forest cover change and by calculating the variability of vegetation over time in Landsat time series.

(5) The remote sensing variables derived from the time series analyses can be applied as inputs in models of aboveground biomass. This approach has the potential to decrease the uncertainty related to land use in forest structure models.

(6) In the last six years, forest loss has greatly increased in the Northern Mountains of Oaxaca. Forest loss is uneven across the region, and affects tropical evergreen forests and cloud forests the most. Although the drivers of forest loss are still uncertain, the area devoted to pasture has increased in the last decades, suggesting that forest or coffee farm conversion to grazing lands could be playing an important role.

(7) Community-based conservation projects taking place in the region are associated to less forest loss. However, their positive effects are local and, overall, the region is experiencing more forest loss than gains.

These results are relevant for several reasons. On the one hand, they highlight the need to consider land use in ecological studies even when the focus is seemingly unrelated to anthropogenic activities. For instance, accurately quantifying AGB across space requires a deep understanding of the composition and configuration of landscapes, including the different uses given to land and management strategies, which greatly influence the factors shaping plant growth, and therefore, forest structure and composition. The high dynamisms of these landscapes show that static land cover categories are insufficient to understand the role of land use in forested landscapes. Moreover, agricultural practices influence forested landscapes in different ways. A large permanent cattle ranch will have a different effect on nearby forests than a low-input shaded coffee farm. These differences have seldom been analyzed at landscape to regional scales.

Based on the results presented here, I suggest conducting further studies on the role of land use in montane forests considering not only broad categories based on land cover (such as cropland, grazing land and forest), but also management strategies and common agricultural practices. This will require analyses across scales: local studies for gaining a deeper understanding on land management and practices as well as their ecological effects in detail; and landscape and regional studies to understand feedbacks and synergies of local changes at larger extents. Both up- and downscaling data implies losing information, thus, continuous dialogue between data acquired on the ground and at larger extents is fundamental. In this sense, remote sensing techniques are excellent candidates to bridge local to regional studies.

The large amount of remote sensing data and computer power currently available allow to study dynamic landscapes considering their complexity and nuances. So far, however, remote sensing techniques have been applied to monitor forest and detect forest loss using series of

images acquired over time, or to describe land features (e.g., land cover, biomass, leaf area) at a single moment. In both approaches anthropogenic activities are usually masked out (except when the objective is to show the direct effect of humans on the environment). Beneath the seemingly objectivity of land cover categories and forest masks lies the complex rural dynamics shaping forests and their agricultural matrix, which are often lost in the process of generalization at regional scales. Thus, remote sensing studies could be enriched by applying different techniques together and, more importantly, by asking questions that have not been explored within mainstream remote sensing research. This includes engaging with the rural reality of the Global South.

In this dissertation I show that there are possible ways to include the recent history of a landscape and the complex dynamics of rural landscapes in the description of land features by combining the two main approaches applied in remote sensing analyses (monitoring over time and single snapshots) and by explicitly including land use in research questions. These are just the first steps in the direction of a remote sensing research situated on the rural context of tropical regions. Many questions are worth exploring in the future, for instance, can the effect of different agricultural practices on forest ecology be accurately study at regional scales using remote sensing techniques? What type of information is lost and gained in the process of generalizing local processes at larger spatial extents? How do global forces driving agrarian change translate into changes in forest ecology and how can remote sensing be used to better understand these processes in tropical regions? In this sense, my suggestion to remote sensing studies of tropical regions is to continue exploring methods and lines of inquiry that engage with rural realities considering their socioeconomic and political context.

The results of my work have implications beyond academic endeavors. Despite major commitments have been made at national and international summits to reduce deforestation and climate change, forest loss continues to increase in tropical regions, and it seems to be accelerating in tropical mountains. Understanding the causes and consequences of land use and agrarian change on forested landscapes is fundamental for developing adequate policies and projects that effectively protect forests. In particular, I would recommend to further explore the effectiveness of payment for ecosystem services and community-based forest conservation projects in the NMO, as well as the expansion of cattle ranches and the decline in coffee production, as I believe these factors are major drivers of forest dynamics in the region.

Moreover, similar processes of agrarian change are probably taking place in other tropical mountains, underscoring the need to understand these dynamics further in the NMO and elsewhere.

       In conclusion, in this dissertation I provide new insights on the spatial patterns of forest structure and aboveground biomass in a tropical mountain range, and how these patterns relate to land use. The results presented here are relevant for understanding forest dynamics in the Northern Mountains of Oaxaca and in other tropical mountains. Besides providing new estimates of aboveground biomass for the region as well as the underlying mechanisms to explain its distribution, I also offer new methods that have the potential to improve models of forest structure and aboveground biomass elsewhere. Finally, this dissertation marks the beginning of a research agenda on the relationship between forest ecology and agrarian change that I would like to develop further in the future.

APPENDIX A
SUPPORTING INFORMATION FOR CHAPTER 2

Tables

Table S2.1. Variables used in this study at three sampling units: site, plot, and tree.

Level	Variable	Units	Explanation	Source
Site	Site ID	-	Unique identifier of site	FI
	Longitude	Decimal degrees	Geographic coordinate at site centroid	FI
	Latitude	Decimal degrees	Geographic coordinate at site centroid	FI
	Altitude	m	Elevation above sea level at site centroid	FI
	Temperature	Degrees C	Annual mean temperature	WorldClim
	Precipitation	mm	Annual mean precipitation	WordClim
	Slope	Degrees	Average slope	Calculated from NASA's Shuttle Radar Topography Mission digital elevation data (~30 m resolution), averaged by plot
	Aspect	Degrees	Average aspect	Calculated from NASA's Shuttle Radar Topography Mission digital elevation data (~30 m resolution), averaged by plot
	Plot number	Plot	Number of plots in site (goes from 1 to 4)	FI (edited after data quality control)
	Tree number	Tree	Site's average number of trees measured	Derived from FI raw data, averaged by plot
	Tree density	stems/ha	Average number of trees per area in site	Derived from FI raw data, averaged by plot
	Basal area	m/ha	Site's average basal area	Derived from FI raw data, averaged by plot
	Tree height	m	Site's average tree height	Derived from FI raw data, averaged by plot
	Lorey's height	m	Mean tree height weighted by their basal area	Derived from FI raw data, averaged by plot
	Aboveground biomass (AGB)	Mg/ha	Site's average AGB	Averaged by plot, calculated with allometric equations

				using FI raw data
	Shannon (H)	bits	Diversity index	Calculated using FI raw data, averaged by plot
	Species richness	Species	Site's average number of species	Calculated using FI raw data, averaged by plot
	Landscape composition	-	Site's patchiness, goes from 0, when all plots in site are mature forests, to 1, when all plots in site are very young forests or agricultural lands	Calculated using plot's successional stage
	Disturbance by agriculture	-	Forest disturbance related to agricultural activities, aggregated, and averaged by site; it goes from 0 when no disturbance was detected to 4 when disturbance was severe	Derived from FI disturbance database
	Disturbance by grazing	-	Forest disturbance related to cattle grazing, aggregated, and averaged by site; it goes from 0 when no disturbance was detected to 4 when disturbance was severe	Derived from FI disturbance database
Plot	Plot ID	-	Unique identifier of plot	FI
	Latitude	Decimal degrees	Geographic coordinate	FI
	Longitude	Decimal degrees	Geographic coordinate	FI
	Altitude	m	Elevation above sea level	FI
	Slope	Degrees	Hillslope steepness	Calculated from NASA's Shuttle Radar Topography Mission digital elevation data (~30 m resolution)
	Aspect	Degrees	Direction that the slope faces (a.k.a., exposure)	Calculated from NASA's Shuttle Radar Topography Mission digital elevation data (~30 m resolution)
	Epiphytes	-	Whether epiphytes are	FI

			present in plot. This variable was only used to select cloud forest sites.	
	Tree number	tree	Total number of trees measured in plot	Calculated using FI raw data
	Tree density	stems/ha	Number of trees per area	Calculated using FI raw data
	Tree height	m	Plot's average tree height	Calculated using FI raw data
	Lorey's height	m	Tree's height weighted by their basal area	Calculated using FI raw data
	Basal area	m/ha	Sum of tree's basal area in relation to plot's area	Calculated using FI raw data
	Aboveground biomass (AGB)	Mg/ha	Sum of tree's AGB per area	Calculated with allometric equations using FI raw data
	Shannon (H)	bits	Diversity index	Calculated using FI raw data with package vegan in R
	Species richness	Species	Total number of species in plot	Calculated using FI raw data
	Successional stage	-	Whether very young, young, or mature forest	Calculated using FI raw data with a non-hierarchical cluster analysis (k-means)
Tree	Site	-	Unique identification of site	FI
	Plot_id	-	Unique identification of plot	FI
	Species	-	Taxonomic name	FI corrected with Taxonomic Name Resolution Service
	Family	-	Taxonomic family	FI corrected with Taxonomic Name Resolution Service with BIOMASS function correctTaxo
	Common name	-	Common name	FI
	Status	-	Alive or dead	FI
	Life form	-	Tree, shrub, palm tree, fern, or liana	FI
	Height	m	Individual total height	FI
	Diameter at breast height (DBH)	cm	Diameter of trunk at 1.3 m from the ground	FI

Basal area	m	Cross sectional area of trunk at 1.3 m from the ground	FI
Mean wood density	g/cm^3	Wood density as recorded in scientific literature	Calculated with BIOMASS function getWoodDensity
Aboveground biomass (AGB)	Mg	Dry mass of the aboveground component (i.e., excluding roots) of plants	Calculated with allometric equations

Table S2.2. Generic and specific allometric equations used in this study to estimate aboveground biomass.

Species	Allometric equation	Reference
Abies sp.	[0.0754]*[DBH^2.513]	Avedaño et al., 2009
Alchornea latifolia	[Exp[-3.363]*[DBH^2.2714]*[TH^0.4984]	Aquino-Ramírez et al., 2015
Alnus acuminata	[Exp[-2.14]*[DBH^2.23]]	Acosta-Mireles et al, 2002
Alnus jorullensis	[0.0195]*[DBH^2.7519]	Carrillo et al., 2014
Brosimum alicastrum	[0.479403]*[DBH^2.0884]	Rodríguez-Laguna et al., 2008
Cecropia obtusifolia	[[0.000022]*[D^1.9]*[H]] + [[-0.56 + 0.02[D^2] + 0.04[H]]/10^3]	Hughes et al., 1999
Citrus sp.	[-6.64]+[0.279*BA]+[0.000514*BA^2]	Schroth et al., 2002
Clethra sp.	[Exp[-1.90]*[DBH^2.15]]	Acosta et al., 2002
Clethra hartwegii	[Exp[-1.90]*[DBH^2.15]]	Acosta et al., 2002
Clethra mexicana	[0.4632]*[DBH^1.8168]	Acosta et al., 2011
Clethra pringlei	[0.067833]*[DBH^2.50972]	Rodríguez et al., 2006
Cordia alliodora	[10^-0.755]*[DBH^2.072]	Segura et al., 2006
Cupressus lusitanica	[0.5266]*[DBH^1.7712]	Vigil, 2010
Dendropanax arboreus	[0.037241]*[DBH^2.99585]	Rodríguez-Laguna et al., 2008
Eugenia sp.	[0.4600]+[[0.0370]*[DBH^2]*TH]	Cairns et al., 2003
Fraxinus uhdei	[362.129]*[[3.1416]*[[[[DBH^2]/4]]^1.100]]	Cano, 1994
Heliocarpus appendiculatus	[[Exp[4.9375]] * [[DBH^2]^1.0583]] * [1.14]/ 1000000	Hughes et al., 1999
Inga sp.	[Exp[-1.76]*[DBH^2.26]]	Acosta et al., 2002
Inga vera	[Exp[-1.76]*[DBH^2.26]]	Acosta et al., 2002
Inga punctata	[Exp[-3.363]*[DBH^2.4809]*[TH^0.4984]	Aquino-Ramírez et

		al., 2015
Juglans olanchana	[10^-1.417]*[DBH^2.755]	Segura et al., 2006
Juniperus flaccida	[0.209142]*[DBH^1.698]	Rodríguez et al., 2009
Liquidambar sp.	[Exp[-2.22]*[DBH^2.45]]	Acosta et al., 2002
Liquidambar styraciflua	[0.180272]*[DBH^2.27177]	Rodríguez et al., 2006
Nectandra ambigens	[[Exp[4.9375]]*[[DBH^2]^1.0583]]*[1.14]/1000000	Hughes et al., 1999
Pinus sp.	[0.058]*[[[DBH^2]*TH]^0.919]	Ayala, 1998
Pinus ayacahuite	[0.058]*[[[DBH^2]*TH]^0.919]	Ayala, 1998
Pinus devoniana	[0.182]*[DBH^1.936]	Méndez et al., 2011
Pinus herrerae	[0.1354]*[DBH^2.3033]	Návar, 2009
Pinus leiophylla	[[Exp^-3.549]*[DBH^2.787]]]	Návar, 2009
Pinus oocarpa	[0.058]*[[[DBH^2]*TH]^0.919]	Ayala, 1998
Pinus patula	[0.0514]*[DBH^2.5222]	Pacheco, 2011
Pinus pseudostrobus	[0.058]*[[[DBH^2]*TH]^0.919]	Ayala, 1998
Prunus persica	[Exp[-2.76]*[DBH^2.37]]	Acosta, 2003
Psidium guajava	[0.246689]*[DBH^2.24992]	Rodríguez-Laguna et al., 2008
Quercus sp.	[0.1269]*[DBH^2.5169]	González, 2008
Quercus candicans	[[Exp[-4.775313]*[DBH^1.798292]*[TH^1.570775]]+[[Exp[-3.547008]*[DBH^2.593972]]+[[Exp[-4.752007]*DBH^2]]	Cortés-Sánchez et al., 2019
Quercus crassifolia	[0.283]*[[[DBH^2]*TH]^0.807]	Ayala, 1998
Quercus laurina	[0.283]*[[[DBH^2]*TH]^0.807]	Ayala, 1998
Quercus obtusata	[[exp[-3.53684]*[DBH^2.043763]*[TH^0.759522]]+[[Exp[-5.803952]*[DBH^2*TH]^1.224292]]+[[Exp[-6.181035]*[DBH^2.488617]]	Cortés-Sánchez et al., 2019
Quercus peduncularis	[Exp[-2.27]*[DBH^2.39]]	Acosta, et al., 2002
Quercus rugosa	[0.283]*[[[DBH^2]*TH]^0.807]	Ayala, 1998
Trema micrantha	[-2.305 + 2.351 * ln[DBH]] * 1.033	Van Breugel et al., 2011
Trichilia havanensis	[0.130169]*[DBH^2.34924]	Rodríguez-Laguna et al., 2008
Trichospermum mexicanum	[0.449]*[DBH^2]-33.565	Montes de Oca-Cano et al., 2020
Zanthoxylum sp.	[0.00166]*[DBH^3.6586]	Manzano, 2010

Tropical trees	0.0673 * (WD * H * DBH^2)^0.976	Chave et al., 2014

Table S2.3. Results of ANOVA and Tukey HSD test on stem density, Lorey's height, basal area, and aboveground biomass (AGB) between forest plots (n= 160) at different successional stages (young fallows (F), young forest (Y), and mature forest (M)). Significant p-values are shown in bold.

Response	ANOVA		Tukey HSD			
	F	p	Comparison	Estimate	95% CI	p
Stem density	80.86	**<2e-16**	F-Y	711.69	(576.74, 846.64)	**9.50e-14**
			F-M	500.86	(330.19, 671.52)	**2.85e-10**
			Y-M	-210.83	(-384.32, -37.33)	**1.27e-02**
Lorey's height	157.90	**<2e-16**	F-Y	2.38	(1.12, 3.65)	**4.63e-05**
			F-M	11.93	(10.33, 13.54)	**9.41e-14**
			Y-M	9.54	(7.92, 11.17)	**9.41e-14**
Basal area	197.50	**<2e-16**	F-Y	17.88	(14.32, 21.43)	**9.81e-14**
			F-M	36.54	(32.04, 41.04)	**9.41e-14**
			Y-M	18.66	(14.09, 23.24)	**1.22e-13**
Wood density	9.77	**<0.001**	F-Y	0.07	(0.03, 0.12)	**3.74e-4**
			F-M	0.08	(0.02, 0.13)	**2.87e-3**
			Y-M	0.005	(-0.05, 0.06)	0.96
AGB	135.70	**<2e-16**	F-Y	118.30	(81.62, 154.99)	**6.50e-12**
			F-M	321.48	(275.08, 367.88)	**9.41e-14**
			Y-M	203.17	(156.00, 250.34)	**1.21e-13**

Table S2.4. Results of ANOVA and Tukey HSD test on tree size contribution to stem density and aboveground biomass (AGB) between tree size classes in TMCF plots (n= 160). Trees were classified in six size classes according to their DBH as follows: class 1: DBH < 10 cm; class 2: DBH 10-20 cm; class 3: DBH 20-30 cm; class 4: DBH 30-40 cm; class 5: DBH 40-50 cm; class 6: DBH > 50 cm. Significant p-values are shown in bold.

Response	ANOVA		Tukey HSD			
	F	p	Comparison	Estimate	95% CI	p
Contribution to stem density proportion	129	**<2e-16**	1-2	0.144	(0.09, 0.19)	**1.75e-10**
			1-3	-0.123	(-0.17, -0.07)	**1.92e-10**
			1-4	-0.193	(-0.24, -0.14)	**1.75e-10**
			1-5	-0.223	(-0.28, -0.16)	**1.75e-10**
			1-6	-0.236	(-0.30, -0.17)	**1.75e-10**
			2-3	-0.267	(-0.31, -0.22)	**1.75e-10**
			2-4	-0.337	(-0.38, -0.28)	**1.75e-10**
			2-5	-0.368	(-0.42, -0.30)	**1.75e-10**
			2-6	-0.380	(-0.44, -0.31)	**1.75e-10**
			3-4	-0.069	(-0.12, -0.01)	**2.69e-03**
			3-5	-0.100	(-0.16, -0.03)	**7.57e-05**
			3-6	-0.112	(-0.17, -0.03)	**1.77e-05**
			4-5	-0.030	(-0.09, 0.03)	0.75
			4-6	-0.043	(-0.11, 0.02)	0.46

			5-6	-0.012	(-0.08, 0.06)	0.99
Contribution to AGB proportion	34.13	**<2e-16**	1-2	0.19	(0.12, 0.25)	**1.75e-10**
			1-3	0.18	(0.11, 0.24)	**1.76e-10**
			1-4	0.18	(0.10, 0.25)	**2.11e-10**
			1-5	0.23	(0.14, 0.31)	**1.76e-10**
			1-6	0.36	(0.27, 0.45)	**1.75e-10**
			2-3	-0.01	(-0.07, 0.05)	0.99
			2-4	-0.01	(-0.08, 0.05)	0.99
			2-5	0.03	(-0.04, 0.12)	0.82
			2-6	0.17	(0.08, 0.26)	**4.92e-07**
			3-4	-0.00	(-0.07, 0.07)	1.00
			3-5	0.04	(-0.03, 0.13)	0.60
			3-6	0.18	(0.09, 0.27)	**1.33e-07**
			4-5	0.04	(-0.04, 0.13)	0.63
			4-6	0.18	(0.09, 0.28)	**4.11e-07**
			5-6	0.13	(0.03, 0.24)	**2.70e-03**

Table S2.5. Results of two-way ANOVA on tree size contribution to stem density and aboveground biomass (AGB) between tree size classes, forest successional stage (young fallows (F), young forest (Y), and mature forest (M)), and their interaction in TMCF plots (n= 160). Trees were classified in six size classes according to their DBH as follows: class 1: DBH < 10 cm; class 2: DBH 10-20 cm; class 3: DBH 20-30 cm; class 4: DBH 30-40 cm; class 5: DBH 40-50 cm; class 6: DBH > 50 cm. Significant p-values are shown in bold. Tukey HSD results in Github repository.

Response	Explanatory	F	*p*
Contribution to stem density proportion	Size class	144.038	**< 2e-16**
	Successional stage	19.048	**9.43e-09**
	Size class:Successional stage	4.641	**2.15e-06**
Contribution to AGB proportion	Size class	41.454	**< 2e-16**
	Successional stage	53.949	**< 2e-16**
	Size class:Successional stage	3.804	**5.35e-05**

Table S2.6. Results of one-way ANOVA on the contribution to stem density and aboveground biomass (AGB) in each tree size class between forest plots at different successional stages (young fallows (F), young forest (Y), and mature forest (M)). Trees were classified in six size classes according to their DBH as follows: class 1: DBH < 10 cm; class 2: DBH 10-20 cm; class 3: DBH 20-30 cm; class 4: DBH 30-40 cm; class 5: DBH 40-50 cm; class 6: DBH > 50 cm. Significant p-values (i.e., p < 0.05) are shown in bold. Tukey HSD results in Github repository.

ANOVA			
Response		F	p
Contribution to stem density	Size class 1	21.28	**9.05e-09**

within size classes between forest successional stage	Size class 2	2.20	0.11
	Size class 3	2.15	0.12
	Size class 4	8.17	**5.29e-04**
	Size class 5	7.93	**9.22e-04**
	Size class 6	6.84	**2.00e-03**
Contribution to AGB within size classes between forest successional stage	Size class 1	11.54	**2.33e-05**
	Size class 2	12.39	**1.03e-05**
	Size class 3	12.66	**9.89e-06**
	Size class 4	16.41	**7.37e-07**
	Size class 5	26.12	**9.67e-09**
	Size class 6	3.37	**0.04**

Table S2.7. Results of one-way ANOVA on the contribution to stem density and aboveground biomass (AGB) in forest plots at different successional stages (young fallows (F), young forest (Y), and mature forest (M)) between tree size classes. Trees were classified in six size classes according to their DBH as follows: class 1: DBH < 10 cm; class 2: DBH 10-20 cm; class 3: DBH 20-30 cm; class 4: DBH 30-40 cm; class 5: DBH 40-50 cm; class 6: DBH > 50 cm. Significant p-values (i.e., $p < 0.05$) are shown in bold. Tukey HSD results in Github repository.

ANOVA			
Response		F	*p*
Contribution to stem density within forest successional stage between size classes	F	18.96	**2.09e-15**
	Y	115.06	**5.18e-64**
	M	54.38	**4.47e-32**
Contribution to AGB within forest successional stage between size classes	F	11.89	**4.44e-10**
	Y	21.31	**6.95e-18**
	M	46.52	**6.47e-29**

Table S2.8. Moran's I statistics for multiple linear regression selected as the best model to explain aboveground biomass patterns in TMCF for neighborhoods of 10, 25, and 50 km of distance between sites (n = 40). This model includes three predictors: slope gradient, landscape composition, and disturbance by agricultural activities.

Distance between sites (km)	Moran's I	*p*
10	-0.049	0.51
25	-0.05	0.60
50	0.02	0.18

Figures

k = 2   k = 3

k = 4   k = 5
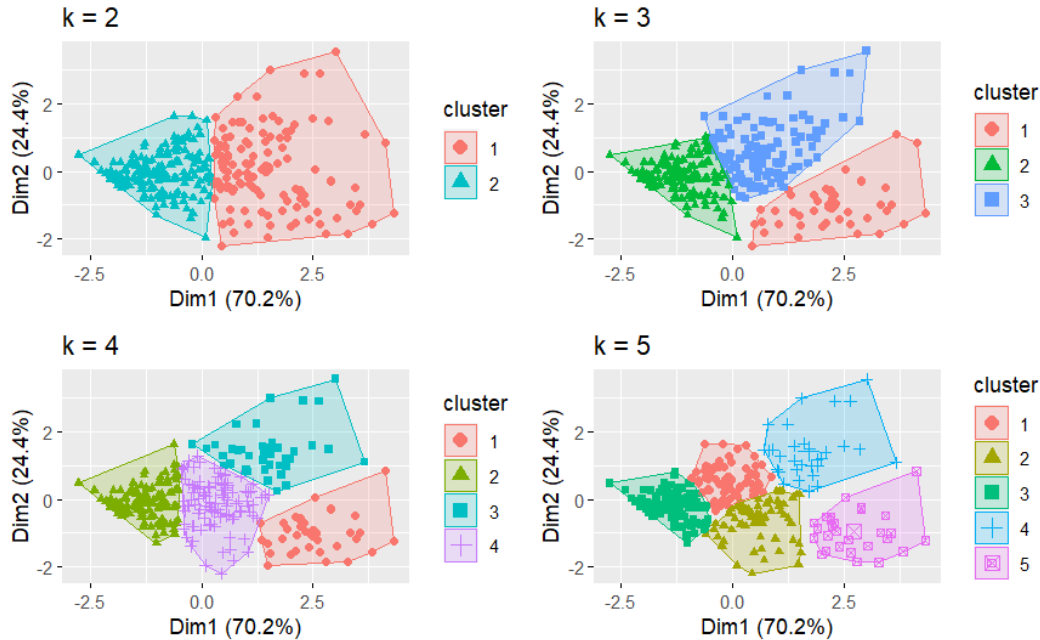
Figure S2.1. K-means cluster analysis on structural attributes (stem density, Lorey's height, and basal area) of TMCF plots showing two (to left), three (top right), four (bottom left) and five (bottom right) clusters. By comparing the four possible classifications with 30 indices, the three cluster classification was selected as the best one based on the majority rule. These three clusters match the expected structure found in young fallows, young forest, and mature forest in TMCFs.

	temp	precip	altitude	aspect_gee	slope_gee	sp_richness_site_av	shannon_av_site	simpson_av_site	av_agb_site	landscape	agriculture	grazing	log_agb
temp	1.00	0.76	-0.96	-0.27	0.32		0.11	-0.14	-0.41	0.59	0.44	0.16	-0.42
precip	0.76	1.00	-0.74	-0.21		0.10			-0.43	0.52	0.34		-0.42
altitude	-0.96	-0.74	1.00	0.23	-0.26	0.15	0.17	0.19	0.46	-0.64	-0.50	-0.18	0.49
aspect_gee	-0.27	-0.21	0.23	1.00	-0.26					0.05	-0.11		
slope_gee	0.32		-0.26	-0.26	1.00	-0.15				0.20	0.24	0.14	
sp_richness_site_av		0.10	0.15		-0.15	1.00	0.91	0.82	0.19	-0.37	-0.37	-0.39	0.38
shannon_av_site			0.17			0.91	1.00	0.98	0.16	-0.32	-0.28	-0.52	0.32
simpson_av_site	-0.14	-0.05	0.19			0.82	0.98	1.00	0.18	-0.32	-0.26	-0.56	0.31
av_agb_site	-0.41	-0.43	0.46			0.19	0.16	0.18	1.00	-0.86	-0.44		0.91
landscape	0.59	0.52	-0.64		0.20	-0.37	-0.32	-0.32	-0.86	1.00	0.53	0.12	-0.86
agriculture	0.44	0.34	-0.50		0.24	-0.37	-0.28	-0.26	-0.44	0.53	1.00	-0.18	-0.64
grazing	0.16		-0.18	-0.11	0.14	-0.39	-0.52	-0.56		0.12	-0.18	1.00	
log_agb	-0.42	-0.42	0.49			0.38	0.32	0.31	0.91	-0.86	-0.64		1.00

Figure S2.2. Correlation matrices showing the correlation between all pair of variables used in this study at site level (n= 40) in a graphic (left) and a numeric (right) way. Red colors indicate negative relations and blue indicate positive relations.
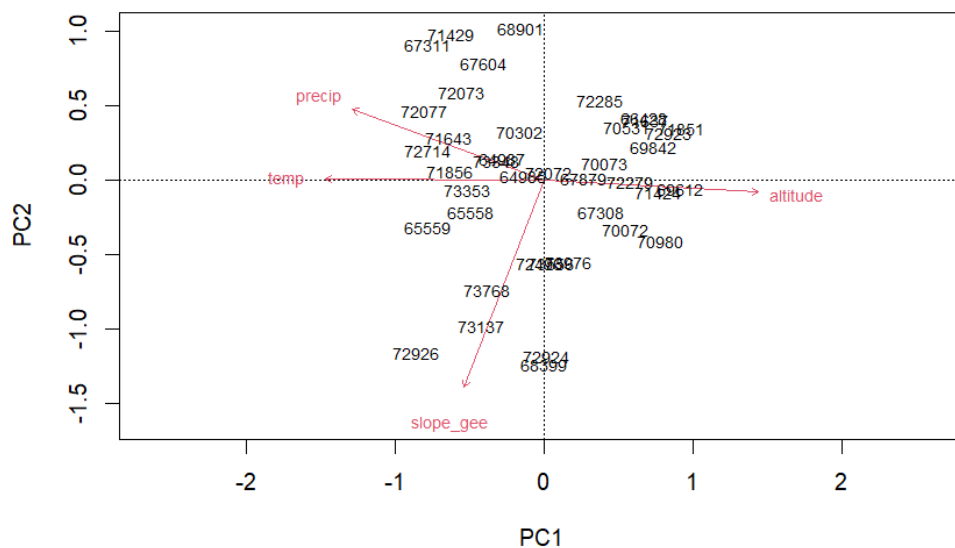
Figure S2.3. Principal component analysis (PCA) of climatic (temperature and precipitation) and topographic variables (slope and elevation) showing the two first principal components (PC1 and PC2). PC1 and PC2 explain 92% of the variation. PC1 explains 68% of variation and shows that there is a positive correlation between temperature and precipitation and a negative correlation between these two and elevation. Thus, PC1 represents an environmental gradient from warmer and wetter sites at lower elevations (negative values) to cooler and drier sites at higher elevations (positive values). Slope is not correlated to the other three variables, and it is the variable driving PC2.
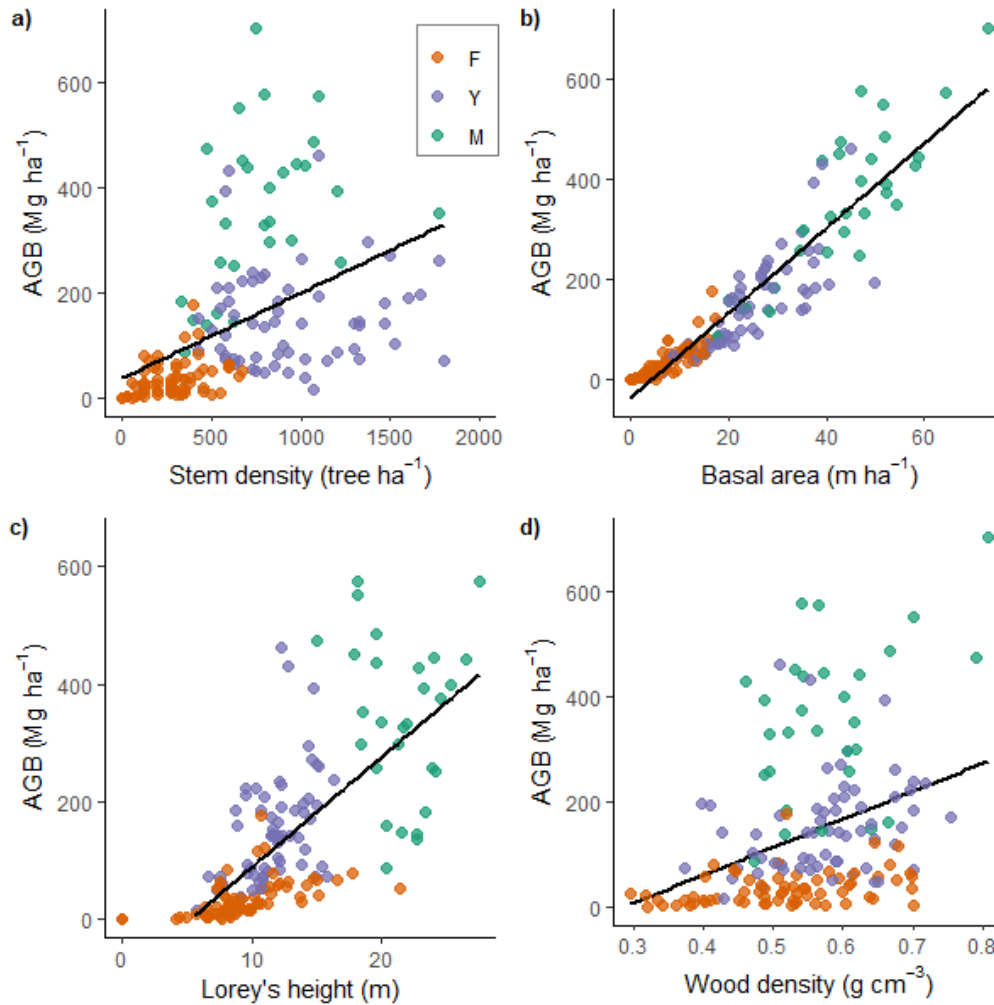
Figure S2.4. Relationship between aboveground biomass (AGB) and (a) stem density, (b) basal area, (c) Lorey's height, and (d) wood density in TMCF plots (n = 160) overlaid by their linear regression curves (black lines). Forest successional stage in plots is displayed in colors as follows: young fallows (F) in orange, young (Y) in purple, and mature (M) forests in green.

a)
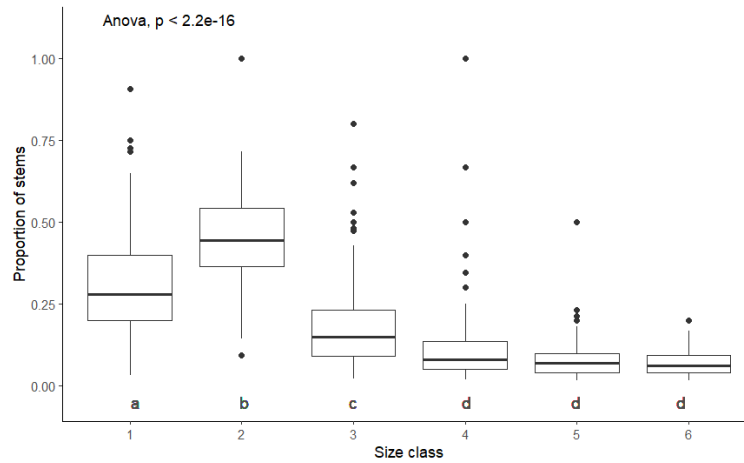
b)
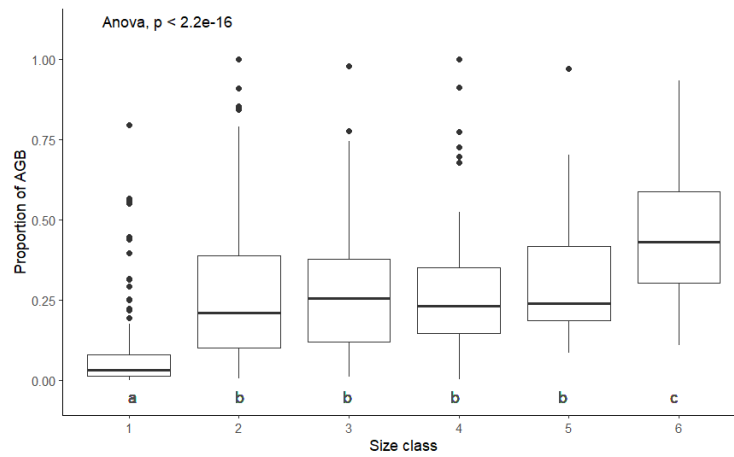
Figure S2.5. Contribution of tree size categories to a) stem density and b) aboveground biomass (AGB) in TMCF sites (n= 40). Trees were classified in six classes according to their DBH as follows: class 1: DBH < 10 cm; class 2: DBH 10-20 cm; class 3: DBH 20-30 cm; class 4: DBH 30-40 cm; class 5: DBH 40-50 cm; class 6: DBH > 50 cm. Letters indicate statistically significant differences between tree size classes assessed with a one-way ANOVA and Tukey HSD test (results shown in Table S2.4). Boxes sharing a letter are not statistically different.
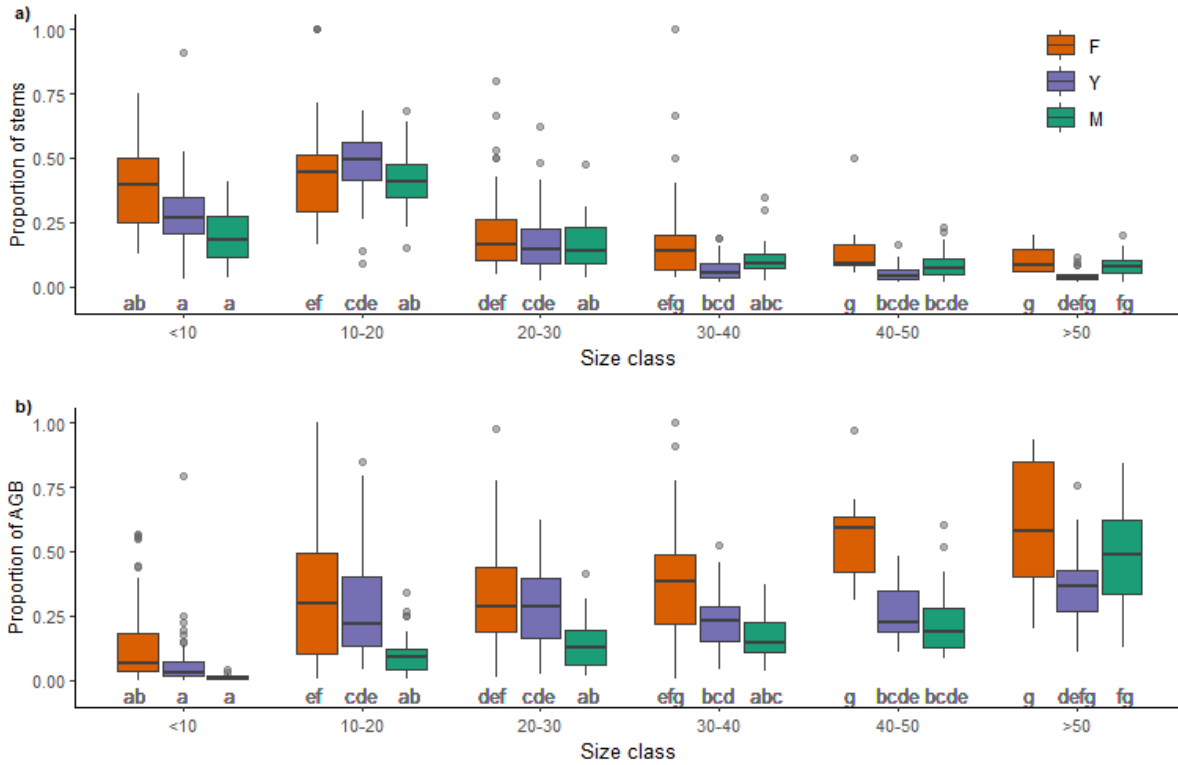
Figure S2.6. Contribution of tree size categories to a) stem density and b) aboveground biomass (AGB) in young fallows (F, shown in orange), young forest (Y, shown in purple), and mature forest (M, shown in green) plots in TMCF (n=160). Trees were categorized in six size classes based on their DBH. Boxes cover the interquartile range (IQR), the horizontal line within boxes shows the median, and values 1.5 times larger or smaller than the IQR are shown in dark gray points. Letters indicate statistically significant differences between tree size classes and forest succession assessed with a two-way ANOVA and Tukey test (ANOVA results shown in Table S2.5). Boxes sharing a letter are not statistically different.

a)

b)

c)

d)
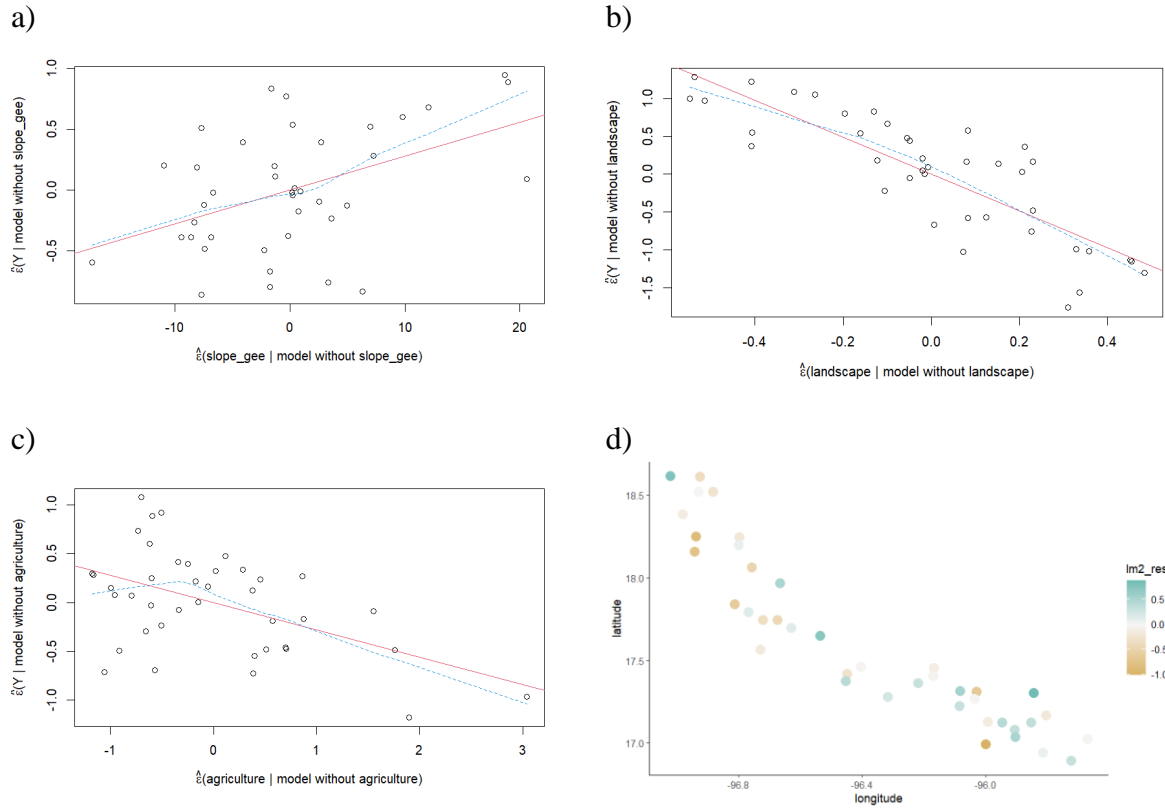
Figure S2.7. Partial residual plots of multiple linear regression selected as the best model to explain aboveground biomass patterns in TMCF based on R^2, Mallows' C_p (CP), and *Bayesian Information Criterion* (BIC) with a stepwise model selection process. Plots show the three predictors included in the model: a) slope, b) land-use intensity gradient, and c) disturbance by agricultural activities. Panel d displays the model residuals according to their geographic location to show there is no spatial autocorrelation between them (Moran's I statistics shown in Table S2.8).

Table S3.1. Confusion matrix showing producer's, user's, and overall accuracy of cloud *vs.* ground classification after applying CFMask and filtering pixels with a cloud index using 500 random pixels.

Predicted	Actual		Row total	User's accuracy
	Cloud	Ground		
Cloud	265	21	286	92.65%
Ground	7	207	214	96.72%
Column total	272	228	500	**Overall accuracy**
Producer's accuracy	97.42%	90.78%		**94.4%**

Table S3.2. Breakpoint validation showing the training point id (tp), date of breakpoint, breakpoint magnitude, validation result indicating whether the break is real (T) or not (F), and the images used for validation of forest cover change.

tp	date	magnitude	validation	images for validation
tp_52	2021-02-13	-0.3082	T	Planet (Nov 26 2020, March 15 2021)
tp_44	2020-11-09	-0.3500	T	Planet (Oct 26 2020, Feb 14 2021)
tp_59	2020-11-09	-0.2404	T	Planet (Oct 26 2020, Feb 14 2021)
tp_73	2020-03-30	-0.2902	T	Planet (Feb 17 2020, May 9 2020)
tp_93	2020-03-30	-0.2895	T	Planet (March 2 2020, May 9 2020)
tp_22	2020-03-14	-0.2579	T	Planet (Feb 24 2020, May 9 2020)
tp_37	2020-01-26	-0.07320	F	Planet (Nov 22 2019, Feb 12 2020)
tp_50	2020-01-26	0.0060	F	Planet (Nov 22 2019, Feb 12 2020)
tp_20	2020-01-10	-0.3354	T	Planet (Jan 6 2020, Feb 12 2020)
tp_53	2019-06-16	0.2092	T *	Planet (Jun 6 2019, Aug 31 2019)
tp_41	2019-04-29	-0.1455	F	Planet (Apr 21 2019, Jul 5 2019)
tp_22	2019-01-23	-0.4323	T	Planet (Jan 11 2019, Feb 20 2019)
tp_37	2019-01-23	-0.3417	T	Planet (Jan 11 2019, Feb 20 2019)
tp_50	2019-01-23	-0.3417	T	Planet (Jan 11 2019, Mar 30 2019)
tp_49	2018-07-31	0.2776	T	Planet (May 11 2018, Aug 11 2018)
tp_53	2018-05-28	-0.0169	F	Planet (May 26 2018, Aug 11 2018)
tp_59	2018-02-05	-0.1978	T	Planet (Nov 21 2017, Mar 29 2018)
tp_82	2018-02-05	-0.1760	T	Planet (Jan 8 2018, Mar 17 2018)
tp_67	2018-01-20	-0.2875	T	Planet (Nov 18 2017, Apr 17 2018)
tp_73	2018-01-20	-0.2615	T	Planet (Nov 21 2017, Mar 17 2018)

tp_49	2017-07-12	0.0140	F	Planet (Jul 11 2017, Aug 03 3017)

* NOTE: Not a clearing but vegetation regrowth after disturbance (hence positive magnitude). Good example of BFAST not detecting vegetation loss but detecting an abrupt change in vegetation regrowth after.

Table S3.3. Results of t-tests of forest structure variables between FI plots with breakpoints (break, n =76) and without breakpoints (no break, n= 208) detected by BFAST.

y	*t*	*df*	*p*
Basal area	-5.91	201	<0.001
log AGB	-5.46	126	< 0.0001
Lorey's height	-6.66	187	<0.0001
Tree density	-1.33	188	0.187

Table S3.4. Results of linear regressions between forest structure variables and time since last disturbance (TSLD) in plots with and without breakpoints detected by BFAST.

All plots (n =284)						
Variable	**y-intercept**	**slope**	**F**	**df**	**p**	**Adj-R^2**
Sqrt-Basal area	1.801	0.122	38.82	(1,282)	<0.0001	0.12
Log-AGB	2.17	0.10	45.32	(1,282)	<0.0001	0.13
Lorey's height	7.05	0.28	27.32	(1, 282)	<0.0001	0.08
Tree density	350.848	15.20	9.207	(1, 282)	0.002	0.02
Plots with breakpoints (n= 76)						
Variable	**y-intercept**	**slope**	**F**	**df**	**p**	**Adj-R^2**
Basal area	7.03	0.39	3.50	(1,74)	0.06	0.03
log AGB	2.38	0.07	6.56	(1,74)	0.01	0.06
Lorey's height	8.14	0.08	1.24	(1,74)	0.26	0.003
Tree density	347.49	20.30	4.02	(1,74)	0.04	0.03
Plots with no breakpoints (n = 208)						
Variable	**y-intercept**	**slope**	**F**	**df**	**p**	**Adj-R^2**
Basal area	-16.35	1.97	8.82	(1,206)	0.003	0.03
log AGB	1.12	0.16	7.48	(1,206)	0.006	0.03
Lorey's height	8.68	0.21	0.89	(1,206)	0.34	0
Tree density	-302.5	49.77	7.37	(1,206)	0.007	0.02

Table S3.5. Comparison of multiple linear regression models of forest structure variables using elevation, slope, and remote sensing variables as predictors, showing the number of predictors considered in each model, as well as their adjusted R^2, Mallows' Cp (CP), and Bayesian Information Criterion (BIC). The highest adjusted R^2, lowest CP, and lowest BIC are in bold.

BASAL AREA

	Number of predictors included in model								
Predictors	1	2	3	4	5	6	7	8	9
Elevation		*	*	*	*	*	*	*	*
Slope			*		*	*	*	*	*
Mean TSLD							*	*	*
Min TSLD							*	*	*
Mean no. breaks									*
NDVIa S.D.				*	*	*	*	*	*
NDVI S.D.	*		*	*	*	*	*	*	*
NDVI min		*				*		*	*
NDWIa min				*	*	*	*	*	*
Adj-R^2	0.294	0.527	0.540	0.575	**0.599**	0.588	0.577	0.565	0.550
CP	23.05	4.819	4.751	3.081	**2.380**	4.253	6.127	8.004	10.00
BIC	-7.31	**-20.35**	-18.88	-19.44	-19.21	-15.72	-12.22	-8.72	-5.07

AGB (log-transformed)

	Number of predictors included in model								
Predictors	1	2	3	4	5	6	7	8	9
Elevation		*	*	*	*	*	*	*	*
Slope			*	*	*	*	*	*	*
Mean TSLD						*	*	*	*
Min TSLD								*	*
Mean no. breaks									*
NDVIa S.D.	*				*	*	*	*	*
NDVI S.D.			*	*	*	*	*	*	*
NDVI min		*					*	*	*
NDWIa min				*	*	*	*	*	*

Adj-R^2	0.241	0.387	0.430	0.425	**0.430**	0.419	0.406	0.387	0.366
CP	9.326	1.811	**0.504**	1.858	2.669	4.362	6.067	8.020	10.00
BIC	-4.492	-10.25	**-10.48**	-7.625	-5.494	-2.237	1.033	4.633	8.269

LOREY'S HEIGHT

	Number of predictors included in model								
Predictors	1	2	3	4	5	6	7	8	9
Elevation		*	*	*	*	*	*	*	*
Slope			*	*	*	*	*	*	*
Mean TSLD								*	*
Min TSLD					*	*	*	*	*
Mean no. breaks					*	*	*	*	*
NDVIa S.D.	*						*	*	*
NDVI S.D.		*	*	*	*	*	*	*	*
NDVI min				*		*	*	*	*
NDWIa min									*
Adj-R^2	0.293	0.448	0.464	0.465	0.476	0.484	**0.492**	0.481	0.463
CP	13.70	3.991	**3.915**	4.872	5.193	5.768	6.306	8.000	10.00
BIC	-7.264	**-14.33**	-12.92	-10.44	-8.759	-6.862	-5.097	-1.843	1.819

TREE DENSITY (sqrt-transformed)

	Number of predictors included in model								
Predictors	1	2	3	4	5	6	7	8	9
Elevation		*	*	*	*	*	*	*	*
Slope									*
Mean TSLD				*	*	*	*	*	*
Min TSLD							*	*	*
Mean no. breaks			*	*	*	*	*	*	*
NDVIa S.D.	*							*	*
NDVI S.D.					*	*	*	*	*
NDVI min						*	*	*	*
NDWIa min		*	*	*	*	*	*	*	*
Adj-R^2	0.187	0.336	**0.352**	0.343	0.345	0.334	0.313	0.290	0.265

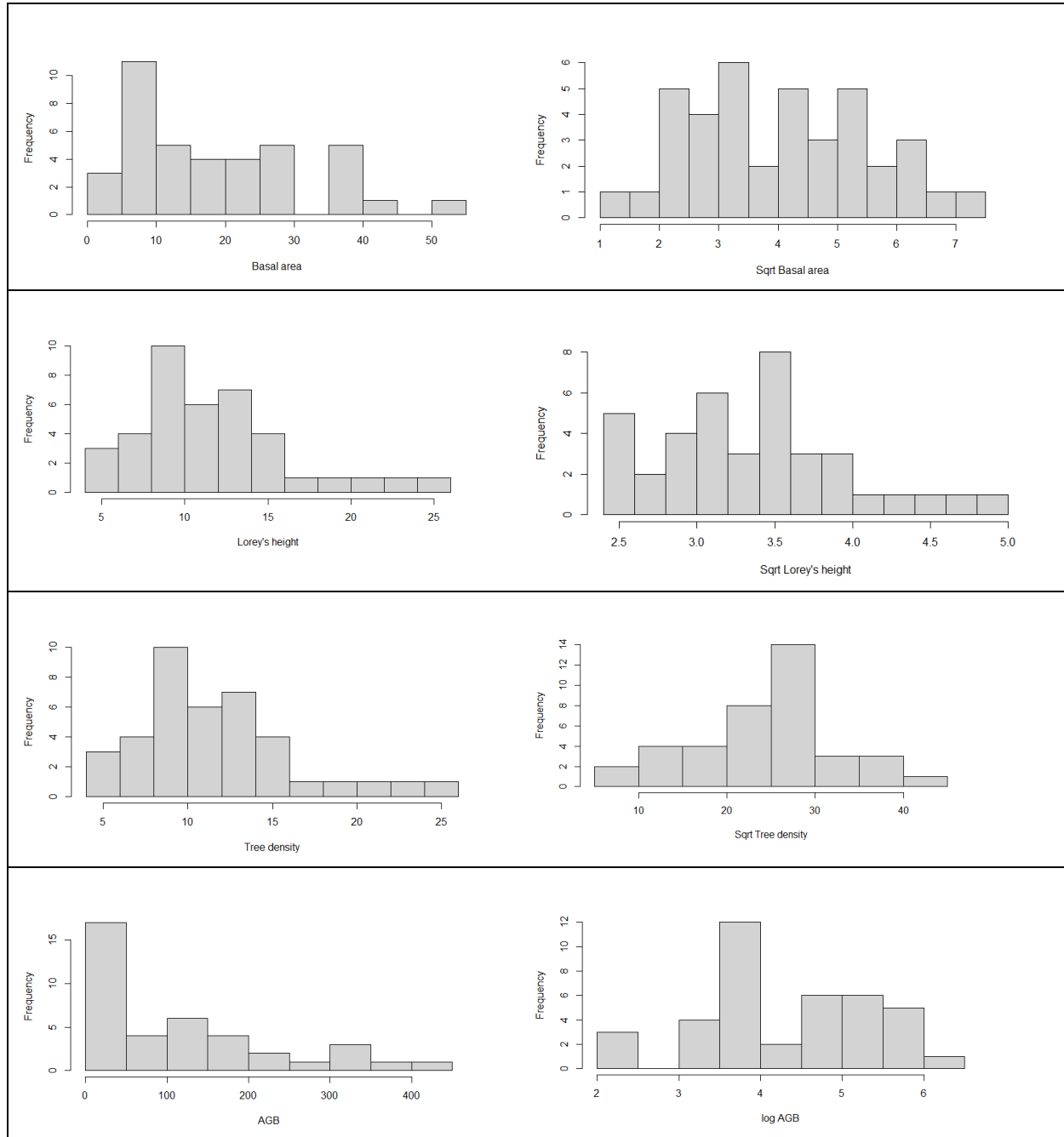| CP	5.963	**-0.448**	-0.128	1.398	2.428	4.012	6.003	8.001	10.00
BIC	-1.803	**-7.104**	-5.507	-2.445	-0.047	3.061	6.712	10.372	14.03

Figures

Figure S3.1. Histograms of forest structure variables before and after transformation.

Figure S3.2. Training points used for validating breakpoints in a tropical montane landscape adjacent to one of the analyzed FI plots.

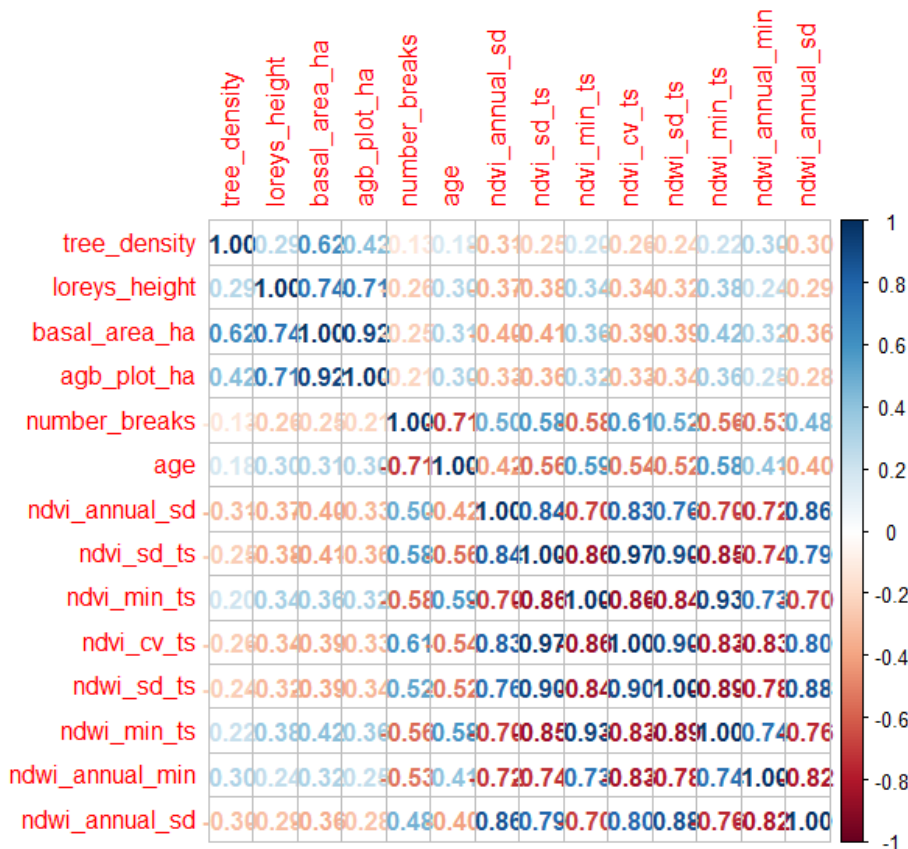|	tree_density	loreys_height	basal_area_ha	agb_plot_ha	number_breaks	age	ndvi_annual_sd	ndvi_sd_ts	ndvi_min_ts	ndvi_cv_ts	ndwi_sd_ts	ndwi_min_ts	ndwi_annual_min	ndwi_annual_sd
tree_density	1.00	0.29	0.62	0.42	0.13	0.18	0.31	0.25	0.20	0.26	0.24	0.22	0.30	0.30
loreys_height	0.29	1.00	0.74	0.71	0.26	0.30	0.37	0.38	0.34	0.34	0.32	0.38	0.24	0.29
basal_area_ha	0.62	0.74	1.00	0.92	0.25	0.31	0.49	0.41	0.36	0.39	0.39	0.42	0.32	0.36
agb_plot_ha	0.42	0.71	0.92	1.00	0.21	0.30	0.33	0.36	0.32	0.33	0.34	0.36	0.28	0.28
number_breaks	0.13	0.26	0.28	0.21	1.00	0.71	0.50	0.58	0.58	0.61	0.52	0.56	0.53	0.48
age	0.18	0.30	0.31	0.39	0.71	1.00	0.42	0.56	0.59	0.54	0.52	0.58	0.41	0.40
ndvi_annual_sd	0.31	0.37	0.49	0.33	0.50	0.42	1.00	0.84	0.70	0.83	0.76	0.79	0.72	0.86
ndvi_sd_ts	0.25	0.38	0.41	0.36	0.58	0.56	0.84	1.00	0.86	0.97	0.90	0.85	0.74	0.79
ndvi_min_ts	0.20	0.34	0.36	0.32	0.58	0.59	0.70	0.86	1.00	0.86	0.84	0.93	0.73	0.70
ndvi_cv_ts	0.26	0.34	0.39	0.33	0.61	0.54	0.83	0.97	0.86	1.00	0.90	0.83	0.83	0.80
ndwi_sd_ts	0.24	0.32	0.39	0.34	0.52	0.52	0.76	0.90	0.84	0.90	1.00	0.89	0.78	0.88
ndwi_min_ts	0.22	0.38	0.42	0.36	0.56	0.59	0.70	0.85	0.93	0.83	0.89	1.00	0.74	0.76
ndwi_annual_min	0.30	0.24	0.32	0.28	0.53	0.41	0.72	0.74	0.73	0.83	0.78	0.74	1.00	0.82
ndwi_annual_sd	0.30	0.29	0.36	0.28	0.48	0.40	0.86	0.79	0.70	0.80	0.88	0.76	0.82	1.00

Figure S3.3. Correlation matrix showing correlation coefficients between forest structure variables and 10 remote sensing variables. Note: age is equivalent to time since last disturbance (TSLD).

REFERENCES CITED

Adhikari, Hari, Janne Heiskanen, Mika Siljander, Eduardo Maeda, Vuokko Heikinheimo, and Petri K.E. Pellikka. 2017. "Determinants of Aboveground Biomass across an Afromontane Landscape Mosaic in Kenya." *Remote Sensing* 9 (8): 1–19. https://doi.org/10.3390/rs9080827.

Akram-Lodhi, A. Haroon, and Cristóbal Kay. 2010. "Surveying the Agrarian Question (Part 1): Unearthing Foundations, Exploring Diversity." *Journal of Peasant Studies* 37 (1): 177–202. https://doi.org/10.1080/03066150903498838.

Ali, Arshad, Si-Liang Lin, Jie-Kun He, Fan-Mao Kong, Jie-Hua Yu, and Hai-Sheng Jiang. 2019. "Climatic Water Availability Is the Main Limiting Factor of Biotic Attributes across Large-Scale Elevational Gradients in Tropical Forests." *Science of The Total Environment* 647 (January): 1211–21. https://doi.org/10.1016/j.scitotenv.2018.08.072.

Altieri, Miguel A., M. Kat Anderson, and Laura C. Merrick. 1987. "Peasant Agriculture and the Conservation of Crop and Wild Plant Resources." *Conservation Biology* 1 (1): 49–58. https://doi.org/10.1111/j.1523-1739.1987.tb00008.x.

Álvarez-Arteaga, G, N García Calderón, P Krasilnikov, and F García-Oliva. 2013. "Almacenes de Carbono En Bosques Montanos de Niebla de La Sierra Norte de Oaxaca, México." *Agrociencia* 47: 171–80.

Álvarez-Dávila, Esteban, Luis Cayuela, Sebastián González-Caro, Ana M. Aldana, Pablo R. Stevenson, Oliver Phillips, Álvaro Cogollo, et al. 2017. "Forest Biomass Density across Large Climate Gradients in Northern South America Is Related to Water Availability but Not with Temperature." *PLoS ONE* 12 (3): 1–16. https://doi.org/10.1371/journal.pone.0171072.

Álvarez Arteaga, G., N. E. García Calderón, P. V. Krasilnikov, S. N. Sedov, V. O. Targulian, and N. Velázquez Rosas. 2008. "Soil Altitudinal Sequence on Base-Poor Parent Material in a Montane Cloud Forest in Sierra Juárez, Southern Mexico." *Geoderma* 144 (3–4): 593–612. https://doi.org/10.1016/j.geoderma.2008.01.025.

Aquino Vásquez, Ciro, Javier Ramírez Juárez, and Ricardo Clark Tapia. 2021. "La Agricultura Familiar En El Contexto de Desarrollo Forestal Comunitario. El Caso de Ixtlán de Juárez, Oaxaca." In *Transformaciones Rurales Desde La Agricultura Familiar En Las Regiones Centro y Sur de México*, 319–42.

Aragón, Susan, Norma Salinas, Alex Nina-Quispe, Vicky Huaman Qquellon, Gloria Rayme Paucar, Wilfredo Huaman, Percy Chambi Porroa, et al. 2021. "Aboveground Biomass in Secondary Montane Forests in Peru: Slow Carbon Recovery in Agroforestry Legacies." *Global Ecology and Conservation* 28 (February): e01696. https://doi.org/10.1016/j.gecco.2021.e01696.

Arasa-Gisbert, Ricard, Jordi Vayreda, Rosa María Román-Cuesta, Sergio Armando Villela, Rafael Mayorga, and Javier Retana. 2018. "Forest Diversity Plays a Key Role in Determining the Stand Carbon Stocks of Mexican Forests." *Forest Ecology and Management* 415–416 (November 2017): 160–71. https://doi.org/10.1016/j.foreco.2018.02.023.

Araza, Arnan, Sytze de Bruin, Martin Herold, Shaun Quegan, Nicolas Labriere, Pedro Rodriguez-Veiga, Valerio Avitabile, et al. 2022. "A Comprehensive Framework for Assessing the Accuracy and Uncertainty of Global Above-Ground Biomass Maps." *Remote Sensing of Environment* 272 (February). https://doi.org/10.1016/j.rse.2022.112917.

Arellanes Cancino, Yaaye. 2000. "Análisis Estructural de Un Bosque Mesófilo de Montaña de Ticodendron Incognitum En La Sierra Norte de Oaxaca, Mexico." Universidad Nacional Autónoma de México.

Arnés Prieto, Esperanza. 2015. "Evaluating Sustainability and Food Security of Peasant Farming Systems in Mesoamerican Highlands," 214.

Asner, G. P., C. B. Anderson, R. E. Martin, D. E. Knapp, R. Tupayachi, F. Sinca, and Y. Malhi. 2014. "Landscape-Scale Changes in Forest Structure and Functional Traits along an Andes-to-Amazon Elevation Gradient." *Biogeosciences* 11 (3): 843–56. https://doi.org/10.5194/bg-11-843-2014.

Asner, Gregory P., R. Flint Hughes, Timothy A. Varga, David E. Knapp, and Ty Kennedy-Bowdoin. 2009. "Environmental and Biotic Controls over Aboveground Biomass throughout a Tropical Rain Forest." *Ecosystems* 12 (2): 261–78. https://doi.org/10.1007/s10021-008-9221-5.

Asner, Gregory P., George V.N. Powell, Joseph Mascaro, David E. Knapp, John K. Clark, James Jacobson, Ty Kennedy-Bowdoin, et al. 2010. "High-Resolution Forest Carbon Stocks and Emissions in the Amazon." *Proceedings of the National Academy of Sciences of the United States of America* 107 (38): 16738–42. https://doi.org/10.1073/pnas.1004875107.

Avitabile, Valerio, Martin Herold, Gerard B.M. Heuvelink, Simon L. Lewis, Oliver L. Phillips, Gregory P. Asner, John Armston, et al. 2016. "An Integrated Pan-Tropical Biomass Map Using Multiple Reference Datasets." *Global Change Biology* 22 (4): 1406–20. https://doi.org/10.1111/gcb.13139.

Baccini, A, W Walker, L Carvalho, M Farina, and R A Houghton. 2017. "Tropical Forests Are a Net Carbon Source Based on Aboveground Measurements of Gain and Loss" 234 (October): 230–34.

Baer, Werner. 1972. "Import Substitution and Industrialization in Latin America: Experiences and Interpretations." *Latin American Research Review* 7 (1): 95–122.

Bellon, Mauricio R., Alicia Mastretta-Yanes, Alejandro Ponce-Mendoza, Daniel Ortiz-Santa
María, Oswaldo Oliveros-Galindo, Hugo Perales, Francisca Acevedo, and José Sarukhán.
2021. "Beyond Subsistence: The Aggregate Contribution of Campesinos to the Supply and
Conservation of Native Maize across Mexico." *Food Security* 13 (1): 39–53.
https://doi.org/10.1007/s12571-020-01134-8.

Benner, J, P M Vitousek, and R Ostertag. 2011. "Nutrient Cycling and Nutrient Limitation in
Tropical Montane Cloud Forests." In *Tropical Montane Cloud Forests: Science for
Conservation and Management*, edited by L A Bruijnzeel, F N Scatena, and L S.Editors
Hamilton, 90–100. International Hydrology Series. Cambridge University Press.
https://doi.org/10.1017/CBO9780511778384.009.

Bennett, Elena M. 2017. "Changing the Agriculture and Environment Conversation." *Nature
Publishing Group* 1. https://doi.org/10.1038/s41559-016-0018.

Berveglieri, Adilson, Nilton N. Imai, Luiz E. Christovam, Maria L.B.T. Galo, Antonio M.G.
Tommaselli, and Eija Honkavaara. 2021. "Analysis of Trends and Changes in the
Successional Trajectories of Tropical Forest Using the Landsat NDVI Time Series." *Remote
Sensing Applications: Society and Environment* 24 (November).
https://doi.org/10.1016/j.rsase.2021.100622.

Betancourt, Mauricio. 2020. "The Effect of Cuban Agroecology in Mitigating the Metabolic
Rift: A Quantitative Approach to Latin American Food Production." *Global Environmental
Change* 63 (July): 102075. https://doi.org/10.1016/j.gloenvcha.2020.102075.

Blanco, Juan A., Yueh-Hsin Lo, James P. Kimmins, and Adrian Weber. 2021. "Highlighting
Complex Long-Term Succession Pathways in Mixed Forests of the Pacific Northwest: A
Markov Chain Modelling Approach." *Forests* 12 (12): 1770.
https://doi.org/10.3390/f12121770.

Bocco, Gerardo. 1991. "Traditional Knowledge for Soil Conservation in Central Mexico."
Journal of Soil and Water Conservation September 46 (5): 346–48.
https://doi.org/https://www.jswconline.org/content/46/5/346.

Bojinski, Stephan, Michel Verstraete, Thomas C. Peterson, Carolin Richter, Adrian Simmons,
and Michael Zemp. 2014. "The Concept of Essential Climate Variables in Support of
Climate Research, Applications, and Policy." *Bulletin of the American Meteorological
Society* 95 (9): 1431–43. https://doi.org/10.1175/BAMS-D-13-00047.1.

Bonan, G. B. 2008. "Forests and Climate Change : Climate Benefits of Forests." *Science* 320
(June): 1444–49.

Bongers, F., R. Chazdon, L. Poorter, and M. Peña-Claros. 2015. "The Potential of Secondary
Forests." *Science* 348 (6235): 642–43. https://doi.org/10.1126/science.348.6235.642-c.

Bordin, Kauane Maiara, Adriane Esquivel-Muelbert, Rodrigo Scarton Bergamin, Joice Klipel, Rayana Caroline Picolotto, Marcelo Araújo Frangipani, Katia Janaina Zanini, et al. 2021. "Climate and Large-Sized Trees, but Not Diversity, Drive above-Ground Biomass in Subtropical Forests." *Forest Ecology and Management* 490 (November 2020). https://doi.org/10.1016/j.foreco.2021.119126.

Bray, David. 2021. "Mexican Communities Manage Their Local Forests, Generating Benefits for Humans, Trees and Wildlife." *The Conversation*, 2021. https://theconversation.com/mexican-communities-manage-their-local-forests-generating-benefits-for-humans-trees-and-wildlife-165647.

Bray, David Barton. 2020. *Mexico's Community Forest Enterprises*. University of Arizona Press. https://doi.org/10.2307/j.ctv191kwrz.

Bray, David Barton, Leticia Merino-Pérez, Patricia Negreros-Castillo, Gerardo Segura-Warnholtz, Juan Manuel Torres-Rojo, and Henricus F.M. Vester. 2003. "Mexico's Community-Managed Forests as a Global Model for Sustainable Landscapes." *Conservation Biology* 17 (3): 672–77. https://doi.org/10.1046/j.1523-1739.2003.01639.x.

Breugel, Michiel van, Johannes Ransijn, Dylan Craven, Frans Bongers, and Jefferson S. Hall. 2011. "Estimating Carbon Stock in Secondary Forests: Decisions and Uncertainties Associated with Allometric Biomass Models." *Forest Ecology and Management* 262 (8): 1648–57. https://doi.org/10.1016/j.foreco.2011.07.018.

Brockington, Daniel, and James Igoe. 2006. "Eviction for Conservation: A Global Overview." *Conservation & Society* 4 (3): 424–70. https://www.jstor.org/stable/26396619.

Brown, Christopher F., Steven P. Brumby, Brookie Guzder-Williams, Tanya Birch, Samantha Brooks Hyde, Joseph Mazzariello, Wanda Czerwinski, et al. 2022. "Dynamic World, Near Real-Time Global 10 m Land Use Land Cover Mapping." *Scientific Data* 9 (1): 251. https://doi.org/10.1038/s41597-022-01307-4.

Brown, Schyler, Lana L. Narine, and John Gilbert. 2022. "Using Airborne Lidar, Multispectral Imagery, and Field Inventory Data to Estimate Basal Area, Volume, and Aboveground Biomass in Heterogeneous Mixed Species Forests: A Case Study in Southern Alabama." *Remote Sensing* 14 (11): 2708. https://doi.org/10.3390/rs14112708.

Bruijnzeel, L A, M Kappelle, M Mulligan, and F N Scatena. 2011. "Tropical Montane Cloud Forests: State of Knowledge and Sustainability Perspectives in a Changing World." In *Tropical Montane Cloud Forests: Science for Conservation and Management*, edited by L A Bruijnzeel, F N Scatena, and L S.Editors Hamilton, 691–740. International Hydrology Series. Cambridge University Press. https://doi.org/10.1017/CBO9780511778384.074.

Bryceson, Deborah Fahy. 2000. "1. Peasant Theories and Smallholder Policies. Past and Present." In *Disappearing Peasantries?*, 1–36. Rugby, Warwickshire, United Kingdom: Practical Action Publishing. https://doi.org/10.3362/9781780440118.001.

Bürgi, Matthias, Lars Östlund, and David J. Mladenoff. 2017. "Legacy Effects of Human Land Use: Ecosystems as Time-Lagged Systems." *Ecosystems* 20 (1): 94–103. https://doi.org/10.1007/s10021-016-0051-6.

Burt, Andrew, Kim Calders, Aida Cuni-Sanchez, Jose Gómez-Dans, Philip Lewis, Simon L. Lewis, Yadvinder Malhi, Oliver L. Phillips, and Mathias Disney. 2020. "Assessment of Bias in Pan-Tropical Biomass Predictions." *Frontiers in Forests and Global Change* 3 (February). https://doi.org/10.3389/ffgc.2020.00012.

Byerlee, Derek, James Stevenson, and Nelson Villoria. 2014. "Does Intensification Slow Crop Land Expansion or Encourage Deforestation?" *Global Food Security* 3 (2): 92–98. https://doi.org/10.1016/j.gfs.2014.04.001.

Calderon-Aguilera, Luis E., Víctor H. Rivera-Monroy, Luciana Porter-Bolland, Angelina Martínez-Yrízar, Lydia B. Ladah, Miguel Martínez-Ramos, Javier Alcocer, et al. 2012. "An Assessment of Natural and Human Disturbance Effects on Mexican Ecosystems: Current Trends and Research Gaps." *Biodiversity and Conservation* 21 (3): 589–617. https://doi.org/10.1007/s10531-011-0218-6.

Cartus, Oliver, Josef Kellndorfer, Wayne Walker, Carol Franco, Jesse Bishop, Lucio Santos, and José María Michel. 2014. "A National. Detailed Map of Forest Aboveground Carbon Stocks in Mexico." *Remote Sensing* 6: 5559–88. https://doi.org/10.3390/rs6065559.

Castillo, Rafael F. del. 2013. "A Conceptual Framework to Describe the Ecology of Fragmented Landscapes and Implications for Conservation and Management." *Ecological Applications* 23 (3): 515–22.

———. 2015. "A Conceptual Framework to Describe the Ecology of Fragmented Landscapes and Implications for Conservation and Management." *Ecological Applications* 25 (6): 1447–55. https://doi.org/10.1890/14-1964.1.

Cavanaugh, Kyle C., J. Stephen Gosnell, Samantha L. Davis, Jorge Ahumada, Patrick Boundja, David B. Clark, Badru Mugerwa, et al. 2014. "Carbon Storage in Tropical Forests Correlates with Taxonomic Diversity and Functional Dominance on a Global Scale." *Global Ecology and Biogeography* 23 (5): 563–73. https://doi.org/10.1111/geb.12143.

Cavelier, Jaime. 1996. "Environmental Factors and Ecophysiological Processes along Altitudinal Gradients in Wet Tropical Mountains." In *Tropical Forest Plant Ecophysiology*, 399–439. Boston, MA: Springer US. https://doi.org/10.1007/978-1-4613-1163-8_14.

Cayuela, Luis, José María Rey Benayas, and Cristian Echeverría. 2006. "Clearance and Fragmentation of Tropical Montane Forests in the Highlands of Chiapas, Mexico (1975-2000)." *Forest Ecology and Management* 226 (1–3): 208–18. https://doi.org/10.1016/j.foreco.2006.01.047.

CEIEG. 2022a. "Presentación de Resultados Censo INEGI 2020: Papaloapan." https://www.oaxaca.gob.mx/ceieg/wp-content/uploads/sites/64/2021/02/Region-Papaloapan_Coplade_definitivo.pdf.

———. 2022b. "Presentación de Resultados Censo INEGI 2020: Sierra Norte." https://www.oaxaca.gob.mx/ceieg/wp-content/uploads/sites/64/2021/02/Region-Sierra-Norte_Coplade_definitivo.pdf.

Chagoya Morgan, Leopoldo. 1986. *La Chinantla En La Epoca Prehispanica*. Mexico: Federación Editorial Mexicana.

Chang, Cynthia C., and Benjamin L. Turner. 2019. "Ecological Succession in a Changing World." Edited by Richard Bardgett. *Journal of Ecology* 107 (2): 503–9. https://doi.org/10.1111/1365-2745.13132.

Chave, Jerome, Richard Condit, Salomon Aguilar, Andres Hernandez, Suzanne Lao, and Rolando Perez. 2004. "Error Propagation and Sealing for Tropical Forest Biomass Estimates." *Philosophical Transactions of the Royal Society B: Biological Sciences* 359 (1443): 409–20. https://doi.org/10.1098/rstb.2003.1425.

Chave, Jérôme, Stuart J. Davies, Oliver L. Phillips, Simon L. Lewis, Plinio Sist, Dmitry Schepaschenko, John Armston, et al. 2019. "Ground Data Are Essential for Biomass Remote Sensing Missions." *Surveys in Geophysics* 40 (4): 863–80. https://doi.org/10.1007/s10712-019-09528-w.

Chazdon, RL. 2003. "Tropical Forest Recovery: Legacies of Human Impact and Natural Disturbances." *Perspectives in Plant Ecology, Evolution and Systematics* 6 (1–2): 51–71. https://doi.org/10.1078/1433-8319-00042.

Chazdon, Robin L., Eben N. Broadbent, Danaë M.A. Rozendaal, Frans Bongers, Angélica María Almeyda Zambrano, T. Mitchell Aide, Patricia Balvanera, et al. 2016. "Carbon Sequestration Potential of Second-Growth Forest Regeneration in the Latin American Tropics." *Science Advances* 2 (5). https://doi.org/10.1126/sciadv.1501639.

Clapp, Jennifer. 2012. "Food." Resources (Polity Press). Cambridge, England ; Malden, Mass.: Polity Press.

Clark, Brett, and Richard York. 2008. "Rifts and Shifts: Getting to the Root of Environmental Crises." *Monthly Review* 60 (6). https://doi.org/https://monthlyreview.org/2008/11/01/rifts-and-shifts-getting-to-the-root-of-environmental-crises/.

Clark, David B., Johanna Hurtado, and Sassan S. Saatchi. 2015. "Tropical Rain Forest Structure, Tree Growth and Dynamics along a 2700-m Elevational Transect in Costa Rica." *PLoS ONE* 10 (4): 1–18. https://doi.org/10.1371/journal.pone.0122905.

Clements, F. E. 1936. "Nature and Structure of the Climax." *Journal of Ecology* 24: 252–84.

Cleveland, Cory C., Alan R. Townsend, Philip Taylor, Silvia Alvarez-Clare, Mercedes M.C. Bustamante, George Chuyong, Solomon Z. Dobrowski, et al. 2011. "Relationships among Net Primary Productivity, Nutrients and Climate in Tropical Rain Forest: A Pan-Tropical Analysis." *Ecology Letters* 14 (9): 939–47. https://doi.org/10.1111/j.1461-0248.2011.01658.x.

CONABIO. 2012. "Principales Regiones y Subregiones Del Bosque Mesófilo de Montaña En México." Mexico: Comisión Nacional para el Conocimiento y Uso de la Biodiversidad. http://www.conabio.gob.mx/informacion/gis/.

CONAFOR. 2009. "INVENTARIO NACIONAL FORESTAL Y DE SUELOS: Manual y Procedimientos Para El Muestreo de Campo (RE-MUESTREO 2009)."

———. 2015. "Inventario Nacional Forestal y de Suelos. Procedimientos de Muestreo."

———. 2018. "Inventario Nacional Forestal y de Suelos – Informe de Resultados 2009-2014." Jalisco, México. https://snigf.cnf.gob.mx/resultados-2009-2014/.

CONANP. 2019. "Áreas Destinadas Voluntariamente a La Conservación." Comisión Nacional de Áreas Naturales Protegidas (CONANP).

Cook-Patton, Susan C., Sara M. Leavitt, David Gibbs, Nancy L. Harris, Kristine Lister, Kristina J. Anderson-Teixeira, Russell D. Briggs, et al. 2020. "Mapping Carbon Accumulation Potential from Global Natural Forest Regrowth." *Nature* 585 (7826): 545–50. https://doi.org/10.1038/s41586-020-2686-x.

Cruz-López, María Isabel, Lilia de Lourdes Manzo-Delgado, Raúl Aguirre-Gómez, Emilio Chuvieco, and Julián Alberto Equihua-Benítez. 2019. "Spatial Distribution of Forest Fire Emissions: A Case Study in Three Mexican Ecoregions." *Remote Sensing* 11 (10): 1185. https://doi.org/10.3390/rs11101185.

Cruz, Ivan. 2022. "Narcotráfico y Feminicidios Alcanzaron a La Sierra Mixe de Oaxaca." *Datanoticias*, 2022. https://datanoticias.com/2022/05/12/narcotrafico-y-feminicidios-alcanzaron-a-la-sierra-mixe-de-oaxaca/.

Cuni-Sanchez, Aida, Marion Pfeifer, Rob Marchant, Kim Calders, Cathrine L. Sørensen, Patrícia V. Pompeu, Simon L. Lewis, and Neil D. Burgess. 2017. "New Insights on above Ground Biomass and Forest Attributes in Tropical Montane Forests." *Forest Ecology and Management* 399: 235–46. https://doi.org/10.1016/j.foreco.2017.05.030.

Cuni-Sanchez, Aida, Martin JP Sullivan, Philip J Platts, Simon L Lewis, Rob Marchant, and Gérard Imani. 2021. "High Above-Ground Carbon Stock of African Tropical Montane Forests." *Nature* 596 (August).

Curtis, Philip G., Christy M. Slay, Nancy L. Harris, Alexandra Tyukavina, and Matthew C. Hansen. 2018. "Classifying Drivers of Global Forest Loss." *Science* 361 (6407): 1108–11. https://doi.org/10.1126/science.aau3445.

Dahlin, Kyla M., Gregory P. Asner, and Christopher B. Field. 2012. "Environmental Filtering and Land-Use History Drive Patterns in Biomass Accumulation in a Mediterranean-Type Landscape." *Ecological Applications* 22 (1): 104–18. https://doi.org/10.1890/11-1401.1.

Defries, Ruth S., Thomas Rudel, Maria Uriarte, and Matthew Hansen. 2010. "Deforestation Driven by Urban Population Growth and Agricultural Trade in the Twenty-First Century." *Nature Geoscience* 3 (3): 178–81. https://doi.org/10.1038/ngeo756.

Delgado, Agustín. 1966. "Arqueología de La Chinantla, Noreste de Oaxaca, México: Su Secuencia Actual." In *Summa Anthropologica En Homenaje a Roberto J. Weitlaner*, 81–90. Mexico: Instituto Nacional de Antropología e Historia/Secretaría de Educación Pública.

DeVries, Ben, Mathieu Decuyper, Jan Verbesselt, Achim Zeileis, Martin Herold, and Shijo Joseph. 2015. "Tracking Disturbance-Regrowth Dynamics in Tropical Forests Using Structural Change Detection and Landsat Time Series." *Remote Sensing of Environment* 169: 320–34. https://doi.org/10.1016/j.rse.2015.08.020.

DeVries, Ben, Jan Verbesselt, Lammert Kooistra, and Martin Herold. 2015. "Robust Monitoring of Small-Scale Forest Disturbances in a Tropical Montane Forest Using Landsat Time Series." *Remote Sensing of Environment* 161: 107–21. https://doi.org/10.1016/j.rse.2015.02.012.

Dinerstein, E., A. R. Joshi, C. Vynne, A. T. L. Lee, F. Pharand-Deschênes, M. França, S. Fernando, et al. 2020. "A 'Global Safety Net' to Reverse Biodiversity Loss and Stabilize Earth's Climate." *Science Advances* 6 (36). https://doi.org/10.1126/sciadv.abb2824.

Domínguez, Lara, and Colin Luoma. 2020. "Decolonising Conservation Policy: How Colonial Land and Conservation Ideologies Persist and Perpetuate Indigenous Injustices at the Expense of the Environment." *Land* 9 (3): 65. https://doi.org/10.3390/land9030065.

Duncanson, L., J. Armston, M. Disney, V. Avitabile, N. Barbier, K. Calders, S. Carter, et al. 2019. "The Importance of Consistent Global Forest Aboveground Biomass Product Validation." *Surveys in Geophysics* 40 (4): 979–99. https://doi.org/10.1007/s10712-019-09538-8.

Duncanson, Laura, Mat Disney, John Armston, Jaime Nickeson, and David Minor. 2021. "Committee on Earth Observation Satellites Working Group on Calibration and Validation Land Product Validation Subgroup Aboveground Woody Biomass Product Validation Good Practices Protocol." *Good Practices for Satellite Derived Land Product Validation*, no. January: 0–236. https://doi.org/10.5067/doc/ceoswgcv/lpv/agb.001.

Duncanson, Laura, James R. Kellner, John Armston, Ralph Dubayah, David M. Minor, Steven Hancock, Sean P. Healey, et al. 2022. "Aboveground Biomass Density Models for NASA's Global Ecosystem Dynamics Investigation (GEDI) Lidar Mission." *Remote Sensing of Environment* 270 (March): 112845. https://doi.org/10.1016/j.rse.2021.112845.

Egerton, F.N. 2015. "History of Ecological Sciences, Part 54: Succession, Community, and Continuum." *The Bulletin of the Ecological Society of America* 96: 426–474. https://doi.org/https://www.jstor.org/stable/pdf/bullecosociamer.96.3.426.pdf.

Ellis, Erle C, and Navin Ramankutty. 2008. "Putting People in the Map: Anthropogenic Biomes of the World." *Frontiers in Ecology and the Environment* 6 (8): 439–47. https://doi.org/10.1890/070062.

Ensslin, Andreas, Gemma Rutten, Ulf Pommer, Reiner Zimmermann, Andreas Hemp, and Markus Fischer. 2015. "Effects of Elevation and Land Use on the Biomass of Trees, Shrubs and Herbs at Mount Kilimanjaro." *Ecosphere* 6 (3). https://doi.org/10.1890/ES14-00492.1.

Erb, Karl-Heinz, Helmut Haberl, Martin Rudbeck Jepsen, Tobias Kuemmerle, Marcus Lindner, Daniel Müller, and Anette Reenberg. 2013. "A Conceptual Framework for Analysing and Measuring Land-Use Intensity." *Current Opinion in Environmental Sustainability* 5 (5): 464–70. https://doi.org/10.1016/J.COSUST.2013.07.010.

Erb, Karl Heinz, Thomas Kastner, Christoph Plutzar, Anna Liza S. Bais, Nuno Carvalhais, Tamara Fetzel, Simone Gingrich, et al. 2018. "Unexpectedly Large Impact of Forest Management and Grazing on Global Vegetation Biomass." *Nature* 553 (7686): 73–76. https://doi.org/10.1038/nature25138.

ESRI Inc. 2020. "ArcGIS Pro." https://www.esri.com/en-us/arcgis/products/arcgis-pro/overview.

Fahey, Timothy J., Ruth E. Sherman, and Edmund V.J. Tanner. 2016. "Tropical Montane Cloud Forest: Environmental Drivers of Vegetation Structure and Ecosystem Function." *Journal of Tropical Ecology* 32 (5): 355–67. https://doi.org/10.1017/s0266467415000176.

Fairhead, James, and Melissa Leach. 2014. "False Forest History, Complicit Social Analysis: Rethinking Some West African Environmental Narratives." In *The Social Lives of Forests*, edited by Susanna B. Hecht, Kathleen D. Morrison, and Christine Padoch, 14–30. Chicago: The University of Chicago.

FAO. 2002. "International Year of Mountains-2002." *Unasylva* 53 (208).

———. 2016. *State of the World's Forests. Forest and Agriculture: Land-Use Challenges and Opportunities*. Rome.

Farr, Tom G., Paul A. Rosen, Edward Caro, Robert Crippen, Riley Duren, Scott Hensley, Michael Kobrick, et al. 2007. "The Shuttle Radar Topography Mission." *Reviews of Geophysics* 45 (2): RG2004. https://doi.org/10.1029/2005RG000183.

Feldpausch, T. R., J. Lloyd, S. L. Lewis, R. J.W. Brienen, M. Gloor, A. Monteagudo Mendoza, G. Lopez-Gonzalez, et al. 2012. "Tree Height Integrated into Pantropical Forest Biomass Estimates." *Biogeosciences* 9 (8): 3381–3403. https://doi.org/10.5194/bg-9-3381-2012.

Feng, Yu, Alan D. Ziegler, Paul R. Elsen, Yang Liu, Xinyue He, Dominick V. Spracklen, Joseph Holden, Xin Jiang, Chunmiao Zheng, and Zhenzhong Zeng. 2021. "Upward Expansion and Acceleration of Forest Clearance in the Mountains of Southeast Asia." *Nature Sustainability* 4 (10): 892–99. https://doi.org/10.1038/s41893-021-00738-y.

Fick, S.E., and R.J. Hijmans. 2017. "Worldclim 2: New 1-Km Spatial Resolution Climate Surfaces for Global Land Areas." *International Journal of Climatology*.

Fischer, Edward F, and Bart Victor. 2014. "High-End Coffee and Smallholding Growers in Guatemala." *Latin American Perspectives* 49 (1).

Fischer, Joern, David J. Abson, Arvid Bergsten, Neil French Collier, Ine Dorresteijn, Jan Hanspach, Kristoffer Hylander, Jannik Schultner, and Feyera Senbeta. 2017. "Reframing the Food–Biodiversity Challenge." *Trends in Ecology & Evolution*. https://doi.org/10.1016/j.tree.2017.02.009.

Fischer, Joern, David J. Abson, Van Butsic, M. Jahi Chappell, Johan Ekroos, Jan Hanspach, Tobias Kuemmerle, Henrik G. Smith, and Henrik von Wehrden. 2014. "Land Sparing versus Land Sharing: Moving Forward." *Conservation Letters*. https://doi.org/10.1111/conl.12084.

Fisher, Joshua B., Yadvinder Malhi, Israel Cuba Torres, Daniel B. Metcalfe, Martine J. van de Weg, Patrick Meir, Javier E. Silva-Espejo, and Walter Huaraca Huasco. 2013. "Nutrient Limitation in Rainforests and Cloud Forests along a 3,000-m Elevation Gradient in the Peruvian Andes." *Oecologia* 172 (3): 889–902. https://doi.org/10.1007/s00442-012-2522-6.

Foga, Steve, Pat L. Scaramuzza, Song Guo, Zhe Zhu, Ronald D. Dilley, Tim Beckmann, Gail L. Schmidt, John L. Dwyer, M. Joseph Hughes, and Brady Laue. 2017. "Cloud Detection Algorithm Comparison and Validation for Operational Landsat Data Products." *Remote Sensing of Environment* 194: 379–90. https://doi.org/10.1016/j.rse.2017.03.026.

França, Filipe M., Cassandra E. Benkwitt, Guadalupe Peralta, James P. W. Robinson, Nicholas A. J. Graham, Jason M. Tylianakis, Erika Berenguer, et al. 2020. "Climatic and Local Stressor Interactions Threaten Tropical Forests and Coral Reefs." *Philosophical Transactions of the Royal Society B: Biological Sciences* 375 (1794): 20190116. https://doi.org/10.1098/rstb.2019.0116.

Frolking, S., M. W. Palace, D. B. Clark, J. Q. Chambers, H. H. Shugart, and G. C. Hurtt. 2009. "Forest Disturbance and Recovery: A General Review in the Context of Spaceborne Remote Sensing of Impacts on Aboveground Biomass and Canopy Structure." *J. Geophys. Res.* 114 (G00E02). https://doi.org/10.1029/2008JG000911.

Fuentealba, Beatriz, and Carlos González-Esquivel. 2016. "Sistemas Silvopastoriles Tradicionales En México." In , 239–62.

Furumo, Paul R., and Eric F. Lambin. 2021. "Policy Sequencing to Reduce Tropical Deforestation." *Global Sustainability* 4 (October): e24. https://doi.org/10.1017/sus.2021.21.

Gao, Bo-cai. 1996. "NDWI—A Normalized Difference Water Index for Remote Sensing of Vegetation Liquid Water From Space." *Remote Sensing of Environment* 266 (April): 257–66. https://doi.org/10.1016/S0034-4257(96)00067-3.

Gardner, Toby A., Jos Barlow, Robin Chazdon, Robert M. Ewers, Celia A. Harvey, Carlos A. Peres, and Navjot S. Sodhi. 2009. "Prospects for Tropical Forest Biodiversity in a Human-Modified World." *Ecology Letters* 12 (6): 561–82. https://doi.org/10.1111/j.1461-0248.2009.01294.x.

Geist, Helmut J., and Eric F. Lambin. 2001. "What Drives Tropical Deforestation?" *LUCC Report Series No.4*. https://doi.org/10.4324/9781315158402-4.

Gibbs, H K, A S Ruesch, F Achard, M K Clayton, P Holmgren, N Ramankutty, and J A Foley. 2010. "Tropical Forests Were the Primary Sources of New Agricultural Land in the 1980s and 1990s" 107 (38): 1–6. https://doi.org/10.1073/pnas.0910275107.

Gibbs, Holly K., Sandra Brown, John O. Niles, and Jonathan A. Foley. 2007. "Monitoring and Estimating Tropical Forest Carbon Stocks: Making REDD a Reality." *Environmental Research Letters* 2 (4). https://doi.org/10.1088/1748-9326/2/4/045023.

Girardin, C. A. J., Y. Malhi, L. E. O. C. Aragão, M. Mamani, W. Huaraca Huasco, L. Durand, K. J. Feeley, et al. 2010. "Net Primary Productivity Allocation and Cycling of Carbon along a Tropical Forest Elevational Transect in the Peruvian Andes." *Global Change Biology* 16: 3176–92.

Girardin, CAJ, William Farfan-Rios, Karina Garcia, Keneth J. Feeley, Peter M. Jørgensen, Alejandro Araujo Murakami, Leslie Cayola Pérez, et al. 2014. "Spatial Patterns of Above-Ground Structure, Biomass and Composition in a Network of Six Andean Elevation Transects." *Plant Ecology and Diversity* 7 (1–2): 161–71. https://doi.org/10.1080/17550874.2013.820806.

Goetz, Scott J, Alessandro Baccini, Nadine T Laporte, Tracy Johns, Wayne Walker, Josef Kellndorfer, Richard A Houghton, and Mindy Sun. 2009. "Mapping and Monitoring Carbon Stocks with Satellite Observations: A Comparison of Methods." *Carbon Balance and Management* 4 (1): 2. https://doi.org/10.1186/1750-0680-4-2.

Gómez-Mendoza, Leticia, Ernesto Vega-Peña, M. Isabel Ramírez, José Luis Palacio-Prieto, and Leopoldo Galicia. 2006. "Projecting Land-Use Change Processes in the Sierra Norte of Oaxaca, Mexico." *Applied Geography* 26 (3–4): 276–90. https://doi.org/10.1016/j.apgeog.2006.09.003.

González-Abraham, Charlotte, Exequiel Ezcurra, Pedro P. Garcillán, Alfredo Ortega-Rubio, Melanie Kolb, and Juan E.Bezaury Creel. 2015. "The Human Footprint in Mexico: Physical Geography and Historical Legacies." *PLoS ONE* 10 (3): 1–17. https://doi.org/10.1371/journal.pone.0121203.

González-Espinosa, M, J A Meave, N Ramírez-Marcial, T. Toledo-Aceves, F G Lorea-Hernández, and G Ibarra-Manríquez. 2012. "Los Bosques de Niebla de México: Conservación y Restauración de Su Componente Arbóreo." *Ecosistemas* 21 (1–2): 36–52.

Goodman, D, and M Watts. 1997. *Globalising Food: Agrarian Questions and Global Restructuring*. Globalising Food: Agrarian Questions and Global Restructuring. Routledge.

Gorelick, Noel, Matt Hancher, Mike Dixon, Simon Ilyushchenko, David Thau, and Rebecca Moore. 2017. "Google Earth Engine: Planetary-Scale Geospatial Analysis for Everyone." *Remote Sensing of Environment* 202 (December): 18–27. https://doi.org/10.1016/j.rse.2017.06.031.

Gotsch, Sybil G, Heidi Asbjornsen, and Gregory R Goldsmith. 2020. "Plant Carbon and Water Fluxes in Tropical Montane Cloud Forests," no. 2016: 404–20. https://doi.org/10.1017/S0266467416000341.

Graham, Catherine H, and Paul V a Fine. 2008. "Phylogenetic Beta Diversity: Linking Ecological and Evolutionary Processes across Space in Time." *Ecology Letters* 11 (12): 1265–77. https://doi.org/10.1111/j.1461-0248.2008.01256.x.

Grantham, H. S., A. Duncan, T. D. Evans, K. R. Jones, H. L. Beyer, R. Schuster, J. Walston, et al. 2020. "Anthropogenic Modification of Forests Means Only 40% of Remaining Forests Have High Ecosystem Integrity." *Nature Communications* 11 (1): 1–10. https://doi.org/10.1038/s41467-020-19493-3.

Guariguata, Manuel R, and Rebecca Ostertag. 2001. "Neotropical Secondary Forest Succession: Changes in Structural and Functional Characteristics." *Forest Ecology and Management* 148 (1–3): 185–206. https://doi.org/10.1016/S0378-1127(00)00535-1.

Hamilton, Sarah, and Edward F. Fischer. 2005. "Maya Farmers and Export Agriculture in Highland Guatemala." *Latin American Perspectives* 32 (5): 33–58. https://doi.org/10.1177/0094582x05279503.

Hansen, M C, P.V. Potapov, R. Moore, M. Hancher, S.A. Turubanova, A. Tyukavina, D. Thau, et al. 2013. "High-Resolution Global Maps of 21st-Century Forest Cover Change." *Science* 342 (6160): 850–53. https://doi.org/10.1126/science.1244693.

Hecht, Susanna. 2010. "The New Rurality: Globalization, Peasants and the Paradoxes of Landscapes." *Land Use Policy* 27 (2): 161–69. https://doi.org/10.1016/j.landusepol.2009.08.010.

Heinrich, Viola H.A., Ricardo Dalagnol, Henrique L.G. Cassol, Thais M. Rosan, Catherine Torres de Almeida, Celso H.L. Silva Junior, Wesley A. Campanharo, et al. 2021. "Large Carbon Sink Potential of Secondary Forests in the Brazilian Amazon to Mitigate Climate Change." *Nature Communications* 12 (1). https://doi.org/10.1038/S41467-021-22050-1.

Hijmans, RJ. 2021. "Raster: Geographic Data Analysis and Modeling." https://cran.r-project.org/package=raster.

Hofhansl, Florian, Jörg Schnecker, Gabriel Singer, and Wolfgang Wanek. 2015. "New Insights into Mechanisms Driving Carbon Allocation in Tropical Forests." *New Phytologist* 205 (1): 137–46. https://doi.org/10.1111/nph.13007.

Hoorn, C., A. Perrigo, and A. Antonelli. 2018. "Mountains, Climate and Biodiversity: An Introduction." In *Mountains, Climate and Biodiversity*, edited by C. Hoorn, A. Perrigo, and A. Antonelli, 1–13. John Wiley & Sons.

Houghton, R. A., Forrest Hall, and Scott J. Goetz. 2009. "Importance of Biomass in the Global Carbon Cycle." *Journal of Geophysical Research: Biogeosciences* 114 (3): 1–13. https://doi.org/10.1029/2009JG000935.

Huang, Chengquan, Samuel N. Goward, Jeffrey G. Masek, Nancy Thomas, Zhiliang Zhu, and James E. Vogelmann. 2010. "An Automated Approach for Reconstructing Recent Forest Disturbance History Using Dense Landsat Time Series Stacks." *Remote Sensing of Environment* 114 (1): 183–98. https://doi.org/10.1016/j.rse.2009.08.017.

Imani, Gerard, Faustin Boyemba, Simon Lewis, Nsharwasi Leon Nsharwasi, Kim Calders, Louis Zapfack, Bernard Riera, Clarisse Balegamire, and Aida Cuni-sanchez. 2017. "Height-Diameter Allometry and above Ground Biomass in Tropical Montane Forests : Insights from the Albertine Rift in Africa." *Plos One*, 1–20.

Imbach, Pablo, Megan Beardsley, Claudia Bouroncle, Claudia Medellin, Peter Läderach, Hugo Hidalgo, Eric Alfaro, et al. 2017. "Climate Change, Ecosystems and Smallholder Agriculture in Central America: An Introduction to the Special Issue." *Climatic Change* 141 (1): 1–12. https://doi.org/10.1007/s10584-017-1920-5.

Immerzeel, W. W., A. F. Lutz, M. Andrade, A. Bahl, H. Biemans, T. Bolch, S. Hyde, et al. 2020. "Importance and Vulnerability of the World's Water Towers." *Nature* 577 (7790): 364–69. https://doi.org/10.1038/s41586-019-1822-y.

INEGI. 2013. "CONJUNTO DE DATOS VECTORIALES DE USO DEL SUELO Y VEGETACIÓN ESCALA 1:250 000, SERIE V." http://www.inegi.org.mx/.

Isakson, S Ryan. 2009. "No Hay Ganancia En La Milpa: The Agrarian Question, Food Sovereignty, and the on-Farm Conservation of Agrobiodiversity in the Guatemalan Highlands." *The Journal of Peasant Studies* 36 (4): 725–59. https://doi.org/10.1080/03066150903353876.

Jackson, L.A., and S. Scherr. 1995. "Non-Degrading Land Use Strategies for Tropical Hillsides."

Janvry, A De. 1981. *The Agrarian Question and Reformism in Latin America*. Johns Hopkins Studies in Development. The Johns Hopkins University Press.

Jarchow, Christopher, Kamel Didan, Armando Barreto-Muñoz, Pamela Nagler, and Edward Glenn. 2018. "Application and Comparison of the MODIS-Derived Enhanced Vegetation Index to VIIRS, Landsat 5 TM and Landsat 8 OLI Platforms: A Case Study in the Arid Colorado River Delta, Mexico." *Sensors* 18 (5): 1546. https://doi.org/10.3390/s18051546.

Jardel Peláez, E.J., R. Cuevas Guzmán, A.L Santiago Pérez, and J.M. Rodríguez Gómez. 2014. "Ecología y Manejo de Los Bosques Mesófilos de Montaña En México." In *Bosques Mesófilos de Montaña de México: Diversidad, Ecología y Manejo*, edited by M. Gual-Díaz and A. Rendón-Correa, 352. Mexico: Comisión Nacional para el Conocimiento y Uso de la Biodiversidad.

Jha, S., and K. S. Bawa. 2006. "Population Growth, Human Development, and Deforestation in Biodiversity Hotspots." *Conservation Biology* 20 (3): 906–12. https://doi.org/10.1111/j.1523-1739.2006.00398.x.

Jiang, Ningsang, Peng Li, and Zhiming Feng. 2022. "Remote Sensing of Swidden Agriculture in the Tropics: A Review." *International Journal of Applied Earth Observation and Geoinformation* 112 (August): 102876. https://doi.org/10.1016/j.jag.2022.102876.

Jong, Bernardus H.J. De. 2013. "Spatial Distribution of Biomass and Links to Reported Disturbances in Tropical Lowland Forests of Southern Mexico." *Carbon Management* 4 (6): 601–15. https://doi.org/10.4155/cmt.13.60.

Kauffman, J. Boone, R. Flint Hughes, and Chris Heider. 2009. "Carbon Pool and Biomass Dynamics Associated with Deforestation, Land Use, and Agricultural Abandonment in the Neotropics." *Ecological Applications* 19 (5): 1211–22. https://doi.org/10.1890/08-1696.1.

Kay, Cristóbal. 2000. "7. Latin America's Agrarian Transformation: Peasantization and Proletarianization." In *Disappearing Peasantries?*, 123–38. Rugby, Warwickshire, United Kingdom: Practical Action Publishing. https://doi.org/10.3362/9781780440118.007.

———. 2008. "Reflections on Latin American Rural Studies in the Neoliberal Globalization Period: A New Rurality?" *Development and Change* 39 (6): 915–43. https://doi.org/10.1111/j.1467-7660.2008.00518.x.

Kennedy, Robert E, Serge Andréfouët, Warren B Cohen, Cristina Gómez, Patrick Griffiths, Martin Hais, Sean P Healey, et al. 2014. "Bringing an Ecological View of Change to Landsat-Based Remote Sensing." *Frontiers in Ecology and the Environment* 12 (6): 339–46. https://doi.org/10.1890/130066.

Körner, Christian, Walter Jetz, Jens Paulsen, Davnah Payne, Katrin Rudmann-Maurer, and Eva M. Spehn. 2017. "A Global Inventory of Mountains for Bio-Geographical Applications." *Alpine Botany* 127 (1): 1–15. https://doi.org/10.1007/s00035-016-0182-6.

Kothandaraman, Subashree, Javid Ahmad Dar, Somaiah Sundarapandian, Selvadurai Dayanandan, and Mohammed Latif Khan. 2020. "Ecosystem-Level Carbon Storage and Its Links to Diversity, Structural and Environmental Drivers in Tropical Forests of Western Ghats, India." *Scientific Reports* 10 (1): 13444. https://doi.org/10.1038/s41598-020-70313-6.

Kremen, Claire. 2015. "Reframing the Land-Sparing/Land-Sharing Debate for Biodiversity Conservation." *Annals of the New York Academy of Sciences*. https://doi.org/10.1111/nyas.12845.

Kuemmerle, Tobias, Karlheinz Erb, Patrick Meyfroidt, Daniel Müller, Peter H Verburg, Stephan Estel, Helmut Haberl, et al. 2013. "Challenges and Opportunities in Mapping Land Use Intensity Globally." *Current Opinion in Environmental Sustainability* 5 (5): 484–93. https://doi.org/10.1016/j.cosust.2013.06.002.

Kutchartt, E., M. Pedron, and F. Pirotti. 2022. "ASSESSMENT OF CANOPY AND GROUND HEIGHT ACCURACY FROM GEDI LIDAR OVER STEEP MOUNTAIN AREAS." *ISPRS Annals of the Photogrammetry, Remote Sensing and Spatial Information Sciences* V-3–2022 (May): 431–38. https://doi.org/10.5194/isprs-annals-V-3-2022-431-2022.

la Cruz-Amo, Lydia de, Guillermo Bañares-de-Dios, Victoria Cala, Íñigo Granzow-de la Cerda, Carlos I. Espinosa, Alicia Ledo, Norma Salinas, Manuel J. Macía, and Luis Cayuela. 2020. "Trade-Offs Among Aboveground, Belowground, and Soil Organic Carbon Stocks Along Altitudinal Gradients in Andean Tropical Montane Forests." *Frontiers in Plant Science* 11 (March): 1–11. https://doi.org/10.3389/fpls.2020.00106.

Lambin, Eric F., Helmut J. Geist, and Erika Lepers. 2003. "Dynamics of Land-Use and Land-Cover Change in Tropical Regions." *Annual Review of Environment and Resources* 28 (1): 205–41. https://doi.org/10.1146/annurev.energy.28.050302.105459.

Lambin, Eric F, B L Turner, Helmut J Geist, Samuel B Agbola, Arild Angelsen, Carl Folke, John W Bruce, et al. 2001. "The Causes of Land-Use and Land-Cover Change: Moving beyond the Myths" 11: 261–69.

Leija-Loredo, Edgar G., Numa P. Pavón, Arturo Sánchez-González, Rodrigo Rodriguez-Laguna, and Gregorio Ángeles-Pérez. 2018. "Land Cover Change and Carbon Stores in a Tropical Montane Cloud Forest in the Sierra Madre Oriental, Mexico." *Journal of Mountain Science* 15 (10): 2136–47. https://doi.org/10.1007/s11629-018-4937-y.

Lewis, Simon L., Bonaventure Sonké, Terry Sunderland, Serge K. Begne, Gabriela Lopez-Gonzalez, Geertje M. F. van der Heijden, Oliver L. Phillips, et al. 2013. "Above-Ground Biomass and Structure of 260 African Tropical Forests." *Philosophical Transactions of the Royal Society B: Biological Sciences* 368 (1625): 20120295. https://doi.org/10.1098/rstb.2012.0295.

Liu, Yang, Alan D. Ziegler, Jie Wu, Shijing Liang, Dashan Wang, Rongrong Xu, Decha Duangnamon, Hailong Li, and Zhenzhong Zeng. 2022. "Effectiveness of Protected Areas in Preventing Forest Loss in a Tropical Mountain Region." *Ecological Indicators* 136 (March): 108697. https://doi.org/10.1016/j.ecolind.2022.108697.

Lumley, T. 2020. "Leaps: Regression Subset Selection." https://cran.r-project.org/package=leaps.

Madrid, Lucía, Juan Manuel Núñez, Gabriela Quiroz, and Yosu Rodríguez. 2009. "La Propiedad Social Forestal En México." *Investigación Ambiental* 1 (2): 179–96.

Magurran, A E. 2013. *Measuring Biological Diversity*. Wiley. https://books.google.com/books?id=fIjsaxmL%5C_S8C.

Maki, M, M Ishiahra, and M Tamura. 2004. "Estimation of Leaf Water Status to Monitor the Risk of Forest Fires by Using Remotely Sensed Data." *Remote Sensing of Environment* 90 (4): 441–50. https://doi.org/10.1016/j.rse.2004.02.002.

Malhi, Y, DD Baldocchi, and PG Jarvis. 1999. "The Carbon Balance of Tropical , Temperate and Boreal Forests," 715–40.

Malhi, Yadvinder, Toby A. Gardner, Gregory R. Goldsmith, Miles R. Silman, and Przemyslaw Zelazowski. 2014. "Tropical Forests in the Anthropocene." *Annual Review of Environment and Resources* 39: 125–59. https://doi.org/10.1146/annurev-environ-030713-155141.

Manzo, Diana, and Lydiette Carrión. 2022. "Se Recrudece Violencia En La Sierra Mixe." *Pie de Página*, 2022. https://piedepagina.mx/se-recrudece-violencia-en-la-sierra-mixe/.

Marshall, A. R., S. Willcock, P. J. Platts, J. C. Lovett, A. Balmford, N. D. Burgess, J. E. Latham, et al. 2012. "Measuring and Modelling Above-Ground Carbon and Tree Allometry along a Tropical Elevation Gradient." *Biological Conservation* 154: 20–33. https://doi.org/10.1016/j.biocon.2012.03.017.

Martínez, M. Luisa, Octavio Pérez-Maqueo, Gabriela Vázquez, Gonzalo Castillo-Campos, José García-Franco, Klaus Mehltreter, Miguel Equihua, and Rosario Landgrave. 2009. "Effects of Land Use Change on Biodiversity and Ecosystem Services in Tropical Montane Cloud Forests of Mexico." *Forest Ecology and Management* 258 (9): 1856–63. https://doi.org/10.1016/j.foreco.2009.02.023.

Masek, J.G., E.F. Vermote, N.E. Saleous, R. Wolfe, F.G. Hall, K.F. Huemmrich, F. Gao, J. Kutler, and T.-K. Lim. 2006. "A Landsat Surface Reflectance Dataset for North America, 1990–2000." *IEEE Geoscience and Remote Sensing Letters* 3 (1): 68–72. https://doi.org/10.1109/LGRS.2005.857030.

Mateo-Vega, Javier, J. Pablo Arroyo-Mora, and Catherine Potvin. 2019. "Tree Aboveground Biomass and Species Richness of the Mature Tropical Forests of Darien, Panama, and Their Role in Global Climate Change Mitigation and Biodiversity Conservation." *Conservation Science and Practice* 1 (8). https://doi.org/10.1111/csp2.42.

McMichael, Philip. 2013. "Value-Chain Agriculture and Debt Relations: Contradictory Outcomes." *Third World Quarterly* 34 (4): 671–90.

Meave, Jorge, Miguel Angel Soto, Luz María Calvo-Irabien, Horacio Paz-Hernández, and Susana Valencia-Avalos. 1992. "Sinecological Analysis of the Montane Rain Forrest of Omiltemi, Guerrero." *Botanical Sciences*, no. 52: 31–77. https://doi.org/10.17129/botsci.1404.

Mejía, Nancy R., Jorge A. Meave, and Carlos A. Ruiz. 2004. "Análisis Estructural De Un Bosque Mesófilo Demontaña En El Extremo Oriental De Lasierramadre Delsur(Oaxaca), México." *Boletín de La Sociedad Botánica de México*, no. 74: 13–19. https://www.redalyc.org/html/577/57707402/.

Melito, Melina, Jean Paul Metzger, and Alexandre A. de Oliveira. 2018. "Landscape-Level Effects on Aboveground Biomass of Tropical Forests: A Conceptual Framework." *Global Change Biology* 24 (2): 597–607. https://doi.org/10.1111/gcb.13970.

Mendoza-Ponce, Alma, Rogelio Corona-Núñez, Florian Kraxner, Sylvain Leduc, and Piera Patrizio. 2018. "Identifying Effects of Land Use Cover Changes and Climate Change on Terrestrial Ecosystems and Carbon Stocks in Mexico." *Global Environmental Change* 53 (August): 12–23. https://doi.org/10.1016/j.gloenvcha.2018.08.004.

Mercier, Audrey, Julie Betbeder, Florent Rumiano, Jacques Baudry, Valéry Gond, Lilian Blanc, Clément Bourgoin, et al. 2019. "Evaluation of Sentinel-1 and 2 Time Series for Land Cover Classification of Forest–Agriculture Mosaics in Temperate and Tropical Landscapes." *Remote Sensing* 11 (8): 979. https://doi.org/10.3390/rs11080979.

Meyfroidt, Patrick, Eric F Lambin, Karl-Heinz Erb, and Thomas W Hertel. 2013. "Globalization of Land Use: Distant Drivers of Land Change and Geographic Displacement of Land Use." *Current Opinion in Environmental Sustainability* 5 (5): 438–44. https://doi.org/10.1016/j.cosust.2013.04.003.

Meyfroidt, Patrick, Thomas K. Rudel, and Eric F. Lambin. 2010. "Forest Transitions, Trade, and the Global Displacement of Land Use." *Proceedings of the National Academy of Sciences* 107 (49): 20917–22. https://doi.org/10.1073/pnas.1014773107.

Mohren, GMJ, H Hasenauer, M Köhl, and G-J Nabuurs. 2012. "Forest Inventories for Carbon Change Assessments." *Current Opinion in Environmental Sustainability* 4 (6): 686–95. https://doi.org/https://doi.org/10.1016/j.cosust.2012.10.002.

Molinario, G, M C Hansen, and P V Potapov. 2015. "Forest Cover Dynamics of Shifting Cultivation in the Democratic Republic of Congo: A Remote Sensing-Based Assessment for 2000–2010." *Environmental Research Letters* 10 (9): 094009. https://doi.org/10.1088/1748-9326/10/9/094009.

Morello, Thiago Fonseca, Marie Gabrielle Piketty, Toby Gardner, Luke Parry, Jos Barlow, Joice Ferreira, and Nicola S. Tancredi. 2018. "Fertilizer Adoption by Smallholders in the Brazilian Amazon: Farm-Level Evidence." *Ecological Economics* 144 (August 2017): 278–91. https://doi.org/10.1016/j.ecolecon.2017.08.010.

Moret, Pierre, Priscilla Muriel, Ricardo Jaramillo, and Olivier Dangles. 2019. "Humboldt's Tableau Physique Revisited." *Proceedings of the National Academy of Sciences* 116 (26): 12889–94. https://doi.org/10.1073/pnas.1904585116.

Morett-Sánchez, J.C., and C Cosío-Ruiz. 2017. "Panorama de Los Ejidos y Comunidades Agrarias En México." *Agricultura, Sociedad y Desarrollo* 14 (1). https://doi.org/http://www.scielo.org.mx/scielo.php?script=sci_arttext&pid=S1870-54722017000100125.

Moser, G., M. Röderstein, N. Soethe, D. Hertel, and C. Leuschner. 2008. "Altitudinal Changes in Stand Structure and Biomass Allocation of Tropical Mountain Forests in Relation to Microclimate and Soil Chemistry," 229–42. https://doi.org/10.1007/978-3-540-73526-7_22.

Mulligan, M, LA Bruijnzeel, FN Scatena, and LS Hamilton. 2011. "Modeling the Tropics-Wide Extent and Distribution of Cloud Forest and Cloud Forest Loss, with Implications for Conservation Priority." In *Tropical Montane Cloud Forests*, 14–38. Cambridge: Cambridge University Press. https://doi.org/10.1017/CBO9780511778384.004.

Mulligan, Mark, and Sophia Burke. 2005. "Global Cloud Forests and Environmental Change in a Hydrological Context." *DFID FRP Project ZF0216. Final Report*.

Mundaca, Antonio. 2019. "El Despojo de Ayutla Mixe." *La Verdad*, 2019. https://laverdadjuarez.com/2019/06/30/el-despojo-de-ayutla-mixe/.

Muñoz-Villers, L. E., and J. López-Blanco. 2008. "Land Use/Cover Changes Using Landsat TM/ETM Images in a Tropical and Biodiverse Mountainous Area of Central-Eastern Mexico." *International Journal of Remote Sensing* 29 (1): 71–93. https://doi.org/10.1080/01431160701280967.

Navarrete Romero, Lourdes. 2015. "El Ejido Mexicano." *Argumentos. Estudios Críticos De La Sociedad* 79: 217–38.

Navarro Cerrillo, Rafael M., Dennis J. Esteves Vieira, Susana Ochoa-Gaona, Bernardus H.J. de Jong, and M. del Mar Delgado Serrano. 2018. "Land Cover Changes and Fragmentation in Mountain Neotropical Ecosystems of Oaxaca, Mexico under Community Forest Management." *Journal of Forestry Research* 30 (1): 143–55. https://doi.org/10.1007/s11676-017-0568-3.

Norden, Natalia, Héctor A. Angarita, Frans Bongers, Miguel Martínez-Ramos, Iñigo Granzow De La Cerda, Michiel Van Breugel, Edwin Lebrija-Trejos, et al. 2015. "Successional Dynamics in Neotropical Forests Are as Uncertain as They Are Predictable." *Proceedings of the National Academy of Sciences of the United States of America* 112 (26): 8013–18. https://doi.org/10.1073/pnas.1500403112.

Ochoa-Gaona, Susana, and Mario Gonzôlez-Espinosa. 2000. "Land Use and Deforestation in the Highlands of Chiapas, Mexico." *Applied Geography* 20 (1): 17–42. https://doi.org/10.1016/S0143-6228(99)00017-X.

Oksanen, JF, G Blanchet, M Friendly, R Kindt, P Legendre, D McGlinn, PR Minchin, et al. 2020. "Vegan: Community Ecology Package." https://cran.r-project.org/package=vegan.

Pan, Yude, RA Birdsey, Fang J, R Houghton, Kauppi PE, WA Kurz, OL Phillips, et al. 2007. "A Large and Persistent Carbon Sink in the World's Forests." *Science* 317 (july): 4.

Pang, Shiyun, Guiying Li, Xiandie Jiang, Yaoliang Chen, Yagang Lu, and Dengsheng Lu. 2022. "Retrieval of Forest Canopy Height in a Mountainous Region with ICESat-2 ATLAS." *Forest Ecosystems* 9: 100046. https://doi.org/10.1016/j.fecs.2022.100046.

Pazos-Almada, Barbara, and David Barton Bray. 2018. "Community-Based Land Sparing: Territorial Land-Use Zoning and Forest Management in the Sierra Norte of Oaxaca, Mexico." *Land Use Policy* 78 (June): 219–26. https://doi.org/10.1016/j.landusepol.2018.06.056.

Peluso, Nancy L., and P. Vandergeest. 2014. "Jungles, Forests, and the Theatre of Wars: Insurgency, Counterinsurgency, and the Political Forest in Southeast Asia." In *The Social Lives of Forests*, edited by Susanna B. Hecht, Kathleen D. Morrison, and Christine Padoch, 55–69. Chicago: The University of Chicago.

Pérez-García, Oscar, and Rafael F. del Castillo. 2016. "The Decline of the Itinerant Milpa and the Maintenance of Traditional Agrobiodiversity: Crops and Weeds Coexistence in a Tropical Cloud Forest Area in Oaxaca, Mexico." *Agriculture, Ecosystems and Environment* 228: 30–37. https://doi.org/10.1016/j.agee.2016.05.002.

———. 2017. "Shifts in Swidden Agriculture Alter the Diversity of Young Fallows: Is the Regeneration of Cloud Forest at Stake in Southern Mexico?" *Agriculture, Ecosystems and Environment* 248 (May): 162–74. https://doi.org/10.1016/j.agee.2017.07.024.

Perfecto, I., and J. Vandermeer. 2010. "The Agroecological Matrix as Alternative to the Land-Sparing/Agriculture Intensification Model." *Proceedings of the National Academy of Sciences*. https://doi.org/10.1073/pnas.0905455107.

Perfecto, I, J H Vandermeer, and A L Wright. 2009. *Nature's Matrix: Linking Agriculture, Conservation and Food Sovereignty*. Earthscan.

Perfecto, Ivette, M. Estelí Jiménez-Soto, and John Vandermeer. 2019. "Coffee Landscapes Shaping the Anthropocene: Forced Simplification on a Complex Agroecological Landscape." *Current Anthropology* 60 (S20): S236–50. https://doi.org/10.1086/703413.

Perfecto, Ivette, and John Vandermeer. 2008. "Biodiversity Conservation in Tropical Agroecosystems: A New Conservation Paradigm." *Annals of the New York Academy of Sciences* 1134: 173–200. https://doi.org/10.1196/annals.1439.011.

Pfaff, Alexander, and Robert Walker. 2010. "Regional Interdependence and Forest 'Transitions': Substitute Deforestation Limits the Relevance of Local Reversals." *Land Use Policy* 27 (2): 119–29. https://doi.org/10.1016/j.landusepol.2009.07.010.

Phelps, Jacob, Luis Roman Carrasco, Edward L. Webb, Lian Pin Koh, and Unai Pascual. 2013. "Agricultural Intensification Escalates Future Conservation Costs." *Proceedings of the National Academy of Sciences* 110 (19): 7601–6. https://doi.org/10.1073/pnas.1220070110.

Piperno, Dolores R. 2011. "The Origins of Plant Cultivation and Domestication in the New World Tropics." *Current Anthropology* 52 (S4): S453–70. https://doi.org/10.1086/659998.

Poorter, L., M. T. van der Sande, J. Thompson, E. J.M.M. Arets, A. Alarcón, J. Álvarez-Sánchez, N. Ascarrunz, et al. 2015. "Diversity Enhances Carbon Storage in Tropical Forests." *Global Ecology and Biogeography* 24 (11): 1314–28. https://doi.org/10.1111/geb.12364.

Poorter, L, Frans Bongers, T. Mitchell Aide, Angélica M. Almeyda Zambrano, Patricia Balvanera, Justin M. Becknell, Vanessa Boukili, et al. 2016. "Biomass Resilience of Neotropical Secondary Forests." *Nature* 530 (7589): 211–14. https://doi.org/10.1038/nature16512.

Poorter, Lourens, Masha T. van der Sande, Eric J.M.M. Arets, Nataly Ascarrunz, Brian Enquist, Bryan Finegan, Juan Carlos Licona, et al. 2017. "Biodiversity and Climate Determine the Functioning of Neotropical Forests." *Global Ecology and Biogeography* 26 (12): 1423–34. https://doi.org/10.1111/geb.12668.

Porter-Bolland, Luciana, Edward A. Ellis, Manuel R. Guariguata, Isabel Ruiz-Mallén, Simoneta Negrete-Yankelevich, and Victoria Reyes-García. 2012. "Community Managed Forests and Forest Protected Areas: An Assessment of Their Conservation Effectiveness across the Tropics." *Forest Ecology and Management* 268 (March): 6–17. https://doi.org/10.1016/j.foreco.2011.05.034.

Potapov, Peter V., Svetlana A. Turubanova, Matthew C. Hansen, Bernard Adusei, Mark Broich, Alice Altstatt, Landing Mane, and Christopher O. Justice. 2012. "Quantifying Forest Cover Loss in Democratic Republic of the Congo, 2000-2010, with Landsat ETM+ Data." *Remote Sensing of Environment* 122: 106–16. https://doi.org/10.1016/j.rse.2011.08.027.

Prach, Karel, and Lawrence R. Walker. 2019. "Differences between Primary and Secondary Plant Succession among Biomes of the World." Edited by Cynthia Chang. *Journal of Ecology* 107 (2): 510–16. https://doi.org/10.1111/1365-2745.13078.

Pulsford, Stephanie A., David B. Lindenmayer, and Don A. Driscoll. 2016. "A Succession of Theories: Purging Redundancy from Disturbance Theory." *Biological Reviews* 91 (1): 148–67. https://doi.org/10.1111/brv.12163.

Quadri, Paulo, Lucas C. R. Silva, and Erika S. Zavaleta. 2021. "Climate-Induced Reversal of Tree Growth Patterns at a Tropical Treeline." *Science Advances* 7 (22). https://doi.org/10.1126/sciadv.abb7572.

Rahbek, Carsten, Michael K. Borregaard, Robert K. Colwell, Bo Dalsgaard, Ben G. Holt, Naia Morueta-Holme, David Nogues-Bravo, Robert J. Whittaker, and Jon Fjeldså. 2019. "Humboldt's Enigma: What Causes Global Patterns of Mountain Biodiversity?" *Science* 365 (6458): 1108–13. https://doi.org/10.1126/science.aax0149.

Raich, James W., Ann E. Russell, Kanehiro Kitayama, William J. Parton, and Peter M. Vitousek. 2006. "TEMPERATURE INFLUENCES CARBON ACCUMULATION IN MOIST TROPICAL FORESTS." *Ecology* 87 (1): 76–87. https://doi.org/10.1890/05-0023.

Ravikumar, Ashwin, Robin R. Sears, Peter Cronkleton, Mary Menton, and Matías Pérez-Ojeda del Arco. 2017. "Is Small-Scale Agriculture Really the Main Driver of Deforestation in the Peruvian Amazon? Moving beyond the Prevailing Narrative." *Conservation Letters* 10 (2): 170–77. https://doi.org/10.1111/conl.12264.

RCoreTeam. 2021. "R: A Language and Environment for Statistical Computing." R Foundation for Statistical Computing, Vienna, Austria. https://www.r-project.org/.

Reid, J. Leighton, Matthew E. Fagan, James Lucas, Joshua Slaughter, and Rakan A. Zahawi. 2019. "The Ephemerality of Secondary Forests in Southern Costa Rica." *Conservation Letters* 12 (2): 1–7. https://doi.org/10.1111/conl.12607.

Réjou-Méchain, Maxime, Ariane Tanguy, Camille Piponiot, Jérôme Chave, and Bruno Hérault. 2017. "BIOMASS: An R Package for Estimating Above-ground Biomass and Its Uncertainty in Tropical Forests." Edited by Sarah Goslee. *Methods in Ecology and Evolution* 8 (9): 1163–67. https://doi.org/10.1111/2041-210X.12753.

Requena Suarez, Daniela, Danaë M.A. Rozendaal, Veronique De Sy, Oliver L. Phillips, Esteban Alvarez-Dávila, Kristina Anderson-Teixeira, Alejandro Araujo-Murakami, et al. 2019. "Estimating Aboveground Net Biomass Change for Tropical and Subtropical Forests: Refinement of IPCC Default Rates Using Forest Plot Data." *Global Change Biology* 25 (11): 3609–24. https://doi.org/10.1111/gcb.14767.

Rivero-Romero, Alexis D., Ana I. Moreno-Calles, Alejandro Casas, Alicia Castillo, and Andrés Camou-Guerrero. 2016. "Traditional Climate Knowledge: A Case Study in a Peasant Community of Tlaxcala, Mexico." *Journal of Ethnobiology and Ethnomedicine* 12 (1): 33. https://doi.org/10.1186/s13002-016-0105-z.

Robinson, Nathaniel, Brady Allred, Matthew Jones, Alvaro Moreno, John Kimball, David Naugle, Tyler Erickson, and Andrew Richardson. 2017. "A Dynamic Landsat Derived Normalized Difference Vegetation Index (NDVI) Product for the Conterminous United States." *Remote Sensing* 9 (8): 863. https://doi.org/10.3390/rs9080863.

Rockström, Johan, Will Steffen, Kevin Noone, Åsa Persson, F Stuart Chapin Iii, Eric Lambin, Timothy M Lenton, et al. 2009. "Planetary Boundaries : Exploring the Safe Operating Space for Humanity." *Ecology and Society* 14 (2): 32.

Rojas-García, Fabiola, Bernardus H.J. De Jong, Pablo Martínez-Zurimendí, and Fernando Paz-Pellat. 2015. "Database of 478 Allometric Equations to Estimate Biomass for Mexican Trees and Forests." *Annals of Forest Science* 72 (6): 835–64. https://doi.org/10.1007/s13595-015-0456-y.

Roman, L, F N Scatena, and L A Bruijnzeel. 2011. "Global and Local Variations in Tropical Montane Cloud Forest Soils." In *Tropical Montane Cloud Forests: Science for Conservation and Management*, edited by L A Bruijnzeel, F N Scatena, and L S.Editors Hamilton, 77–89. International Hydrology Series. Cambridge University Press. https://doi.org/10.1017/CBO9780511778384.008.

Rozendaal, Danaë M A, Daniela Requena Suarez, Veronique De Sy, Valerio Avitabile, Sarah Carter, C Y Adou Yao, Esteban Alvarez-Davila, et al. 2022. "Aboveground Forest Biomass Varies across Continents, Ecological Zones and Successional Stages: Refined IPCC Default Values for Tropical and Subtropical Forests." *Environmental Research Letters* 17 (1): 014047. https://doi.org/10.1088/1748-9326/ac45b3.

Ruiz-Jiménez, Carlos Alberto, Jorge Meave, and José Luis Contreras-Jiménez. 1999. "El Bosque Mesófilo de La Región de Puerto Soledad (Oaxaca), México: Análisis Estructural." *Botanical Sciences*, no. 65: 23–37. https://doi.org/10.17129/botsci.1592.

Saatchi, Sassan S., Nancy L. Harris, Sandra Brown, Michael Lefsky, Edward T.A. Mitchard, William Salas, Brian R. Zutta, et al. 2011. "Benchmark Map of Forest Carbon Stocks in Tropical Regions across Three Continents." *Proceedings of the National Academy of Sciences of the United States of America* 108 (24): 9899–9904. https://doi.org/10.1073/pnas.1019576108.

Salinas, Norma, Eric G. Cosio, Miles Silman, Patrick Meir, Andrew T. Nottingham, Rosa Maria Roman-Cuesta, and Yadvinder Malhi. 2021. "Editorial: Tropical Montane Forests in a Changing Environment." *Frontiers in Plant Science* 12 (August). https://doi.org/10.3389/fpls.2021.712748.

Santoro, Maurizio, Oliver Cartus, Nuno Carvalhais, Danaë M.A. Rozendaal, Valerio Avitabile, Arnan Araza, Sytze De Bruin, et al. 2021. "The Global Forest Above-Ground Biomass Pool for 2010 Estimated from High-Resolution Satellite Observations." *Earth System Science Data* 13 (8): 3927–50. https://doi.org/10.5194/essd-13-3927-2021.

Scatena, F N, L A Bruijnzeel, P Bubb, and S Das. 2011. "Setting the Stage." In *Tropical Montane Cloud Forests: Science for Conservation and Management*, edited by L A Bruijnzeel, F N Scatena, and L S.Editors Hamilton, 3–13. International Hydrology Series. Cambridge University Press. https://doi.org/10.1017/CBO9780511778384.003.

Seymour, Frances, and Nancy L. Harris. 2019. "Reducing Tropical Deforestation." *Science* 365 (6455): 756–57. https://doi.org/10.1126/science.aax8546.

Sheil, D, B Ladd, LCR Silva, S Laffan, and M Van Heist. 2016. "How Are Soil Carbon and Tropical Biodiversity Related?" *Environmental Conservation*, 1–11. https://doi.org/10.1017/S0376892916000011.

Shen, Yong, Shixiao Yu, Juyu Lian, Hao Shen, Honglin Cao, Huanping Lu, and Wanhui Ye. 2016. "Tree Aboveground Carbon Storage Correlates with Environmental Gradients and Functional Diversity in a Tropical Forest." *Scientific Reports* 6 (1): 25304. https://doi.org/10.1038/srep25304.

SIAP. 2020. "Estadística de La Producción Agrícola." Servicio de Información Agroalimentaria y Pesquera. http://infosiap.siap.gob.mx/gobmx/datosAbiertos.php.

Silver, W. L., R. Ostertag, and A. E. Lugo. 2000. "The Potential for Carbon Sequestration Through Reforestation of Abandoned Tropical Agricultural and Pasture Lands." *Restoration Ecology* 8 (4): 394–407. https://doi.org/10.1046/j.1526-100x.2000.80054.x.

Slik, J. W.F., Shin Ichiro Aiba, Francis Q. Brearley, Chuck H. Cannon, Olle Forshed, Kanehiro Kitayama, Hidetoshi Nagamasu, et al. 2010. "Environmental Correlates of Tree Biomass, Basal Area, Wood Specific Gravity and Stem Density Gradients in Borneo's Tropical Forests." *Global Ecology and Biogeography* 19 (1): 50–60. https://doi.org/10.1111/j.1466-8238.2009.00489.x.

Solórzano, Jonathan Vidal, José Alberto Gallardo-Cruz, and Candelario Peralta-Carreta. 2020. "Potencial Del Acervo de Imágenes Landsat Disponible En Google Earth Engine Para El Estudio Del Territorio Mexicano." *Investigaciones Geográficas*, no. 101 (March). https://doi.org/10.14350/rig.59821.

Spehn, Eva M., Katrin Rudmann-Maurer, and Christian Körner. 2011. "Mountain Biodiversity." *Plant Ecology & Diversity* 4 (4): 301–2. https://doi.org/10.1080/17550874.2012.698660.

Spracklen, D. V., and R. Righelato. 2014. "Tropical Montane Forests Are a Larger than Expected Global Carbon Store." *Biogeosciences* 11 (10): 2741–54. https://doi.org/10.5194/bg-11-2741-2014.

Sullivan, Martin J.P., Joey Talbot, Simon L. Lewis, Oliver L. Phillips, Lan Qie, Serge K. Begne, Jerôme Chave, et al. 2017. "Diversity and Carbon Storage across the Tropical Forest Biome." *Scientific Reports* 7 (January): 1–12. https://doi.org/10.1038/srep39102.

Taylor, Philip G., Cory C. Cleveland, William R. Wieder, Benjamin W. Sullivan, Christopher E. Doughty, Solomon Z. Dobrowski, and Alan R. Townsend. 2017. "Temperature and Rainfall Interact to Control Carbon Cycling in Tropical Forests." *Ecology Letters* 20 (6): 779–88. https://doi.org/10.1111/ele.12765.

Tellman, Beth, Steven E. Sesnie, Nicholas R. Magliocca, Erik A. Nielsen, Jennifer A. Devine, Kendra McSweeney, Meha Jain, et al. 2020. "Illicit Drivers of Land Use Change: Narcotrafficking and Forest Loss in Central America." *Global Environmental Change* 63 (April): 102092. https://doi.org/10.1016/j.gloenvcha.2020.102092.

Teresa, Ana Paula de. 1999. "Población y Recursos En La Región Chinanteca de Oaxaca." *Desacatos* 1: 1–24.

———. 2011. *Quia-Na. La Selva Chinanteca y Sus Pobladores*. 1.ª ed. Universidad Autónoma Metropolitana.

Terraube, Julien, and Álvaro Fernández-Llamazares. 2020. "Strengthening Protected Areas to Halt Biodiversity Loss and Mitigate Pandemic Risks." *Current Opinion in Environmental Sustainability* 46 (October): 35–38. https://doi.org/10.1016/j.cosust.2020.08.014.

Ticehurst, Catherine, Alex Held, and Stuart Phinn. 2004. "Integrating JERS-1 Imaging Radar and Elevation Models for Mapping Tropical Vegetation Communities in Far North Queensland, Australia." *Photogrammetric Engineering and Remote Sensing* 70 (11): 1259–66. https://doi.org/10.14358/PERS.70.11.1259.

Tito, Richard, Heraldo L. Vasconcelos, and Kenneth J. Feeley. 2020. "Mountain Ecosystems as Natural Laboratories for Climate Change Experiments." *Frontiers in Forests and Global Change* 3 (March). https://doi.org/10.3389/ffgc.2020.00038.

Toledo-Aceves, Tarin, Jorge A. Meave, Mario González-Espinosa, and Neptalí Ramírez-Marcial. 2011. "Tropical Montane Cloud Forests: Current Threats and Opportunities for Their Conservation and Sustainable Management in Mexico." *Journal of Environmental Management* 92 (3): 974–81. https://doi.org/10.1016/j.jenvman.2010.11.007.

Topik, Steven, John M. Talbot, and Mario Samper. 2010. "Introduction Globalization, Neoliberalism, and the Latin American Coffee Societies." *Latin American Perspectives* 37 (2): 5–20. https://doi.org/10.1177/0094582X09356955.

Torres Castillo, Nora E., Elda M. Melchor-Martínez, Jhosseph S. Ochoa Sierra, Ricardo A. Ramirez-Mendoza, Roberto Parra-Saldívar, and Hafiz M.N. Iqbal. 2020. "Impact of Climate Change and Early Development of Coffee Rust – An Overview of Control Strategies to Preserve Organic Cultivars in Mexico." *Science of The Total Environment* 738 (October): 140225. https://doi.org/10.1016/j.scitotenv.2020.140225.

Torres Colín, Rafael. 2004. "Tipos de Vegetación." In *Biodiversidad de Oaxaca*, edited by A.J. García-Mendoza, M.J. Ordoñez, and M. Briones-Salas, 605. Mexico: UNAM.

Tredennick, Andrew T., Giles Hooker, Stephen P. Ellner, and Peter B. Adler. 2021. "A Practical Guide to Selecting Models for Exploration, Inference, and Prediction in Ecology." *Ecology* 102 (6). https://doi.org/10.1002/ecy.3336.

Trew, Brittany T., and Ilya M. D. Maclean. 2021. "Vulnerability of Global Biodiversity Hotspots to Climate Change." Edited by Brian McGill. *Global Ecology and Biogeography* 30 (4): 768–83. https://doi.org/10.1111/geb.13272.

Tscharntke, Teja, Alexandra M. Klein, Andreas Kruess, Ingolf Steffan-Dewenter, and Carsten Thies. 2005. "Landscape Perspectives on Agricultural Intensification and Biodiversity - Ecosystem Service Management." *Ecology Letters* 8 (8): 857–74. https://doi.org/10.1111/j.1461-0248.2005.00782.x.

Tsui, Chun-Chih, Zueng-Sang Chen, and Chang-Fu Hsieh. 2004. "Relationships between Soil Properties and Slope Position in a Lowland Rain Forest of Souther Taiwan." *Geoderma* 123: 131–42.

Turkelboom, F., J. Poesen, and G. Trébuil. 2008. "The Multiple Land Degradation Effects Caused by Land-Use Intensification in Tropical Steeplands: A Catchment Study from Northern Thailand." *CATENA* 75 (1): 102–16. https://doi.org/10.1016/j.catena.2008.04.012.

Urquijo Torres, Pedro Sergio. 2012. "El Uso de Suelo En México. Síntesis Histórica," 1–28.

Valencia, Vivian, Luis García-Barrios, Eleanor J. Sterling, Paige West, Amayrani Meza-Jiménez, and Shahid Naeem. 2018. "Smallholder Response to Environmental Change: Impacts of Coffee Leaf Rust in a Forest Frontier in Mexico." *Land Use Policy* 79 (February): 463–74. https://doi.org/10.1016/j.landusepol.2018.08.020.

Vargas, Martín. 2016. "Cambian Cafetales Por Ganadería En La Sierra Mixe Zapoteca." *IstmoPress*, 2016. http://www.istmopress.com.mx/istmo/cambian-cafetales-por-ganaderia-en-la-sierra-mixe-zapoteca/.

Velasco-Murguía, Abril, Rafael F. del Castillo, Matthias Rös, and Raúl Rivera-García. 2021. "Successional Pathways of Post-Milpa Fallows in Oaxaca, Mexico." *Forest Ecology and Management* 500 (August): 119644. https://doi.org/10.1016/j.foreco.2021.119644.

Velasco Murguía, Abril, Elvira Durán Medina, Raúl Rivera, and David Barton Bray. 2014. "Cambios En La Cobertura Arbolada de Comunidades Indígenas Con y Sin Iniciativas de Conservación, En Oaxaca, México." *Investigaciones Geográficas, Boletín Del Instituto de Geografía* 2014 (83): 55–73. https://doi.org/10.14350/RIG.34975.

Velázquez, Alejandro, Elvira Durán, Isabel Ramírez, Jean François Mas, Gerardo Bocco, Gustavo Ramírez, and José Luis Palacio. 2003. "Land Use-Cover Change Processes in Highly Biodiverse Areas: The Case of Oaxaca, Mexico." *Global Environmental Change* 13 (3): 175–84. https://doi.org/10.1016/S0959-3780(03)00035-9.

Verbesselt, Jan, Rob Hyndman, Glenn Newnham, and Darius Culvenor. 2010. "Detecting Trend and Seasonal Changes in Satellite Image Time Series." *Remote Sensing of Environment* 114 (1): 106–15. https://doi.org/10.1016/j.rse.2009.08.014.

Vizcaíno-Bravo, Quetzalli, Guadalupe Williams-Linera, and Heidi Asbjornsen. 2020. "Biodiversity and Carbon Storage Are Correlated along a Land Use Intensity Gradient in a Tropical Montane Forest Watershed, Mexico." *Basic and Applied Ecology* 44: 24–34. https://doi.org/10.1016/j.baae.2019.12.004.

Wang, Cuizhen, Zhenqian Lu, and Timothy L. Haithcoat. 2007. "Using Landsat Images to Detect Oak Decline in the Mark Twain National Forest, Ozark Highlands." *Forest Ecology and Management* 240 (1–3): 70–78. https://doi.org/10.1016/j.foreco.2006.12.007.

Weisse, Mikaela, and Elizabeth Goldman. 2022. "Forest Loss Remained Stubbornly High in 2021." 2022. https://research.wri.org/gfr/latest-analysis-deforestation-trends.

West, Paige, James Igoe, and Dan Brockington. 2006. "Parks and Peoples: The Social Impact of Protected Areas." *Annual Review of Anthropology* 35 (1): 251–77. https://doi.org/10.1146/annurev.anthro.35.081705.123308.

White, Joanne C., Michael A. Wulder, Txomin Hermosilla, Nicholas C. Coops, and Geordie W. Hobart. 2017. "A Nationwide Annual Characterization of 25 Years of Forest Disturbance and Recovery for Canada Using Landsat Time Series." *Remote Sensing of Environment* 194 (June): 303–21. https://doi.org/10.1016/j.rse.2017.03.035.

Williams-Linera, Guadalupe. 1991. "Nota Sobre La Estructura Del Estrato Arboreo Del Mosque Mesofilo de Montaña En Los Alrededores Del Campamento 'El Triunfo', Chiapas." *Acta Botánica Mexicana* 13: 1–7.

Wu, Lin, Hongxia Wang, Yuan Li, Zhengwei Guo, and Ning Li. 2021. "A Novel Method for Layover Detection in Mountainous Areas with SAR Images." *Remote Sensing* 13 (23): 4882. https://doi.org/10.3390/rs13234882.

Wulder, Michael A., Thomas R. Loveland, David P. Roy, Christopher J. Crawford, Jeffrey G. Masek, Curtis E. Woodcock, Richard G. Allen, et al. 2019. "Current Status of Landsat Program, Science, and Applications." *Remote Sensing of Environment* 225 (May): 127–47. https://doi.org/10.1016/j.rse.2019.02.015.

Xia, Jiangzhou, Wenping Yuan, Sebastian Lienert, Fortunat Joos, Philippe Ciais, Nicolas Viovy, Ying-ping Wang, et al. 2019. "Global Patterns in Net Primary Production Allocation Regulated by Environmental Conditions and Forest Stand Age: A Model-Data Comparison." *Journal of Geophysical Research: Biogeosciences* 124 (7): 2039–59. https://doi.org/10.1029/2018JG004777.

Zabel, Florian, Ruth Delzeit, Julia M. Schneider, Ralf Seppelt, Wolfram Mauser, and Tomáš Václavík. 2019. "Global Impacts of Future Cropland Expansion and Intensification on Agricultural Markets and Biodiversity." *Nature Communications* 10 (1): 2844. https://doi.org/10.1038/s41467-019-10775-z.

Zeng, Zhenzhong, Drew B. Gower, and Eric F. Wood. 2018. "Accelerating Forest Loss in Southeast Asian Massif in the 21st Century: A Case Study in Nan Province, Thailand." *Global Change Biology* 24 (10): 4682–95. https://doi.org/10.1111/gcb.14366.

Zhai, Han, Hongyan Zhang, Liangpei Zhang, and Pingxiang Li. 2018. "Cloud/Shadow Detection Based on Spectral Indices for Multi/Hyperspectral Optical Remote Sensing Imagery." *ISPRS Journal of Photogrammetry and Remote Sensing* 144 (August): 235–53. https://doi.org/10.1016/j.isprsjprs.2018.07.006.

Zhu, Xiaolin, Eileen H. Helmer, David Gwenzi, Melissa Collin, Sean Fleming, Jiaqi Tian, Humfredo Marcano-Vega, Elvia J. Meléndez-Ackerman, and Jess K. Zimmerman. 2021. "Characterization of Dry-Season Phenology in Tropical Forests by Reconstructing Cloud-Free Landsat Time Series." *Remote Sensing* 13 (23): 4736. https://doi.org/10.3390/rs13234736.

Zomer, Robert J., Deborah A. Bossio, Rolf Sommer, and Louis V. Verchot. 2017. "Global Sequestration Potential of Increased Organic Carbon in Cropland Soils." *Scientific Reports*. https://doi.org/10.1038/s41598-017-15794-8.

Zomer, Robert J, Henry Neufeldt, Jianchu Xu, Antje Ahrends, Deborah Bossio, Antonio Trabucco, Meine van Noordwijk, and Mingcheng Wang. 2016. "Global Tree Cover and Biomass Carbon on Agricultural Land: The Contribution of Agroforestry to Global and National Carbon Budgets." *Scientific Reports* 6 (1): 29987. https://doi.org/10.1038/srep29987.